Alma Mater Studiorum
Università degli Studi di Bologna

Facoltà di Scienze Matematiche, Fisiche e Naturali

Corso di Laurea Specialistica in Astrofisica e Cosmologia

Relaxation of dynamical systems with long range interactions

Candidato:
Pierfrancesco Di Cintio

Relatore:
Chiar.mo Prof. Luca Ciotti

Anno Accademico 2008/2009 - Sessione II

ALMA MATER STUDIORUM
UNIVERSITÀ DEGLI STUDI DI BOLOGNA

Facoltà di Scienze Matematiche, Fisiche e Naturali

Corso di Laurea Specialistica in ASTROFISICA E COSMOLOGIA

Relaxation of dynamical systems with long range interactions

Candidato:
Pierfrancesco Di Cintio

Relatore:
Chiar.mo Prof. Luca Ciotti

Anno Accademico 2008/2009 - Sessione II

Contents

1 Outline **5**

2 Preliminaries: Long range interactions and relaxation mechanisms **7**

2.1 N-body systems with long range interactions 8
2.2 What do we mean by Relaxation? 12
2.2.1 Different forms of relaxation 13
2.3 A short review of the Virial Theorem 15
2.4 Astrophysical implications 17

3 A toy model for systems with long range forces **21**

3.1 The model 22
3.2 The field produced by a shell 23
3.2.1 The general equation for $\mathcal{F}(r)$ case 24
3.3 Examples 26
3.3.1 Classical Gravity: The Newton's theorems 26
3.3.2 The $1/r$ case 27
3.4 The $1/r^{\alpha}$ force 28
3.5 The collapse of a shell under self-gravity 30
3.5.1 Single shell collapse in Newton's gravity 30
3.5.2 Single shell collapse under general $1/r^{\alpha}$ law 31

4 The numerical model **33**

4.1 The code 34
4.1.1 The choice of the softening lenght 35
4.2 The tests 37
4.2.1 Reproducing Hénon's experiments 37
4.2.2 The single shell collapse in Newton's gravity (Numerical) . . 47
4.3 Simulations and results for other $1/r^{\alpha}$ laws 47
4.3.1 Phase space evolution 48
4.3.2 The virial ratio evolution 59

4.3.3 Final velocity and energy distributions 61
4.3.4 Density profiles and global radial oscillations 67
4.4 Flow diagrams 70

5 Discussion and conclusions **75**
5.1 General Results 76
5.2 Open problems 77
5.3 Possible future studies 78

A Two body relaxation time with $1/r^{\alpha}$ force **81**

B The MOND case **87**

C The code's listing **99**

Bibliography **116**

Chapter 1

Outline

In this thesis we will deal with the problem of relaxation in dynamical systems regulated by long range interactions with particular interest in the gravitational N-body problem. We are interested in how the mechanism of relaxation is related with the range and strenght of the interaction. In order to do this we will point out both analytic facts and numerical results.
In classical and even in quantum multiparticle systems the correlation between the relaxation time scale and the range of the interaction governing the dynamics is a very tricky subject to deal with, and leads to a large number of unsolved points both in statistical and dynamical approaches. According to common sense, systems with short-range interactions (for example a gas of particles subjected only on hard core collisions), are supposed to relaxe to equilibrium configurations on longer time-scales than those of the systems dominated by long range interaction [6], [42], [40] (for example a non-neutral plasma where the mean field overcomes the collisional term). This is also for the fact that the two systems have different Thermodynamics.
If we consider gravity in the Newtonian case $1/r^2$, and in the MOND case in the asymptotic limit (low acceleration regime)[1] $1/r$, we have opposite results: A stellar system with dark matter halo in Newtonian gravity has a collisional relaxation scale smaller than the one of an analogous system described without dark matter in MOND while the time scales for collisionless mechanisms such as Phase Mixing are longer in the modified gravity. Remember that unless MOND is not a metric theory, in the limit of low acceleration and large distance (deep MOND regime) it could be considered a "longer-than-gravity range theory". Such fact leads to think that something deeper hides under this problem.
The dependence of the relaxation time on the nature of the force law has obviously a lot of implications in different parts of physics, like Thermodynamics, Statistical

[1] It must be pointed out as we will see later that MOND is not a metric theory, the large r limit is not the only case where its deviance from $1/r^2$ Newton Law is evident.

Mechanics and Stellar Dynamics. This Thesis focuses on the study of a numerical toy model of such class of systems. For the model we have used the simplest possible example of a spherical dissipationless collapse of a family of N concentric shells with uniform surfacial density under a genearilzed $\mathcal{F}(r)$ form of the Gravity Law. In our model we have used long-range interactions in the form $1/r^{\alpha}$ for which the intensity of the force decreases when the distance r increases. To treat our model we have implemented a numerical code that integrates the equations of motion of a system of N dust shells collapsing under a long range force law that can be chosen for each experiment. Further complications of the model could be taking into consideration the angular momentum or the introduction of an external field. The final goal of our work is to investigate the relaxation of an N-body dynamical system governed by an interaction depending from the distance r, and in particular how the relaxation time scale is correlated with the range of such interaction.
In our work the collapsing shell model is, as we have stated, the basic exemplification of a non equlibrium system experiencing a relaxation process. The possibility of changing the form of the interaction in different numerical experiments enable us to see how its range acts on the relaxation time scale. The Thesis starts with an introduction where we briefly treat some properties of the N-body systems and the mechanisms of relaxation. The following chapter is about the mathematical background of the model. Another chapter is about the numerical model with tests and experiments and the results. Finally we end with the conclusions and by pointing out some astrophysical applications.
After the conclusions one can find three appendices, one focusing on dynamical friction in long range systems, another on Modified Dynamics and the last containing the complete listing of our numerical code. Each chapter and appendix is preceded by a short summary of its content.

Chapter 2

Preliminaries: Long range interactions and relaxation mechanisms

In this chapter we first review the concepts of long range interaction systems and relaxation in order to discuss later the motivations behind our model. Herein we present some important definitions in the theory of long range interacting systems, and a handful of concepts taken from Statistical Mechanics and Stellar Dynamics that will be useful to comprehend our discussion. At the end of the chapter after a short review of the Virial Theorem a list of important astrophysical problems related to relaxation is presented.

2.1 N-body systems with long range interactions

A long range interaction could be naively defined as a force F depending on the distance r from its source whose effects are evident also at large r. We can make a rough division between strong long-range interactions and weak long range interactions, the first case concerns interactions such as the harmonic force that are non-zero at $r \to +\infty$, the second case concerns instead interactions such as Gravity and Coulomb force where in this limit the force is zero. Weak long range interactions differ from short-range interaction, mainly because the latter go to zero for $r \to \tilde{r}$ where $\tilde{r}$ is a finite distance. Short-range forces have a completely different behaviour and will not be explored here.
In our discussion we will treat weak forces obeying the Superposition Principle (i.e. given two or more pointlike sources the force in a generic point of the space is merely the vectorial sum of the contribution of the sources) and having the form in the case of a binary interaction

$$\vec{F}_{1,2} = -\frac{K m_1 m_2}{\|\vec{r}_1 - \vec{r}_2\|^{\alpha+1}}(\vec{r}_1 - \vec{r}_2), \tag{2.1}$$

where m_1 and m_2 are the charges (masses) of the interacting particles, $\vec{r}_1$ and $\vec{r}_2$ are their position vectors, K is a coupling constant (G in the gravitation case for example) and α is a real positive quantity. In such kind of interactions the intensity of the field decreases with the distance r from the source, with the law $1/r^{\alpha}$; normalizing to one the contributions of the coupling constant and the charge we can state that for higher values of α the field converges to zero with $r \to +\infty$ faster than for lower values. In this sense we are speaking of Long Range Interaction. Furtheron, equation 2.1 can be seen as a special case of a more general law:

$$\vec{F}_{1,2} = -K m_1 m_2 \mathcal{F}(\|\vec{r}_1 - \vec{r}_2\|)\frac{(\vec{r}_1 - \vec{r}_2)}{\|\vec{r}_1 - \vec{r}_2\|}, \tag{2.2}$$

where $\mathcal{F}(\|\vec{r}_1 - \vec{r}_2\|)$ is a smooth scalar function of the distance. By taking into account the before mentioned Superposition Principle and the fact that a force $1/r^{\alpha}$ is linked with a potential $-1/(\alpha-1)r^{\alpha-1}$, let us suppose to have a system of N of those particles of mass μ_i, mutally interacting with law 2.1. The dynamics of such system is fully described in hamiltonian formalism by

$$\mu_i \frac{d\,\vec{r}_i}{dt} = \frac{\partial H}{\partial\,\vec{v}_i} \tag{2.3}$$

and

$$\mu_i \frac{d\,\vec{v}_i}{dt} = -\frac{\partial H}{\partial\,\vec{r}_i}, \tag{2.4}$$

where the N-body Hamiltonian function takes the usual form

$$H = \frac{1}{2}\sum_{i=1}^{N} \mu_i v_i^2 + K \sum_{i\neq j=1}^{N} \frac{m_i m_j}{(1-\alpha)\,\|\vec{r_i} - \vec{r_j}\|^{\alpha-1}}; \tag{2.5}$$

again it must be pointed out that the late expression works out only in the case of inverse power law force with inverse power law potential. Note that we symbolyze the gradient with $\partial/\partial\,\vec{r}$ with a little formalism abuse.
If we take a look on nature we can see that systems with long range interactions tend to give origin to coherent structures, for example stellar systems with Gravitation, Clusters in the HMF model and so on. Describing the dynamical evolution of such systems in Hamiltonian formalism (direct approach) is obviously incredibly complex, in the so called thermodynamic limit $N \to +\infty$ one can use a statistical approach based upon the concept of Distribution Function. Let us suppose that our N particles are displaced in an open subset of $\Re^3$, each one is still characterized by its mass μ, velocity $\vec{v_i}$, position $\vec{r_i}$ and charge. In this framework we can immagine our particles inside an $8N$-dimensional parameter space (the Γ-phase space) where we now define the N-body distribution function $P_N(r_1, v_1, \mu_1, m_1, ..., r_N, v_N, \mu_N, m_N)$ wich counts how many particles there are for cell of position, velocity, mass and charge. At this point, for reasons of simplicity, let us consider only particles of equal mass interacting via mass-depending $1/r^\alpha$ interactions so that μ_i=m_i=m, in such case the Γ-space becomes isomorphic to $\Re^{6N}$ and the hamiltonian is rewritten as

$$H = \frac{m}{2}\sum_{i=1}^{N} v_i^2 + Km^2 \sum_{i\neq j=1}^{N} \frac{1}{(1-\alpha)\,\|\vec{r_i} - \vec{r_j}\|^{\alpha-1}}. \tag{2.6}$$

If each particle moves smoothly from a cell to another the time evolution of P_N is governed by the Liouville equation

$$\frac{\partial P_N}{\partial t} + \sum_{i=1}^{N}\left(\vec{v_i}\cdot\frac{\partial P_N}{\partial\,\vec{r_i}} + \frac{\vec{F_i}}{m}\cdot\frac{\partial P_N}{\partial\,\vec{v_i}}\right) = 0 \tag{2.7}$$

that arises simply fron the continuity equation in $6N$-dimensional space. Here the force by unit of mass can be obtained defining a scalar field, the potential Φ due to the distribution of the masses in space $\rho(\vec{r})$, as

$$\frac{\vec{F_i}}{m} = -\frac{\partial\Phi}{\partial\,\vec{r_i}}. \tag{2.8}$$

The potential is related to density through a field equation wich is formaly written as

$$\mathcal{O}\phi = \psi\left[\rho(\vec{r})\right] \tag{2.9}$$

where $\mathcal{O}$ is a differential operator acting on ϕ and ψ is a smooth function of density. In the Gravitational case the last equation is the well known Poisson equation where $\mathcal{O}$ is simply the Laplacian operator and ψ is only the multiplicative constant $4\pi G$. Note that even in the simple $1/r^{\alpha}$ case we do not have an explicit form of that equation but only one of its solution

$$\phi(\vec{r}) = \frac{K}{\alpha - 1} \int \frac{\rho(\vec{r_*})}{\|\vec{r} - \vec{r_*}\|^{\alpha-1}} d\,\vec{r_*} \tag{2.10}$$

arising from the superposition principle. This formulation of our N-body problem is completely equivalent to the previous one but it focuses more on statistic aspects rather than exploring the dynamics of every single particle. In this spirt we now introduce the Statistical Equilibrium as the macroscopic configuration of the system for whom all the microscopic configurations in the Γ-space with a given value of total energy E are equiprobable. This means in other words that a particular state of the systems in the real-life space corresponds to one of a set of realizations in its parameter space, none of them having more weight than another. Here, nonetheless, we must point a caveat. What we have just stated relies upon the hypothesis of ergodicity (the time average of a macroscopic obsevable equals the average of the same quantity overe the all the phase space realizations of the system at given time t), but in chaotic systems there could be some regions of the Γ-space that are more probable than others, so the idea of equivalent realizations becomes quite unclear and thus, even the Statistical Equilibrium cannot be taken as a strict definition. This fact is named Ergodicity Breaking. We now write in a more explicit fashion the N-body distribution function at equilibrium as

$$P_N(\vec{r_1}, \vec{v_1}, ..., \vec{r_N}, \vec{v_N}) = \frac{1}{g(E)} \delta(E - H), \tag{2.11}$$

where the normalization[1] factor given by the density of micro-states of energy E is

$$g(E) = \int \delta(E - H) \prod_{i=1}^{N} d\,\vec{r_i}\, d\,\vec{v_i}\,. \tag{2.12}$$

Furtheron, if we want the reduced probability $P_j(\vec{r_j}, \vec{v_j}, ..., \vec{r_N}, \vec{v_N})$, this is simply

$$P_j(\vec{r_j}, \vec{v_j}, ..., \vec{r_N}, \vec{v_N}) = \int P_N \prod_{k=j}^{N} d\,\vec{r_k}\, d\,\vec{v_k}\,. \tag{2.13}$$

[1] As P_N is related to a probability we must impose that $\int_{\Re^{6N}} P_N \prod_i d\,\vec{r_i}\, d\,\vec{v_i} = 1$; in this sense we use the expression normalization factor.

In our case concerning identical particles we can define the one-body distribution function in μ-phase space isomorphic to $\Re^6$ from $P_1(\vec{r},\vec{v})$ as

$$f(\vec{r},\vec{v}) = \langle \sum_{i=1}^{N} m\delta(\vec{r}-\vec{r_i})\delta(\vec{v}-\vec{v_i})\rangle = NmP_1(\vec{r},\vec{v}) \tag{2.14}$$

where $\langle ... \rangle$ means average. With this definition the function $f(\vec{r},\vec{v})$ can be seen as the average density of particles in the six-dimensional μ-space. Note that $\partial\ \vec{v}\ /\partial t$ is simply the force per unit o mass. Again if we suppose that each particle moves smoothly from cell to cell inside the phase space we can state that the time evolution of f satisfies a continuity equation:

$$\frac{\partial f}{\partial t} = -\nabla\cdot(f\ \vec{v}) - \nabla_{\vec{v}}\cdot(f\frac{\partial\ \vec{v}}{\partial t}). \tag{2.15}$$

Considering that in the phase space $\vec{r}$ and $\vec{v}$ are just like independent varibles, by the means of simple vectorial identities the last equation becomes

$$\frac{\partial f}{\partial t} + \vec{v}\cdot\nabla f + \frac{\partial\ \vec{v}}{\partial t}\cdot\nabla_{\vec{v}} f = 0. \tag{2.16}$$

We have now written the so called collisionless Boltzmann equation wich has great importance for example in Stellar Dynamics. It must be pointed also that if we substitute $\partial\ \vec{v}\ /\partial t$ with the Lorentz Force by unit of mass we obtain the Vlasov equation, that is the analogous in the specific case of Plasma Physics. In this formalism studing the dynamical evolution of the system is studing the time evolution of the funciton $f(\vec{r},\vec{v},t)$. If one knows the field equation for the interaction it is possible to link f to the potential using the density $\rho(\vec{r})$; in general this is possible only formally, but for the gravitational/electromagnetic case where we have the Poisson equation we can explicitly write:

$$\nabla^2\phi(\vec{r},t) = -4\pi G\rho(\vec{r},t) = -4\pi Gm\int f(\vec{r},t)d\ \vec{v}\ . \tag{2.17}$$

In this case we say that the system is Vlasov-Poisson. One last quantity related to the distribution function that has to be defined is the velocity dispersion tensor σ^2_{ij}, by $i,j = 1,2,3$ we write:

$$\sigma^2_{ij}(\vec{r},t) = \frac{1}{\rho(\vec{r},t)}\int_{\Re^3}(v_i - \bar{v_i})(v_j - \bar{v_j})f d\ \vec{v} \tag{2.18}$$

where v_i and $\bar{v_i}$ are the components of the velocities and the average velocity. For certain special systems, those that are isothropic, the velocity dispersion tensor

can be written everywhere as $\sigma_{ij}^2 = \sigma^2 \delta_{ij}$, in this case the velocity dispersion of the particles is the same in every direction of space. At this point we have linked our N-body system to the time evolution of two functions in two higher dimensional spaces, let us define now before entering the discussion on relaxation a couple basic concepts arising from the thermodynamic limit (i.e. they are meaningful only in the case when N is virtualy infinite). The first is the microcanonical entropy, defined as

$$S(E) = k_B \ln g(E), \tag{2.19}$$

where k_B is the Boltzmann constant; taking the derivative of S in respect of the energy E we obtain the quantity $\beta(E)$ and then we can define the temperature as

$$T(E) = \frac{1}{k_B \beta(E)}. \tag{2.20}$$

Note that in a long range boudend self-gravitating sysems this definition leads to a negative temperature, this occours because the binding energies of the particles are defined negative while $S(E)$[2] is always increasing.

2.2 What do we mean by Relaxation?

We now give a brief review of relaxation in many-body dynamical systems. In the statistic approach we say that a system is relaxed when it reaches the Statistical Equilibrium. Consider again the N-body system with total energy E, Every particle has its own energy e_i written as the sum of individual kinetic energy k_i and potential energy u_i, the first is the usual $mv_i^2/2$ and the second is determined by the spatial distribution of the other particles plus eventualy the effect of an external potential (we will neglect for the moment the latter contribution). Stating that the individual energy of a particle is function only of velocity and of other particles positions we can treat f and thus P_N at each time as functions of the one particle energy e and particle energies e_i with $i = 1, N$. We introduce now another function that will be very important in the next chapters, the fractional energy distribution $n(E)$, defined in such a way that $n(E)dE$ counts how may particle are per interval of energy $E + dE$. This object looks also more simple to imagine. The relationship with $f(e)$(see for example [7]) is expressed as

$$n(E)dE = \int_\Omega f(e) d\,\vec{r}\; d\,\vec{v} \tag{2.21}$$

[2]One can define the entropy of the system also with f. In this case we have $S_L = -\int\int f \ln f d\,\vec{r}\; d\,\vec{v}$. Notice also that such quantities are named entropy but can not be expressed in the wisdom of classical thermodynamics as $\frac{\partial Q}{\partial T}$

where Ω is the region in μ-phase space where energy lies in the limit $(e, e+de)$. At this point, due to energy exchange between particles moving inside the collective potential ϕ, we must note that the form of $n(e)$ changes in time, for $t \to +\infty$ one can formaly reach the limit of $n(e)$ corresponding to the P_N of Statistical Equilibrium, this, due to the fact of particle being indistinguible can be obtained for an infinite number of phase-space assets. Under the assumpions of Statistical Mechanics[3] when a system has P_N at the statistical equilibrium the form of $n(e)$ is a Maxwell-Boltzmann distribution arising from the corresponding to the entropy maximizing f:

$$n(E) = n_0 \exp(-\frac{E}{k_B T}). \tag{2.22}$$

So now we can say that when in its macroscopic configuration the system has the total energy E parted between the particles with a Maxwell-Boltzmann $n(e)$ the system is relaxed and we call relaxation the set of collective and binary phenomena that lead to this configuration. It is now useful to give a brief description of some relaxation mechanisms.

2.2.1 Different forms of relaxation

First we have to distinguish between two forms of relaxation, say collisional and collisionless relaxation. The first case is due only to the contribution of two body interactions and dominates in systems with short-range interactions or where the granularity is much evident (i.e. few-body systems or screened-interaction systems); whilst the second happens when we have a strong mean field effect, a strongly variating collective potential or resonances betwen internal modes and collective oscillations. As the energy exchange is a matter of two body encounters, in many body systems, collisional relaxation has very long relaxation timescales, these are strongly dependent from the number of particles in the system, and can be written in general as

$$t_{CR} = g(\mathcal{F})h(N) \tag{2.23}$$

where with $g(\mathcal{F})$ we mind a function that contains the dependence from the form of the interaction, and with $h(N)$ a function of the number of particles N. Notice that the latter is not necessarely monotonically increasing, for example consider

[3] In the framework of classical Statistical Mechanics one must state that the one particle Hamiltonian can be written in the form $H_i = \frac{p_i^2}{2m_i} + H_{int}$ where H_{int} is the so called interaction Hamiltonian which is essentially impossible to be written explicitely and is *energetically* negligible in comparison with the other term. Following this wisdom we mean that H_{int} beheaves like a noise in redistributing energy between the modes (particles) of the system.

a system of a few particles, say 10, in this case is completely meaningless to define a relaxation time, the system will undergo indefinitely irregular oscillations never reaching a stationary state nor a quasi-stationary regime, on the other hand everyone will agree that intuitively t_{CR} is lagrer for a 10^9 particle system than for a 10^6 particle system. It has to mentioned that for the gravitational N-body problem, in Chandrasekhar's statistical theory of Stellar Dynamics (for the original theory consult [10], for an exhaustive review [44]), under certain assumptions one can define the two body relaxation time t_{2b} which is the time scale of relaxation given by the two body dynamical collision as

$$t_{2b} \simeq \frac{0.04N}{\ln(N)} t_{cross} \tag{2.24}$$

with t_{cross} being the characteristic crossing time of the system. For a derivation of t_{2b} for general weak long range interactions one can take a look at appendix A and references therein. Under the general name of Collisionless relaxation there are lots of different mechanisms leading to energy partitioning amognst whom there is a strong distintion. Some of them such as Violent Relaxation, Phase Mixing and Gravitational Landau damping, are related to variations of the self-consistent potential and can be all reconduced to the time evolution of the distribution function via the collisionless Boltzmann equation (for example see [28]) while the others need an external agent to perturb or contribute to the interaction field, so the system is no more considered as isolated, this make the story much different. In our discussion we deal mainly with systems interacting via self-consistent potental so we will momentanealy forget about the last subclass. We now give an intuitive idea of Phase Mixing and Violent relaxation. Consider for simplicity a one dimensional system were N particles move inside their potential; at $t = 0$ they are packed in a compact region of the $2d$ phase space, each one of them as it moves, perturbates the total potential and has contemporarely its trajectory perturbated by the time variating potential, this leads in phase space to a collective derive of phase points in a way that the original compact set is spread in regions where the phase points are dense in empty points. If a macroscopic observer computes at each time the coarse-grained entropy[4] $\bar{S}$ defined as

$$\bar{S} = -\int_{\Omega} \bar{f} \ln \bar{f} \, d\tau \tag{2.25}$$

[4]This quantity is related to the previous defined S, the two are equal in the case of Phase Mixing just a $t = 0$, at other times $\bar{S}$ is supposed to increase because as the coarse-grained diluites, the probability of finding a phase point in a certain region of μ space increases, so the integral entropy also gets bigger.

where $\bar{f}$ is the coarse-grained distribution function and $d\tau$ is the phase space element, he notices that it decreases as the phase point spread, in this sense as it goes towards a minimum entropy state Phase Mixing is to be considered a relaxation mechanism. In Violent Relaxation (Lynden-Bell 1967 [32]) we have that in a recently formed formed object the large scale gravitational potential is strongly variating, both spatialy and in time, this with the fact that inidvidual particle energy do not conservates leads to a rapid energy redistribution so here the point is that every single particle feels the effect of a global change in ϕ. This differs from Phase Mixing mainly because it is a rapid phenomena while the latter tooks longer time. Moreover a system relaxed via Violent Relaxation if it is observed at a finer scale looks still unrelaxed while at greater scales it could be seen as relaxed. In addiction they show an equilibrium distribution in the form

$$n(E) = \frac{n_0}{1 + \lambda \exp(E/k_B T)} \tag{2.26}$$

where $\lambda = e^{\gamma}$ is a parameter called fugacity connected to the lagrange multiplier γ. The reader familiar with Quantum Mechanics will note immediately the striking similarity with Fermi-Dirac statistic, in this our case this fourth type of statistics cames for a set of distinguishble particles with exclusion. The Lynden-Bell expression reduces to the Maxwell-Boltzmann in the limit $\lambda \exp(\phi/k_B T) \to +\infty$.

2.3 A short review of the Virial Theorem

It is useful now to discuss a little on the classical virial theorem. Although it is just a special moment (i.e. second order) of the equation of motion in the form

$$\rho \frac{dv_i}{dt} = -\frac{\partial P}{\partial x_i} + \frac{\rho F_i}{m} \tag{2.27}$$

which has been written by components and explicitating the pressure term P, this result will be used later and has some interesting applications in dynamical astronomy so we decided to spend some lines on it. For first let us define some time depending tensorial quantities for $i, j = 1, 2, 3$; we call inertia tensor

$$I_{ij}(t) = \int_{\Re^3} \rho x_i x_j d\,\vec{r} \tag{2.28}$$

by taking its track we obtain the total moment of inertia defined also by

$$I = \sum_{i=1}^{N} m_i \, \|\vec{r_i}\|^2, \tag{2.29}$$

the second tensor is the total kinetic energy tensor

$$K_{ij}(t) = \frac{1}{2}\int_{\Re^3} \rho\overline{v_i v_j} d\ \vec{r}, \tag{2.30}$$

the third is the pressure integral

$$\Pi\delta_{ij} = \int_{\Re^3} P d\ \vec{r}\ \delta_{ij} \tag{2.31}$$

that comes from the first positional momentum of equation 2.27 multiplied by x_j and integrated ove the total volume; then we introduce one last tensor, the potential energy tensor

$$W_{ij} = \frac{1}{2}\int_{\Re^3} \rho\phi_{ij} d\ \vec{r}, \tag{2.32}$$

in this case ϕ_{ij} referres only to the self consisten potential, in case of presence external forces another tensor is to be added, the external potentia energy tensor E_{ij} defined in the same way but with ϕ_{ext} in the place of ϕ. It can be demonstrated (see for example [8] or [44]), but here we omit the calculations that

$$\frac{1}{2}\frac{d^2 I_{ij}}{dt^2} = 2T_{ij} + W_{ij} + \Pi\delta_{ij} \tag{2.33}$$

this identity is known as the tensor virial theorem. Setting $i = j$ and contracting we obtain the scalar identity

$$\frac{1}{2}\frac{d^2 I}{dt^2} = 2T + W + 3\Pi \tag{2.34}$$

called the scalar virial theorem. One can see immediately the striking similarity with the Lagrange-Jacobi identity

$$\frac{d^2 I}{dt^2} = 2(2T + W) \tag{2.35}$$

where W is the total potential energy and that it is obtained instead directly from the equations of the N-body problem while the virial theorem comes from the collisionless continuum approach. Now when a system is in the steady state (say equilibrium configuration or relaxed state) $d^2 I/dt^2 = 0$ and pressure, gravitational collapse and bulk motions balance toghether so one obtains in the scalar form the identity which is commonly (and erroneusly) called virial theorem

$$2T = -W \tag{2.36}$$

where again W is the total potential energy. In the end we must define another quantity called the virial ratio as

$$q = \frac{2T}{|W|}. \tag{2.37}$$

q will oscillate around 1 during the system's relaxation process.

2.4 Astrophysical implications

Since many of the results that we have just mentioned here originate from dynamical astronomy we are going to spend some lines on the problems concerning the relaxation of dynamical systems in an astrophysical context. We focus on the fact that gravity is a long range force and so learning something about the properties of general long range theories can help us to better understand classical $1/r^2$ gravity. The main problem, and certainly the most famous, is how structures such as elliptical galaxies or galaxy clusters can look so relaxed while having relaxation time scales so long in comparison to their age. This, due to the fact that galaxies are essentialy collisionless systems, leads to theorize other mechanisms of relaxation which are different from the simple dynamical mixing with velocities exchanges, such as for example the mentioned before Violent relaxation. It must be also pointed out that Dark Matter haloes of both elliptical and spiral galaxies seem to be relaxed structures, and Dark Matter itself even if we do not know the nature of its components yet is a collisionless fluid and so collisionless mechanisms of relaxation must apply also to that case. Moreover it is interesting to mention for the elliptical galaxies the connection between surface brightness profiles $I(R)$ and their dynamical evolution. Many observative studies have shown that

$$I(R) = I_e \exp\left\{-b(m)\left[\left(\frac{R}{R_e}\right)^{1/m} - 1\right]\right\} \tag{2.38}$$

known as Sersic law [45], where R_e is a certain typical radius and I_e is the surface brightness at such radius while $b(m)$ and m are numerical fitting parameters linked by the relation $b(m) \sim 2m - 1/3 + 4/(405m)$. The observed galaxies present different values of m spanning form ~ 2 to ~ 6; It has been found that for the majorities of galaxies the value of m is about 4 so the surface brightness law is the de Vaucouleurs' law of 1948 [16]

$$I(R) = I_e \exp\left\{-7.67\left[\left(\frac{R}{R_e}\right)^{1/4} - 1\right]\right\}. \tag{2.39}$$

In this case it has been proved (see for example[7],[12]) that the fraction of the mass in the Boltzmannian regime is maximized. That is to say a greater part of the stars lie in the relaxed energy distribution. This important fact can be read as the more the parameter m approaches 4 the more the galaxy is close to the equilibrium (i.e. it is dynamically evolved). Another interesting fact that has to be mentioned is the correlation between mass segregation and relaxation. This is evident for example in galaxie clusters where the larges galaxies have less velocity dispersion and tend to accumulate at the center of the cluster while the

lighter ones have more velocity dispersion and are in the external part. In this case the situation is more complex because of the fact that galaxies are extended objects. But questions connected to the mass spectrum arise also in collisional stellar systems like the globular clusters. Here, due to the collisionality, relaxation via dynamical friction seems to be the most important. There are a lot of features concernig the dynamical evolution of globular clusters (for a general review see [46]). We must point out that from numerical simulations it was long ago clear [24] that the relaxation history of those objects is essentially divided into two phases: a violent phase of dynamical mixing and a long phase of gentle relaxation. The study of globular clusters is important because they are also subjected to environement driven evolution. Galactic globular cluster moving inside the galaxy's gravitational field and crossing it hundred of times during their lives suffer from phenomena like tidal shocks and compressions. This has lots of effects on the dynamics inside the globulars especially when internal pulsations are resonant with the external galctic triggering.

Unfortunatly we have to state that a final theory of relaxation of stellar and galactic systems is still missing. For example it is not known if some dynamical friction contributions are important even in collisionless systems. We do not know exactly if the Violent Relaxation really happens and how is efficent, we do not know why Boltzmann equilibrium arises also in those systems where one cannot realy say that the contributions of the interaction hamiltonian H_{int} are treatable as a noise (i.e. the Most Probable Distribution Principle holds). We do not have precise information on initial conditions of the cosmic structures so it is quite impossible to state how they really dynamically discriminant during the evolution and thus we are essentially relegated to perform numerical experiments.

To the present days many efforts have been made towards a general theory of relaxation. For example we now know [27] that Phase Mixing, Violent Relaxation and Landau Damping, as we have said before are just three different phases of the Boltzmann evolution equation for f and so they can bee seen as different moments of the same process and not as independent mechanisms. Violent Relaxation seems also to happen in non-neutral plasmas as found in [31]. This is a very important point because it relates such phenomena to the form of the interaction (both Gravity and Coulomb have in fact the $1/r^2$ trend) and not to the nature of the interaction (mass dependent force and charge dependent force), and because it is possible to compare theory and numerical simulations to laboratory experiments as the techniques in plasma physics have been rapidly increasing in the last years.

One last thing that has to be mentioned is the question with MOND or modified gravity. Although being very debated, such non linear theory is very interesting from a mathematical point of view and shows a lot of curious aspects even in relaxation's functioning.

We will develop some aspects of relaxation in MOND in Appendix B. Here we are

simply pointing out that MOND is an intensive theory, so that in the field equation there is a stronger dependence on field's intensity, it happens strangely that where the equivalent Newtonian field is weaker the MONDian field is more intense in proportion. So MOND is not precisely a long range theory in our sense (in fact even on the scale of very small masses the equivalent modified field dominates the Newtonian) but if one considers naively the asymptotic trend in the limit of far field the modified gravity could be treated as a $1/r$ long range interaction. It has been noticed that in this theory the collisionless mechanisms have longer timescales while the collisional contribution with dynamical friction seems to be more efficient than its Newtonian analogous.

20: white page

Chapter 3

A toy model for systems with long range forces

In this chapter we describe in detail the toy model of long range system that we have evolved numerically in our experiments, motivating our choices in matters of approximations and assumptions. First we explain the basic ideas then we show some examples and in the end we prepare the reader for a description of the code that will be presented in the next chapter.

3.1 The model

As stated before the main goal of this work is to understand by the means of analitic and numerical arguments the correlation between relaxation and form of the interaction in long range systems. In order to investigate numericaly this problem the idea is to perform a bunch of direct N-body experiments with different laws of force and to compare their evolutions towards equilibrium. the tools that we will use are essentialy the virial ratio $2K/W$ and the energy distribution $n(E)$. If the most probable distribution principle works also for generic long range interactions we expect that in the relaxed state such distribution has an exponential form that is barely reconducible to $\exp(-E/k_BT)$. At this point arises a big technical difficulty, as everyone knows in direct N-body simulations, even in the familiar Gravitation problem, the numerical complexity increases vertiginously with the number of particles used in the simulations. As we want to study the collective evolution of the whole system of many particles and the distribution function and so so we do not pay interest of singele orbits evolution, here we have the solution. Instead of using a direct code that tracks down each particle's evolution we will use an old idea by M. Hénon [23],[24], for the study of dynamical evolution in globular clusters. Let us suppose that we have our spherical system of N particles interacting with $1/r^\alpha$ force; consider in its μ-space a system of N^* shells each one containing particles having distance from the center of the cluster between r_i and $r_i + dr_i$, radial velocity between u_i and $u_i + du_i$ and tangential velocity between v_i and $v_i + dv_i$, at this point, sending to zero the of the shells we can define a sort of surfacial density

$$\sigma_i = \frac{mn_i}{4\pi r_i^2} \tag{3.1}$$

where n_i is the number of particles on the shell and m is their mass. Each shell ineracts with the others and with itself by the integral contribution of the particles on its surface. If we evolve the system of those shells during time will contract and expand following their dynamics in the μ-space. We now neglect the particles and study the system as a gas of spherical dust[1] shells, the symmetry of the system is the same but we have gained the fact that the degree of freedom is very lower now, we have recondcted the problem to a one dimensional. The equation of motion for the i-th shell are

$$\frac{dr_i}{dt} = u_i \tag{3.2}$$

[1]We say dust because the shells, being made of particles, are not solid entities so they can cross each other while expanding and collapsing.

and

$$\frac{du_i}{dt} = \frac{v_i^2}{r_i} - A_i^s - \sum_{j\neq i=1}^{N^*} A_j. \tag{3.3}$$

Here we write with A_i^s the self-force by unity of mass for each single shell and with $\sum_{j\neq i=1}^{N^*} A_j$ the contribution of the others. In our experimens we will neglect the contribution of the angular momentum v_i^2/r_i as v_i remains a constant an so it could be put equal to zero. With this cosmesis in our problem we now consider the reduced distribution $n^*(E)dE$ defined as the number of shells having energy between E and $E + dE$. If we suppose that in first approximation each shell contains the same number p of particles $n(E)$ and $n^*(E)$ are related by the simple relation

$$n(E) = pn^*(E). \tag{3.4}$$

As stated before with such assumptions we have now to study the evolution of a one dimensional[2] system, the numerical investigation of its properties are much easier now, as the numerical complexity has sensibily reduced. We now have to write and then to compute the expression for the acceleration produced by a shell of particles interacting via generic long range force. To do this we will follow the classical wisdom to compute the gravitational field of a thin shell of matter, and then we will use the result to write the interaction between the dust shells in our model.

3.2 The field produced by a shell

On the way to build a consistent model of shell collapse we have to write firstly a general expression for the field produced by a single shell of uniform surface density; note that we are assuming the nature of the interaction to be central. In this sections after extracting the general expression for the field due to a single shell we will write the self-force of the shell. Furthermore we will show some examples with Newtonian gravity and various $1/r^\alpha$ laws; the latter will be central in our study. Then we will write and integrate analiticaly the differential equation for the evolution of a single collapsing shell in some of those cases; this will be a strong test for the numerical experiments with an ensemble of mutual interacting shells that will be latter constructed. As we are going to show, in general, the i-th shell S_i undergoes the combined effect of selfgravity and the contribution of the others,

[2]Shells have only one spatial degree of freedom, their radius r_i

internal and external such that the field acting on it is:

$$\vec{F}_i^T = \sum_{j\neq i=1}^{N^*} \vec{F}_{ji} + \vec{F}_i^s \tag{3.5}$$

where $\vec{F}_i^s$ is the self-force. Note that if the field is Newtonian the contribution of the external shells vanishes in virtue of the second Newton's theorem and so the summation in the first addendum goes from 1 to $i-1$.

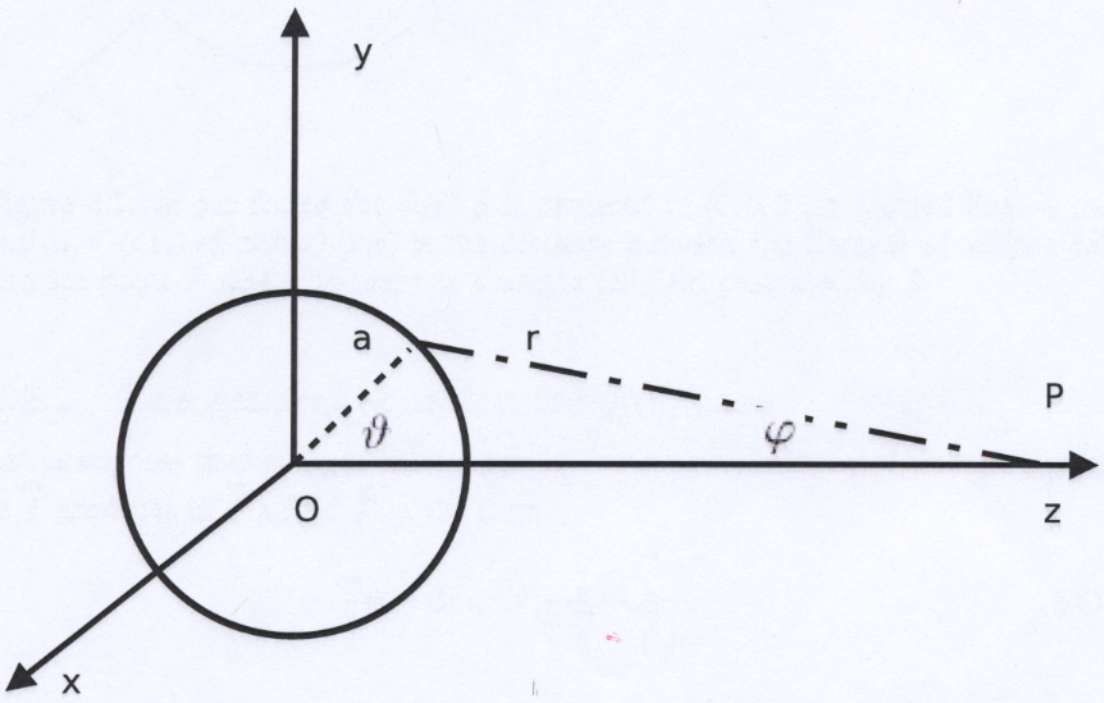

Figure 3.1: In our frame the shell S is centered in $(0,0,0)$, a (dotted line) is its radius, r (dashed-dotted line) is the distance between the element of surface dS and the point P where we want to evaluate the field generated by S.

3.2.1 The general equation for $\mathcal{F}(r)$ case

Let us suppose that in a generalized gravity law a pointlike body of mass m placed in $\vec{\xi}$ produces in $\vec{\zeta}$ a field $\vec{F}$ in the form

$$\vec{F} = -Km\mathcal{F}(r)\frac{\vec{\xi}-\vec{\zeta}}{\|\vec{\xi}-\vec{\zeta}\|}, \tag{3.6}$$

where K is a dimensional constant and $\mathcal{F}(r)$ is a smooth function of the distance $r = || \vec{\xi} - \vec{\zeta} ||$. For simplicity and for the fact that we are working only with radial fields, hereafter we will neglect the vector arrows. Consider now a shell S of uniform surface density σ and radius a, in a Cartesian frame where the origin coincides with its center, and a point P on the z axis of coordinates $(0, 0, z)$. Without loss of generality we can fix the point at which the gravitational field is to be evaluated at P; here the field due to an element of surface dS is, (see figure 3.1):

$$dF_z = -Kdm\mathcal{F}(r)\cos\varphi \tag{3.7}$$

where r is the distance between P and dS, $dm = 4\pi\sigma a^2 d\varphi \sin\vartheta d\vartheta$ and $\cos\varphi = (z - a\cos\vartheta)/r$. In order to evaluate the total field F_z in $(0, 0, z)$ we have to perform an integration over S:

$$F_z = -K\sigma a^2 \int_S \frac{(z - a\cos\vartheta)\mathcal{F}(r)dS}{r}. \tag{3.8}$$

Referring again to figure 2.1, by the means of trivial trigonometric relations we set $r = (a^2 + z^2 - 2az\cos\vartheta)^{1/2}$ and $dS = a^2 d\varphi \sin\vartheta d\vartheta$, so the integral becomes:

$$F_z = -K\sigma a^2 \int_0^{\pi}\int_0^{2\pi} \frac{(z - a\cos\vartheta)\mathcal{F}(r)d\varphi\sin\vartheta d\vartheta}{(a^2 + z^2 - 2az\cos\vartheta)^{1/2}}, \tag{3.9}$$

then the integration in $d\varphi$ gives

$$F_z = -2K\pi\sigma a^2 \int_0^{\pi} \frac{(z - a\cos\vartheta)\mathcal{F}(r)\sin\vartheta d\vartheta}{(a^2 + z^2 - 2az\cos\vartheta)^{1/2}}. \tag{3.10}$$

If we perform the change of variable $cos\vartheta = t$ and we use the definition of surfacial density $\sigma = m/4\pi a^2$, we obtain:

$$F_z = \frac{-Km}{2} \int_{-1}^{1} \frac{(z - at)\mathcal{F}(r)dt}{(a^2 + z^2 - 2azt)^{1/2}}. \tag{3.11}$$

At This point before giving some explict examples we give an expression for the self-field of an isolated collapsing shell. Let us consider in this scenario a shell of radius a collapsing under its self-gravity. Essentialy the differential equation for the time evolution of a is in the form

$$\frac{d^2a}{dt^2} = F_z(a) \tag{3.12}$$

where $F_z(a)$ is the gravitational acceleration field calculated $z = a$, the usual way to separate that kind of equation is an energy methot, we multiply by da/dt in order to obtain:

$$\frac{da}{dt}\frac{d^2a}{dt^2} = F_z(a)\frac{da}{dt}; \tag{3.13}$$

note that

$$\frac{1}{2}\frac{d}{dt}\left(\frac{da}{dt}\right)^2 = \frac{da}{dt}\frac{d^2a}{dt^2} \tag{3.14}$$

thus

$$\frac{1}{2}\frac{d}{dt}\left(\frac{da}{dt}\right)^2 = F_z(a)\frac{da}{dt}. \tag{3.15}$$

Eliminating dt on both sides and integrating one has:

$$\frac{\dot{a}^2}{2} = \int F_z(a)da \tag{3.16}$$

where the dot as usual represents the time derivative. At this point we can extract the square root and separate the resulting expression obtaining

$$\frac{da}{\sqrt{\int F_z(a)da}} = dt \tag{3.17}$$

that we will finally integrate in different cases.

3.3 Examples

We will now treat the case where $\mathcal{F}(r)$ is a simple inverse power law as it will be central in our discussion, but for first we start with two known special cases and then we will generalize it to the $1/r^\alpha$ form. The first is the well explored Newtonian gravity, with power law force and power law potential, and the second is the $1/r$ force with logaritmic potential wich occours for example in the dynamics of charged wires in a plane.

3.3.1 Classical Gravity: The Newton's theorems

By substituting $\mathcal{F}(r)$ with the usual newtonian $1/r^2$ force and taking $K = G$ we can get for example the analytic proof of the two first Newton's theorems. The integral expression for the field becomes:

$$F_z = -\frac{Gm}{2}\int_{-1}^{1}\frac{(z-at)dt}{(a^2+z^2-2azt)^{3/2}}, \tag{3.18}$$

if we set $2azt = x$ and $a^2 + z^2 = A^2$ and we integrate the resulting expression

$$-\frac{Gm}{8az^2}\int_{-2az}^{2az}\frac{(2z^2 - x)dx}{(A^2 - x)^{3/2}} \tag{3.19}$$

over x we obtain:

$$F_z = -\frac{Gm}{z^2}, \tag{3.20}$$

for $z \geq a$ and

$$F_z = 0 \tag{3.21}$$

for $0 \leq z < a$. The reader will immediately recognize the two results due to Newton stating that, a shell of uniform surfacial density produces on the exterior a field as if its mass were concentrated at its center, and that it has null field in the interior. The reader can find the full calculations for this case in the superb textbook by Kellogg on potential theory [30]. In a system of N^* concentric shells these last results in imply that the i-th shell is subjected only on the contributiuon of the interior ones and on its autogravity. As we will see in the next sections this is no more true if the force is not the familiar $1/r^2$. In those latter cases as we have stated before, also the external shells act a force on the internal ones.

3.3.2 The $1/r$ case

In order to obtain this latter case we have to substitute $\mathcal{F}(r)$ with $1/(a^2 + z^2 - 2azt)^{1/2}$ in equation 3.6 , we have now to integrate

$$F_z = -2K\pi\sigma a^2\int_{-1}^{1}\frac{(z - at)dt}{a^2 + z^2 - 2azt}, \tag{3.22}$$

setting $x = 2azt$ this becomes:

$$\begin{aligned} F_z &= -\frac{2K\pi\sigma a^2}{2az}\int_{-2az}^{2az}\frac{(z - \frac{x}{2z})dx}{a^2 + z^2 - x} \\ &= -\frac{K\pi\sigma a}{2z^2}\int_{-2az}^{2az}\frac{(2z^2 - x)dx}{a^2 + z^2 - x}, \end{aligned} \tag{3.23}$$

now by adding and subtracting z^2 in the integrand denominator we can pose $y = 2z^2 - x$ and thus the last equation now equals to

$$-\frac{K\pi\sigma a}{2z^2}\int_{-2az+2z^2}^{2az+2z^2}\frac{ydy}{a^2 - z^2 + y}, \tag{3.24}$$

then, labeling $B^2 = a^2 - z^2$, by the change $\xi = y + B^2$ and some basic algebric manipulations we can write

$$\begin{aligned} F_z &= -\frac{K\pi\sigma a}{2z^2}\int_{-B^2-2az+2z^2}^{-B^2+2az+2z^2}\frac{(\xi - B^2)d\xi}{\xi} \\ &= -\frac{K\pi\sigma a}{2z^2}\int_{-B^2-2az+2z^2}^{-B^2+2az+2z^2} d\xi + \frac{K\pi\sigma a}{2z^2}\int_{-B^2-2az+2z^2}^{-B^2+2az+2z^2}\frac{B^2}{\xi}d\xi. \end{aligned} \tag{3.25}$$

at this point if we perform separately the integration of the two members of the r.h.s. and we insert the expression for σ we obtain:

$$F_z = -\frac{Km}{8az^2}\xi\,|_{-B^2-2az+2z^2}^{-B^2+2az+2z^2} + \frac{KB^2m}{8az^2}\log\xi\,|_{-B^2-2az+2z^2}^{-B^2+2az+2z^2} \tag{3.26}$$

and finaly explicitating we have

$$F_z = -\frac{Km}{2z} + \frac{KB^2m}{8az^2}\log\left(\frac{2az - B^2 + 2z^2}{-B^2 - 2az + 2z^2}\right). \tag{3.27}$$

It must be stated out as we will see in appendix B that the $1/r$ form is also fitting with the asymptotic beheviour of weak field in Milgrom's Modified Dynamics; in this theory where the field equation for the Gravitation is non linear, the intensity of field produced by a pointlike mass m when is sensibly lower than a certain constant (for example this may happen at very large radius[3]) is approximatively

$$F = -\frac{\sqrt{Gma_0}}{r} \tag{3.28}$$

where a_0 is the Milgrom's scale acceleration, r is the distance from the source and G the familiar gravitational constant. Let us pose $K = \sqrt{Ga_0/m}$ in order to write this equation in a form analogous to equation 3.6, this in an action derived theory could be interpreted as a mass dependence of the coupling constant; in our simple treatment, which does not concerns the real MOND, we neglect that annoying problem simply stating that the mass is also a constant.

3.4 The $1/r^\alpha$ force

After those two examples we can go back to the general case and write its expression. By replacing in equation 3.11 $\mathcal{F}(r)$ with $1/r^\alpha$ we have to integrate

$$F_z = -\frac{Km}{2}\int_{-1}^{1}\frac{(z - at)dt}{(a^2 + z^2 - 2azt)^{\frac{\alpha+1}{2}}}. \tag{3.29}$$

[3]Also for very small masses it is the same, remind that the MOND is not a metric theory as we will see in the appendix.

It is useful to separate the last integral in order to carry on separately two simpler integrations, so now we deal with:

$$F_z = \frac{Km}{2}\int_{-1}^{1}\frac{atdt}{(a^2+z^2-2azt)^{\frac{\alpha+1}{2}}} - \frac{Km}{2}\int_{-1}^{1}\frac{zdt}{(a^2+z^2-2azt)^{\frac{\alpha+1}{2}}}, \tag{3.30}$$

multiplying and dividing the first member of the rhs by $2z$ and using the changing $2azt = x$ the last expression equals to:

$$+\frac{Km}{8az^2}\int_{-2az}^{2az}\frac{xdx}{(a^2+z^2-x)^{\frac{\alpha+1}{2}}} - \frac{Km}{4a}\int_{-2az}^{2az}\frac{dx}{(a^2+z^2-x)^{\frac{\alpha+1}{2}}}, \tag{3.31}$$

which can be solved integrating by parts the first member and integrating the second as a simple inverse power law, thus:

$$\begin{aligned} F_z &= -\frac{2Kmx(a^2+z^2-x)^{\frac{1-\alpha}{2}}}{(1-\alpha)8az^2}\Big|_{-2az}^{2az} \\ &+ \frac{2Km}{(1-\alpha)8az^2}\int_{-2az}^{2az}(a^2+z^2-x)^{\frac{1-\alpha}{2}}dx \\ &+ \frac{2Km}{(1-\alpha)4a}(a^2+z^2-x)^{\frac{1-\alpha}{2}}\Big|_{-2az}^{2az} \end{aligned} \tag{3.32}$$

and then

$$\begin{aligned} F_z &= -\frac{2Kmx(a^2+z^2-x)^{\frac{1-\alpha}{2}}}{(1-\alpha)8az^2}\Big|_{-2az}^{2az} \\ &- \frac{Km}{2az^2(3-\alpha)(1-\alpha)}(a^2+z^2-x)^{\frac{3-\alpha}{2}}\Big|_{-2az}^{2az} \\ &+ \frac{2Km}{(1-\alpha)4a}(a^2+z^2-x)^{\frac{1-\alpha}{2}}\Big|_{-2az}^{2az} \end{aligned} \tag{3.33}$$

It must be stated now that the parameter α should be also different from 3 in order to avoid divergences. Expliciting the integration, we obtain this expression for the field:

$$\begin{aligned} F_z &= \frac{Km(a+z)\left[(a^2+z^2-2az)^{\frac{1-\alpha}{2}} + (a^2+z^2+2az)^{\frac{1-\alpha}{2}}\right]}{2az(1-\alpha)} \\ &- \frac{Km\left[(a^2+z^2-2az)^{\frac{3-\alpha}{2}} + (a^2+z^2+2az)^{\frac{3-\alpha}{2}}\right]}{2az^2(3-\alpha)(1-\alpha)}; \end{aligned} \tag{3.34}$$

in this case it can be seen that if $z < a$ in general $F_z \neq 0$. In such class of models we are allowed to adapt the range of F with different choices of the α parameter. Note that if $\alpha = 1$ or $\alpha = 3$ the latter expression diverges, so in our we will consider only α exponents inside the open interval $(1;3)$.

3.5 The collapse of a shell under self-gravity

In the next subsections we write and integrate the differential equations for a single collapsing shell to obtain an expression for the free fall time. This is the only case wher the equations of motion are analiticaly integrable even in the general power law case. For first, again, we analyze the Newtonian case and then the general power law model with α strictly included between 1 and 3. Here we exclude from the discussion the $1/r$ example as it has to be analyzed separately having logaritmic potential and not being obtained by equation 3.34. In the next chapter where we will describe in detail the numerical model we will use as a test the following results by comparing them to the results of single shell experiments. The self-field for a thin shell is well studied in the $1/r^2$ Coulombian case and can be found in every textbook on classical Electrodynamics, see for example [17] or [26]. Essentialy one has to extract the limit $z \to a$ in equation 3.34 and equate the result to the second time derivative of the radius a to obtain the differential equation for the shell collapse.

3.5.1 Single shell collapse in Newton's gravity

In this case the differential equation describing the time evolution for a, is simply:

$$\frac{d^2a}{dt^2} = -\frac{Gm}{2a^2}. \tag{3.35}$$

. This second order differential equation, is best solved starting with an energy method. We multiply the two sides by da/dt obtaining

$$\frac{da}{dt}\frac{d^2a}{dt^2} = -\frac{Gm}{2a^2}\frac{da}{dt}, \tag{3.36}$$

at this point, using rearranging it and eliminating on both sides dt, we get:

$$d(\frac{\dot{a}^2}{2}) = -\frac{Gm}{2a^2}da. \tag{3.37}$$

If we perform the integration on the l.h.s. and the r.h.s. we can now write

$$\frac{\dot{a}^2}{2} = \frac{Gm}{2a} + E_0, \tag{3.38}$$

where the constant E_0 represents the initial (conserved) energy by unity of mass. If we take the square root we now deal with:

$$\dot{a} = \sqrt{2E_0 + \frac{Gm}{a}}, \tag{3.39}$$

in order to solve it we carry on by separation obtaining:

$$\frac{da}{\sqrt{2E_0 + \frac{Gm}{a}}} = dt. \tag{3.40}$$

Let us consider the integration between the initial radius a_0 and the generic radius $\tilde{a}$, so

$$t = \int_{a_0}^{\tilde{a}} \frac{da}{\sqrt{\frac{Gm}{a} - \frac{Gm}{a_0}}}, \tag{3.41}$$

by mulitping and dividing by $a_0^{1/2}$, with the substitution $\theta^2 = a_0/a$ this becomes

$$t = -2a_0\sqrt{\frac{a_0}{Gm}} \int_{\sqrt{a_0/a}}^{1} \frac{d\theta}{\theta\sqrt{\theta^2 - 1}} \tag{3.42}$$

that can be easily integrated as an arcosecant. Turning back to our original variable we have:

$$t = 2a_0\sqrt{\frac{a_0}{Gm}} arcsec\left(\sqrt{\frac{a_0}{a}}\right)|_{a_0}^{\tilde{a}} \tag{3.43}$$

3.5.2 Single shell collapse under general $1/r^{\alpha}$ law

Following what we have done for the Newtonian gravity we consider the limit $z \to a$ in equation 3.34 and then we equate it to equation 3.12 obtainig

$$\begin{aligned} \frac{d^2a}{dt^2} &= \frac{Km}{2a(1-\alpha)}\left[\frac{(4a^2)^{\frac{3-\alpha}{2}} - 2a^2(3-\alpha)(4a^2)^{\frac{1-\alpha}{2}}}{2a^2(3-\alpha)}\right] \\ &= -\frac{2Km}{(2a)^{\alpha}(3-\alpha)}, \end{aligned} \tag{3.44}$$

note that if $K = G$ and $\alpha = 2$ we return to the the Newtonian gravity analyzed before. According to the standard procedure used in the previous section we carry on the separation and thus

$$t = \int \frac{da}{\sqrt{\frac{4Kma^{1-\alpha}}{2^{\alpha}(1-\alpha)(3-\alpha)} + 2E_0}}. \tag{3.45}$$

By substituting $4Mm/2^{\alpha}(1-\alpha)(3-\alpha)$ with C and considering the shell at rest at a_0 we have now to evaluate

$$t = -\int_{a_0}^{\tilde{a}} \frac{da}{\sqrt{-|C|a^{1-\alpha} + |C|a_0^{1-\alpha}}}, \tag{3.46}$$

if we set $a/a_0 = \xi$ and we change sign to the integration we get

$$t = \frac{a_0^{\frac{\alpha-1}{2}}}{\sqrt{|C|}} \int_{\widetilde{a}/a_0}^{1} \frac{d\xi}{\sqrt{1-\xi}}, \tag{3.47}$$

further on, by posing $\xi^{1-\alpha} = Y$ we arrive to

$$t = \frac{a_0^{\frac{\alpha-1}{2}}}{(\alpha-1)\sqrt{|C|}} \int_{(\widetilde{a}/a_0)^{\frac{1}{1-\alpha}}}^{1} Y^{\frac{2-\alpha}{1-\alpha}} (1-Y)^{-\frac{1}{2}} dY \tag{3.48}$$

that may be expressed in terms of Euler's Beta-functions in q and p setting $q = 1/2$ and $p = (3-2\alpha)/(1-\alpha)$ in such a way that:

$$t = \frac{a_0^{\frac{\alpha-1}{2}}}{(\alpha-1)\sqrt{|C|}} \int_{s}^{1} Y^{p-1}(1-Y)^{q-1} dY \tag{3.49}$$

where $s = (\widetilde{a}\ /a_0)^{1/1-\alpha}$. At this point with the shift $\theta = Y - 1$ we can write

$$t = -\frac{a_0^{\frac{\alpha-1}{2}}}{(\alpha-1)\sqrt{|C|}} \int_{s-1}^{0} \theta^{q-1}(1-\theta)^{p-1} d\theta \tag{3.50}$$

that is, reverting the extremes of integration, an incomplete Beta-function, so finaly we have:

$$t = \frac{a_0^{\frac{\alpha-1}{2}}}{(\alpha-1)\sqrt{|C|}} B_{s-1}\left(\frac{1}{2}, p\right). \tag{3.51}$$

To evaluate Euler's function one can consult for example [4] and references therein, or do it numericaly with the efficent algorithms proposed in [41].

Chapter 4

The numerical model

In this chapter we describe and explain the numerical code that we have developed for our experiments. Then we pay some attention on the first experiments made to test it, and finally we deal with the simulations made with different long range forces with their results.

4.1 The code

We start this discussion with the description of the code that we have developed and used during this thesis. The numerical model of the problem presented in the previous chapter essentialy implements the system of equations 3.5 with different forms of the interaction and solves it in time with a direct summation algorithm. We decided to keep the implementation of the algorithms as simle as possible in the wisdom that the more essential is the treatment, the more reasonable are the results. Although this initial need for simplicity in the code it is possible to change a large set of parameters and features apart from the form of the interaction; for example: the number of shells n^*, the coupling constant, the total mass M, the mass spectrum for the shells, the initial phase space disposition and the presence or not of angular momentum. In our experiments we have managed mainly with radial collapses neglecting the rotation, but analyzing for example how the radial orbital instability is important in the different force models would be an interesting topic for further studies. The structure of the code (developed in FORTRAN 90) itself is thought as linear as possible, There is a main where the parameters and the initial conditions are set while the integration, the calculations of the force and the potential, the final velocity distributions, the mass profile $m(R)$ and the random numbers generators are carried in separated routines that can be substituted by the need, leaving unaltered the general structure. The quantities of interest such as the total kinetic energy, K, the virial ratio $2K/|W|$ and the second derivative of the inertia momentum $\ddot{I}$ are saved on files during the integration in order to be plotted at the end. No plotting routine was implemented as the files come in a format that can be easely processed by every simple plotting program like Smongo or GNUplot. For the integration of particle's equations of motion various numerical schemes have been tested

- first order Euler algorithm;
- second order Euler algorithm;
- first order leapfrog;
- second order leapfrog;
- second order Runge-Kutta;
- fourth order Runge-Kutta.

For a specific review of them, one can refer for example to [41] (general) or [1] (with specific interest to the astrophysical case). By the means of some tests with the well known Newtonian force we have opted for the second order leapfrog

scheme with fixed timestep Δt which combines CPU time efficency with acceptable energy conservation over long integration times. The scheme solves the couple of differential equations for each shell iterating in time

$$v_i(t_0 + \Delta t) = v_i(t_0) + F_i \Delta t; \tag{4.1}$$

and

$$r_i(t_0 + \Delta t/2) = r_i(t_0) + 0.5\Delta t^2 F_i + v_i(t_0 + \Delta t/2) \tag{4.2}$$

Where F_i is intendet to be a force by unity of mass (acceleration). One must at need use other algorithms by simply replacing the integration routine with another containing the wanted scheme and with a few minor changes inside the main. It is now useful to say something about the force regularization as this is a tedious problem that affects all the dynamical numerical simulations. For the flow charts of the code one can look at the end of this chapter while for listing it has been reprinted in appendix C.

4.1.1 The choice of the softening lenght

Due to their mathematical singularity for $r \to 0$ weak long range power law interactions give a serious difficulty in direct numerical computations. When the distance between two particles is zero the force and thus the acceleration diverges and so the numerical integration breaks down; in addiction also the problem of the computers ability in representing the real numbers gives other problems; while approaching the singularity the force's estimate becomes worst and its value diverges faster than in the reality. In Newtonian direct N-body simulations one usually introduces a force softening that modifies the Newton's law at short scales [15] from

$$\vec{F}_{ij}^{real} = G m_i m_j \frac{\vec{r}_j - \vec{r}_i}{\|\vec{r}_j - \vec{r}_i\|^3} \tag{4.3}$$

to

$$\vec{F}_{ij}^{soft} = G m_i m_j \frac{\vec{r}_j - \vec{r}_i}{(\|\vec{r}_j - \vec{r}_i\|^2 + \epsilon^2)^{3/2}} \tag{4.4}$$

where ϵ is the softening lenght and it is not rigorousely defined but it is just adapted to the code where it is introduced. In a work of 1996 by Merritt [33] it has been derived an algorithm for the best ϵ choice and in a subsequent paper of 2004 by Rodionov and Sotnikova [43] the algorithm has been extended to the

choice of the optimal timestep Δt combined with ϵ. For a given distribution of N masses Merritt defined the average square error on the force as

$$ASE = \frac{1}{N}\sum_{i=1}^{N} |F_i^{soft} - F_i^{true}|^2, \tag{4.5}$$

if one assumes a given density function $\rho(\vec{r})$ he can define also its continuous analogous, the integrated square error

$$ISE = \int \rho(\vec{r})|F(\vec{r_i})^{soft} - F(\vec{r_i})^{true}|^2 d\ \vec{r} \tag{4.6}$$

By generating a certain number m of Monte Carlo realizations of the same system, he defined one more quantity, the expectation value of the ISE called the mean integrated square error that is expressed by

$$MISE = \langle ISE \rangle_m = \langle \int \rho(\vec{r})|F(\vec{r_i})^{soft} - F(\vec{r_i})^{true}|^2 d\ \vec{r} \rangle_m \tag{4.7}$$

where $\langle ... \rangle_m$ is the mean over the Monte Carlo ensemble. In Merritt's idea the optimal ϵ is defined as the one that minimizes the $MISE$. It has been proved empiricaly that with this algorithm, for a Plummer sphere distribution the optimal softening lenght ϵ_m is related to the number of particles[1] N by

$$\epsilon_m \sim 0.58 N^{-0.26} \tag{4.8}$$

having used virial units with $G = M_{tot} = 1$ and $E_{tot} = -1/4$. In our code which is using shell we have two moints where equation 3.5 becomes singular: when two shells cross each other and when a shell crosses itself in the origin. So one has to take care of what happens to the self force when the radius of a shell goes to zero and what happens to the force between two shells when the two cross. The last is not a problem in Newtonian gravity because the force is not depending from the distance of the surfaces of the two shells but only on the radius of the external one but arises when one considers a different force where this contribution is important while the other is crucial in both cases. To efficently soften the force we have implemented numericaly in a separated code Merritt's algorithm to find ϵ_m by minimizing the mean integral square error, using the ASE instead of the ISE as we are working with a discrete spherical density profile. This second program substantialy generated different realizations of the system under study, calculated a discrete version of the $MISE$ and then by a procedure of interpolation

[1] The next formula has been shown to be valid by Athanassoula et al. (1998) [3] only for N between 30 and 3×10^5.

extracted the optimal softening lenght. The procedure was repeated for all the different $1/r^{\alpha}$ interactions that we have studied giving an average value of 0.098 for the softening parameter for a system of 2×10^3 interacting via $1/r^{\alpha}$ law with α between 1.1 and 2.6 and having radius $R = 5$ in normalized unities. it must be specified that the value that we have found numericaly is consistent with the value obtained empiricaly doing different tests until the divergences were eliminated while the energy remained sufficently constant apart from uneliminable numerical fluctuations during the integration. Another thing that has to be mentioned is that we have verified that for Newtonian force the relation 4.8 holds still for the shell model[2] with virial units unless the coefficent may not be precisely 0.58 but some other constant of the same order of magnitude.

4.2 The tests

As the main idea behind the numerical part of this work arises from the studies of Hénon ([23] and [24]) on dynamical evolution of globular cluster, one the first testing experiment that we managed was to try reproduce his results with our own code, the other, more simple is to verify in Newtonian gravity the consistence of the numerical results for a single shell collapse (i.e. computing the free fall time t_{ff}) with the solution of equation 3.43 when $t = t_{ff}$, that is the only case where the analytic solution is possible and well known.

4.2.1 Reproducing Hénon's experiments

In this test we have performed a set of experiments that were essentialy similar to the ones performed by M. Hénon in 1964; for first we have evolved for $54t_{dyn}$ systems of 12 shells, 50 shells, 100 shells as in [24] but with cold initial conditions and no angular momentum; we have verified that the trends with the number of shells for $K_{total}(t)$ and $W_{total}(t)$ are essentialy the same as in the original work. We have also computed and plotted with time the virial ratio and $\ddot{I}$, observing that in agreement with the previsions, the lesser is the number of shells the more it takes to dump the oscillations around 1 and 0 of the two quantities. It must be said also that due to the discreteness of the mass profile of the system ,with a low number of shells (say $N < 500$) the time series of every quantity look more noisy. In the next pages there are the results for these experimens reproduced with our code.

[2]Keep in mind that here we are working with shells and not with test particles so the systems are 1-dimensonal.

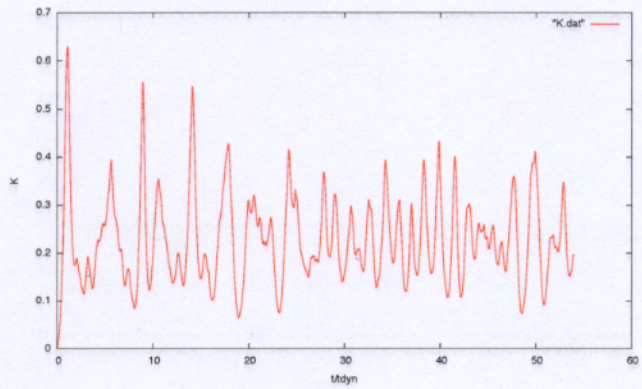

(a)

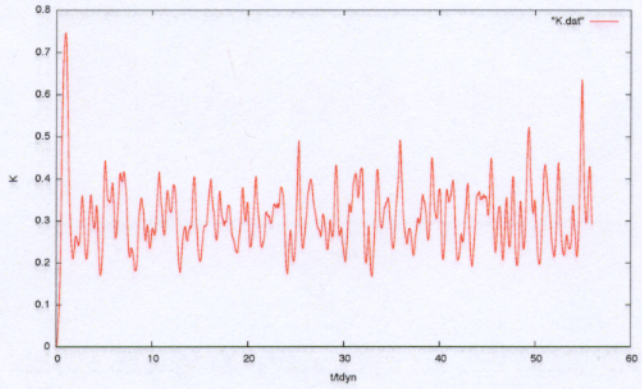

(b)

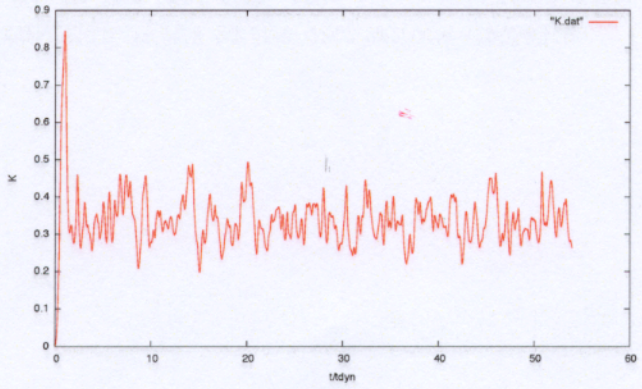

(c)

Figure 4.1: Total kinetic energy for systems (from top panel to lower panel) of 12, 50 and 100 shells. The noiseness here seems to increase with the number of shells but this is due only to the fact that also the encounters increase with N^*. See infact that the amplitude of the of the oscillations decreses.

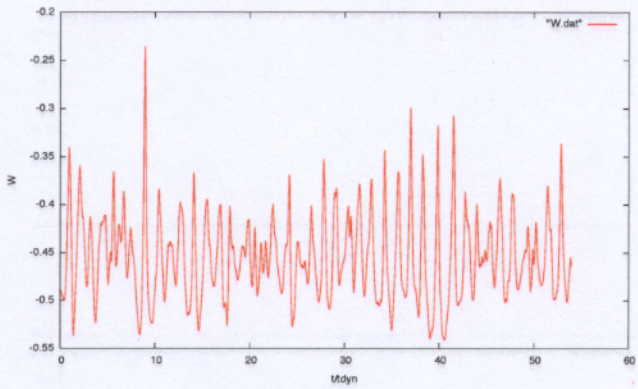

(a)

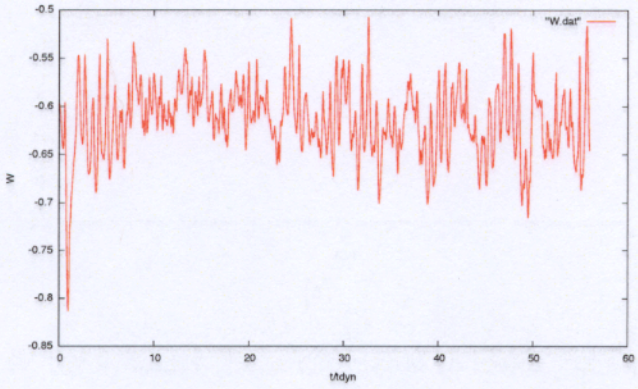

(b)

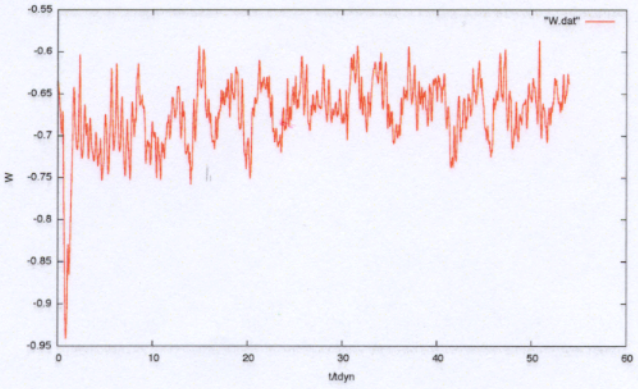

(c)

Figure 4.2: Total W for systems (from top panel to lower panel) of 12, 50 and 100 shells.

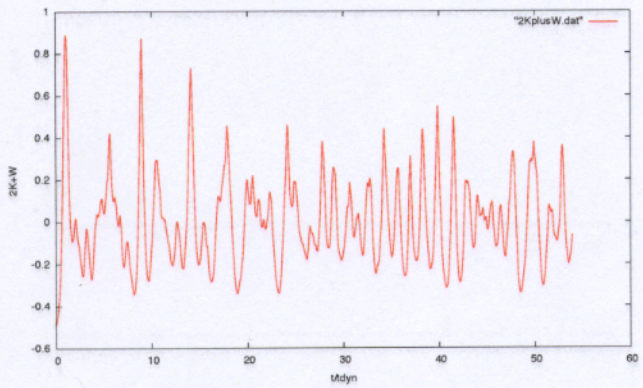

(a)

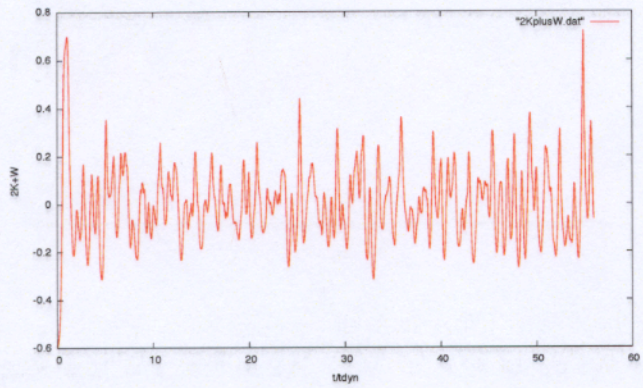

(b)

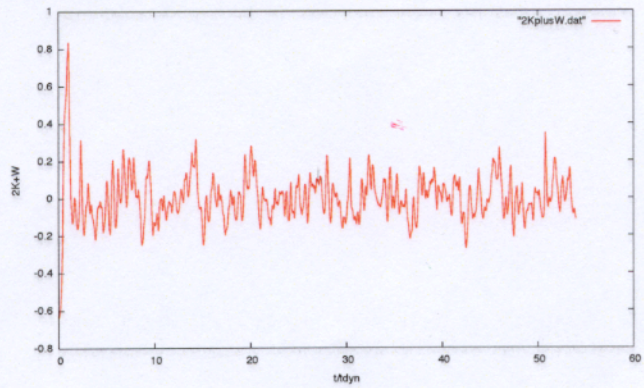

(c)

Figure 4.3: $d^2I/dt^2 = 2K + W$ for the same systems.

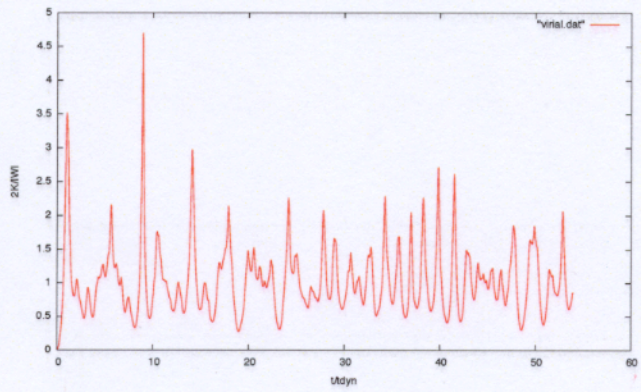

(a)

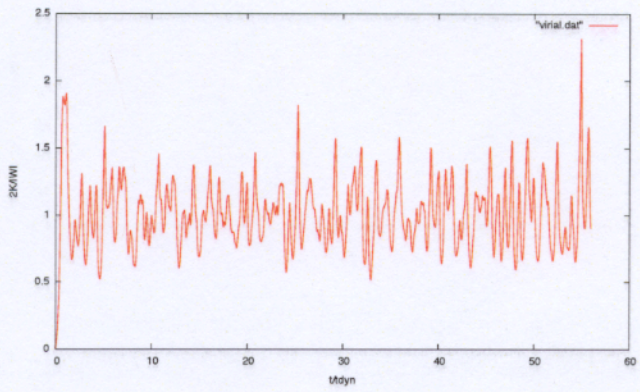

(b)

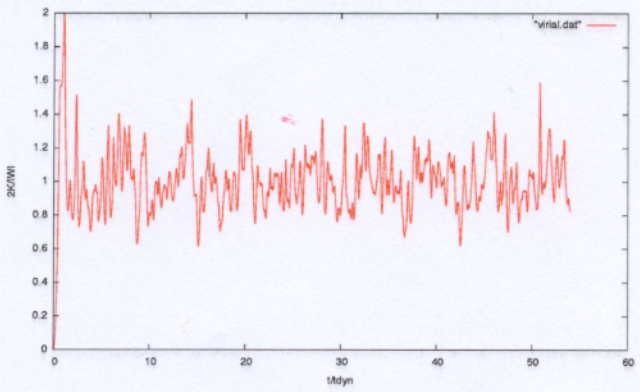

(c)

Figure 4.4: Virial ratio $2K/|W|$ for the same systems. Note that the scales of the plots are different. As it was expected increasing the number of shells the oscillations are of lower amplitude and dump to 1 faster.

Apart from the fact that here we have shown only radial collapses, our tests seems to be according with Hénon's work. Continuing with Newtonian experiments, although in the original paper the next tests where not made, we have also evolved a system of 2500 radialy collapsing shells (impossible with the original code of the sixties) for 20 t_{dyn} from $K(t_0) = 0$ and $K(t_0) \neq 0$ initial states and observed the phase space properties of both cases by plotting Poincaré sections of the phase plane at 0, 0.5, 1, 5, 10, and 20 dynamical times. in the next page there are the results for a simulation with zero initial kinetic energy. The phase space after a few dynamical times appear well mixed while the virial ratio and the Jacobi identity present a violent initial phase in both cases and then a gentle oscillation arount the equilibrium values.

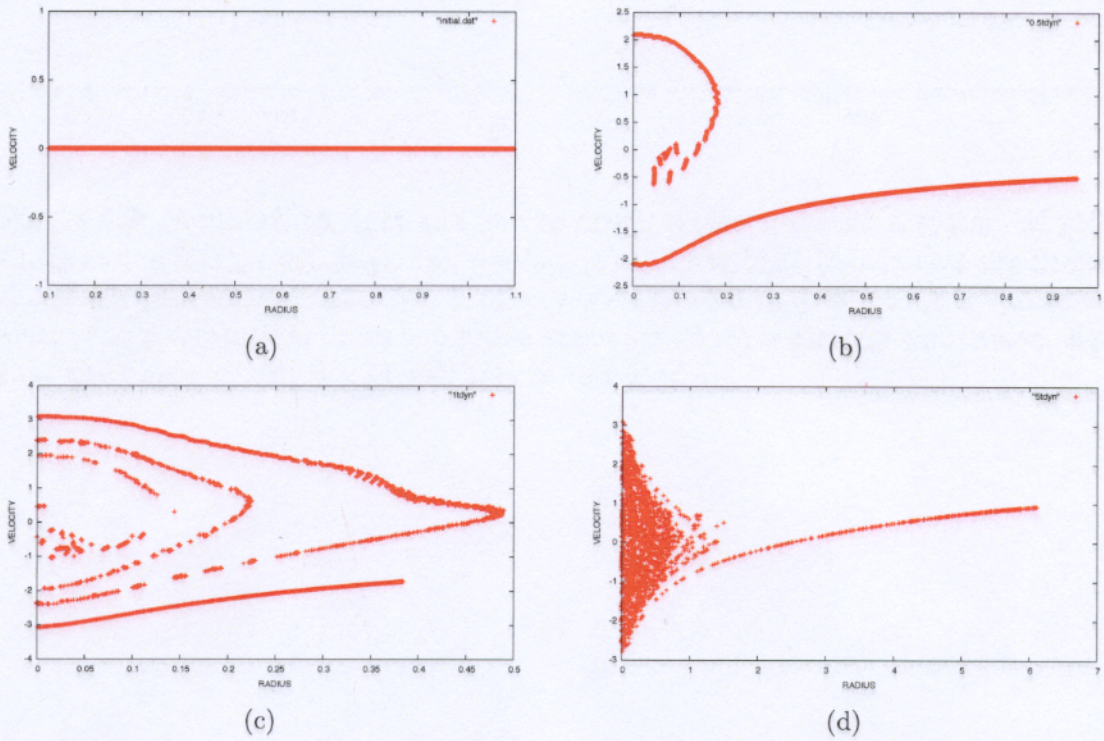

Figure 4.5: From left to right and top to down, phase space for a system of 2500 shells at $t = 0$ (a), $t = 0.5t_{dyn}$ (b), $t = t_{dyn}$ (c) and $t = 5t_{dyn}$ (d). In this simulation the shells started from an initial motionless state with $r_{max} = 1.1$. It is clear that even after 5 dynamical times the phase space structure is already well mixed, sign that the phase mixing works well also in this model.

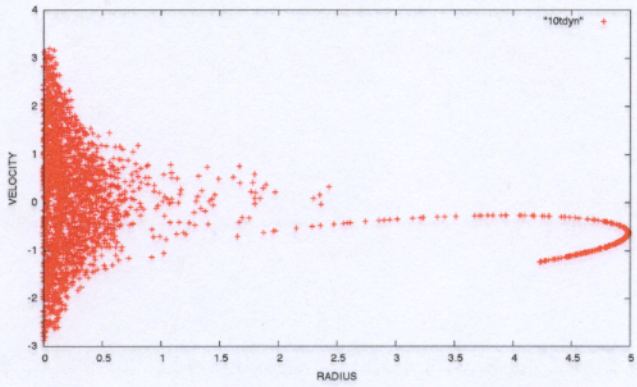

(a)

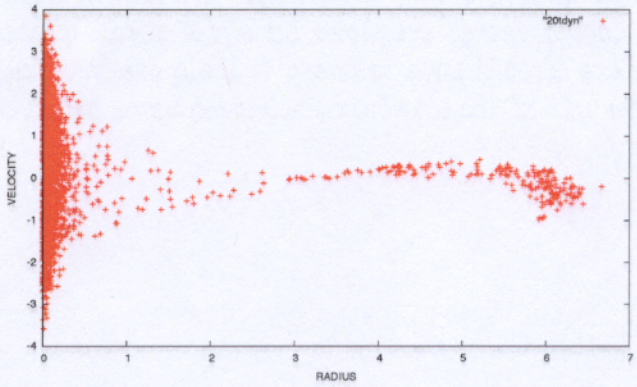

(b)

Figure 4.6: Phase space for the system of 2500 shells at $t = 10t_{dyn}$ (upper panel) and $t = 20t_{dyn}$ (lower panel). Here we can see that this Newtonian system shows a clear core-halo segregation. At high radius (say 6 in this units) appears a population of low velocity shells while no excapers (great radius and high positive velocity) are evident in these plots. Note that even if total energy is negative and so the system is bounded some particles could excape. In this experiment the total energy was -0.728.

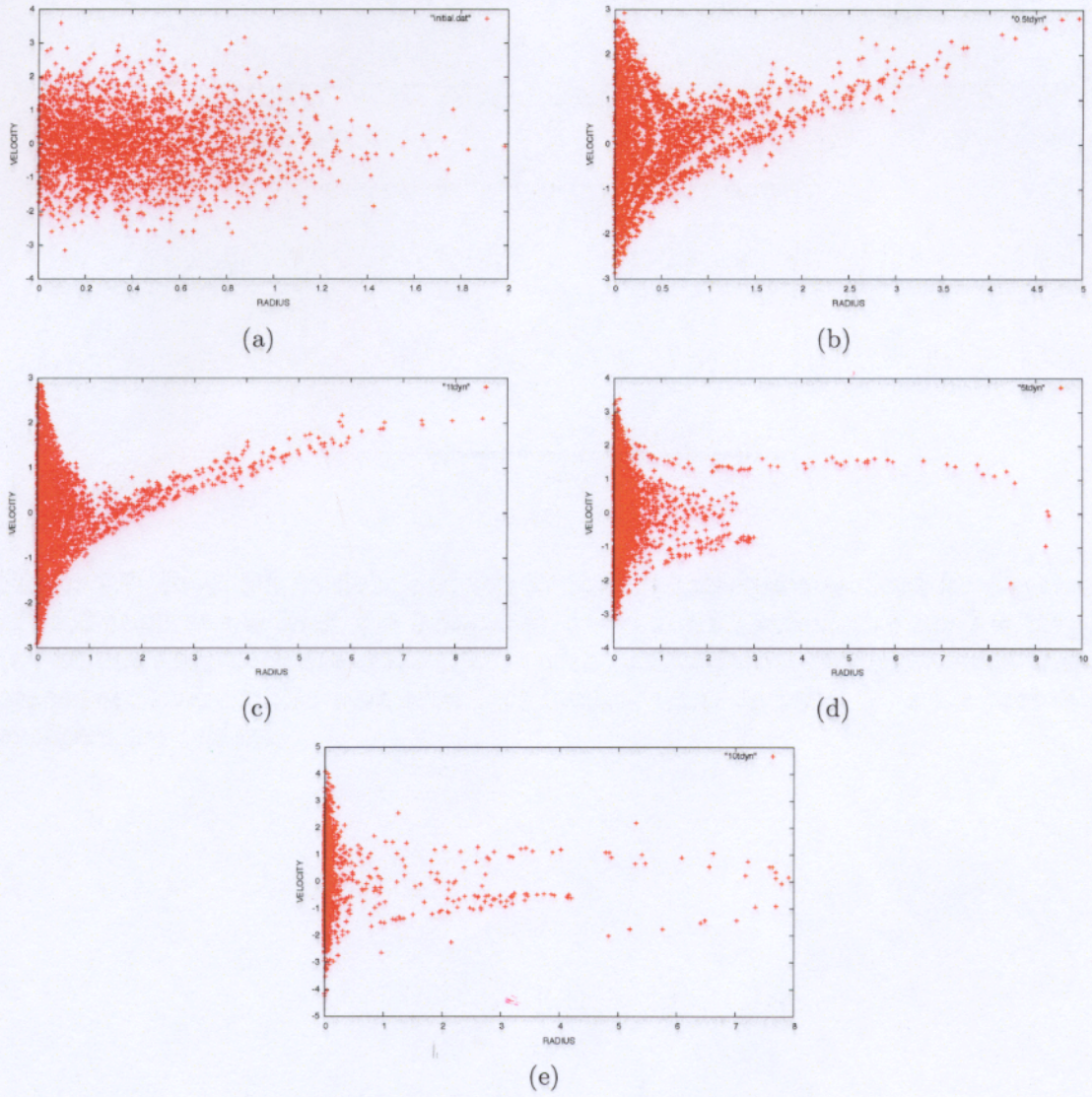

Figure 4.7: From left to right and top to down, phase space sections for a system of 2500 shells at $t = 0$ (a), $t = 0.5t_{dyn}$ (b), $t = t_{dyn}$ (c), $t = 5t_{dyn}$ (d) and $t = 10t_{dyn}$ (e). In this simulation the shells started with random initial conditions. The phase space seems very mixed even after 1 dynamical time. In panel (e) some probable excapers are evident.

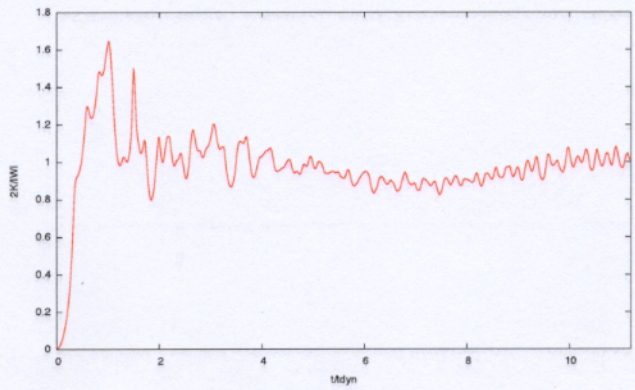

(a)

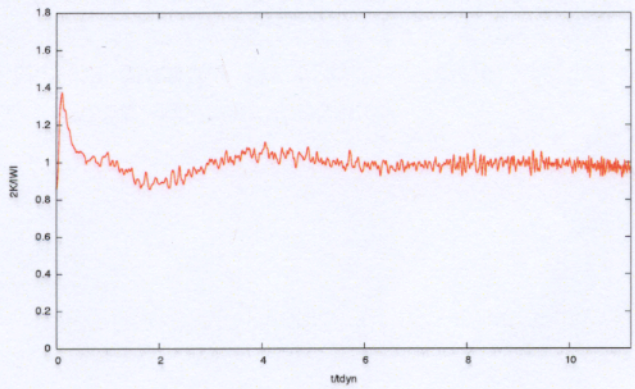

(b)

Figure 4.8: Virial ratio until $t = 11.2t_{dyn}$ for two systems of 2500 shells, one starting with $K = 0$ and total energy -0.728 (top panel); and the other starting with $K = 0.462$ and total energy -0.613 state (bottom panel). Unless the initial conditions are very simple the evolution of $2K/W$ for the two systems is nicely similar. The two system undergo the common initial violent phase and then fall on to the quasi-equilibrium oscillating phase.

4.2.2 The single shell collapse in Newton's gravity (Numerical)

In order to check the consistence with the analytic solutions, in this test we have made some minor changes in the code adding the some lines into the integration loop that output the value of time when the radius of the shell with index 1 reaches its minimum radius and we have performed some one-shell Newtonian collapse with $G = 1$, $M_{tot} = M_{shell} = 1$ for different values of its radius. Then we have confronted the outputs with the results for the related solutions of equation 3.43 finding a sufficently good agreement with the analytic solutions. For example considering a shell falling from $r = 1$ with 0 initial radial velocity, setting $\epsilon = 9 \times 10^{-3}$ and $\Delta t = 10^{-3}$, it has been found that it contracts to $r = 0$ in $t \sim 2.8$ that has less than the 10% of error on the analytic solution tha predicts ~ 2.2. Repeating the experiment with different values of ϵ and Δt and starting with different initial radius does not changes significatively the error. When we consider a system with a large number of shells, one may think that due to the error propagation the entire consistence of the simulation will be erased, but one has also to keep in mind that when the number of shells is large the noise introduced by the force produced on each shell's unperturbed trajectory is greater than any intrinsec numerical fluctuation, this works more or less like when in a big choir a few singers (not too many) are out of tune and their clashing effect is covered by the contribution of the others.

4.3 Simulations and results for other $1/r^{\alpha}$ laws

To explore the dynamical evolution of long range systems with generalized power law force $1/r^{\alpha}$ and compare it to Newton gravity, we have performed a set of experiments with $1 < \alpha < 2$ and a set with $2 < \alpha < 3$. The $\alpha = 1$ case, excluded for the moment as it comes from a logarithmic potential, is partialy explored in appendix B and the cases with $\alpha \geq 3$ are also out of the discussion being unphysical for the fact that α excedes the dimension of the configurations space that in our case is meant to be $\Re^3$. We have evolved seven systems of 10^3 shells from the same initial condition with 0 kinetic energy, for 15 dynamical times, in the different cases with α =1.2, 1.4, 1.6, 1.8, 2, 2.2, 2.4. In each case following the reasonement that that one does for gravity, t_{dyn} was euristicaly estimated with dimensional and order of magnitude arguments as

$$t_{dyn}(\alpha) \simeq \frac{R}{\sqrt{C_c M_{tot}/R^{\alpha-1}}} \tag{4.9}$$

with R the total radius, that in this first group of simulations was always set ~ 1, and where C_c is the coupling constant that was also set equal to 1 in all the

explored cases. From the experiments we have extracted the phase space structure at the different dynamical times, the virial ratio, the final velocity distribution $n(V)$, the final $M(r)$ profile, the final energy distribution $n(E)$ and the evolution of the system's radius R_{max}. We now start to show and discuss the results for each feature of interest.

4.3.1 Phase space evolution

The pictures in the next pages show the phase space of the simulated systems at different dynamical times. The first group (figures 4.9, 4.10, 4.11, 4.12 and 4.13) contains the experiments with $\alpha < 2$ and the second (figures 4.14, 4.15, 4.16, 4.17 and 4.18) the experiments with $\alpha > 2$ and the result for the Newtonian simulation. We have found an increasing trend of the mixing efficiency with the exponent α; so interaction with lower α (longer range) have a more regular phase space than shorter-ranged interactions at the same time. This means that the phase space mixing time increases with the range.
Also the way in which chaos originates and spreads across the phase space is different between systems with $\alpha > 2$ and systems with $\alpha < 2$. For example in the case of interactions with $\alpha < 1$ the chaos takes more dynamical times to spread from the external regions of the phase space into the inner regions while for the cases with $\alpha > 2$ chaotic point start to dominate between regular curves already at $t = 5t_{dyn}$ for all the tested exponents and in both internal and external parts of the region occupied by the phase points. Despite to the seaming trend with α the Newtonian case seems at every dynamical time the best mixed amongst the others; this is most probably due to the fact that in virtue of the second Newton Theorem, when two spherical shells cross each other the one that was before the external one ends to undergo the field of the other, that at this point starts to be subjected to the field of the one that has crossed it. Such fact gives rise to a violent noise effect that increases in this case the energy exchange between the shells, while for non-newtonian systems, where this result is not valid and so the field changing during a crossing is not discrete, the shell crossing has a more gentle effect. As one can see from picture 4.16 for the Newtonia system (panel (c)) the chaotic points are already dominat over the regular lines, this means tha the system is at this time have relaxed on small scales; we call this feature Local Relaxation. Notice that this difference is sensible only for spherical dissipationless collapses while for anisotropic systems the situation may be different.

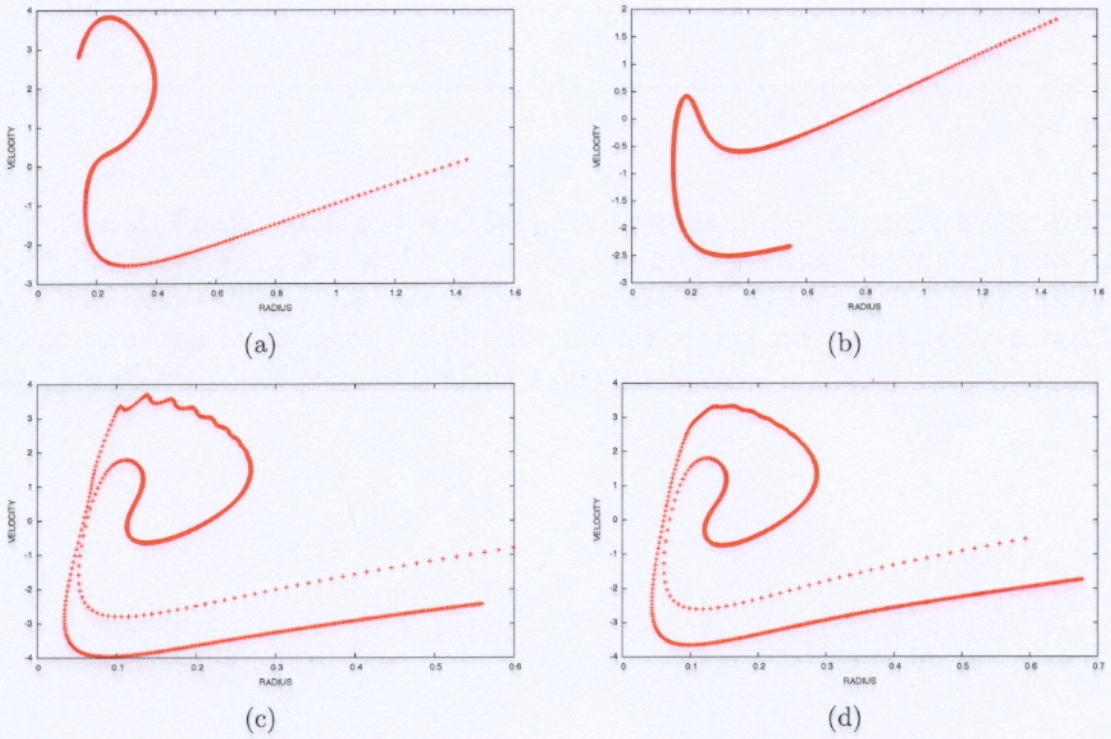

Figure 4.9: Phase space at $t = 0.5t_{dyn}$ for systems of 10^3 shells interacting via $1/r^{\alpha}$ law (each point is a shell). $\alpha = 1.2$ (top left), $\alpha = 1.4$ (top right), $\alpha = 1.6$ (bottom left) and $\alpha = 1.8$ (bottom right). After 0.5 dynamical times the phase space structure looks more complex for the higher exponents, while for $\alpha = 1.2$ and 1.4 all the phase points are along a distinct curve.

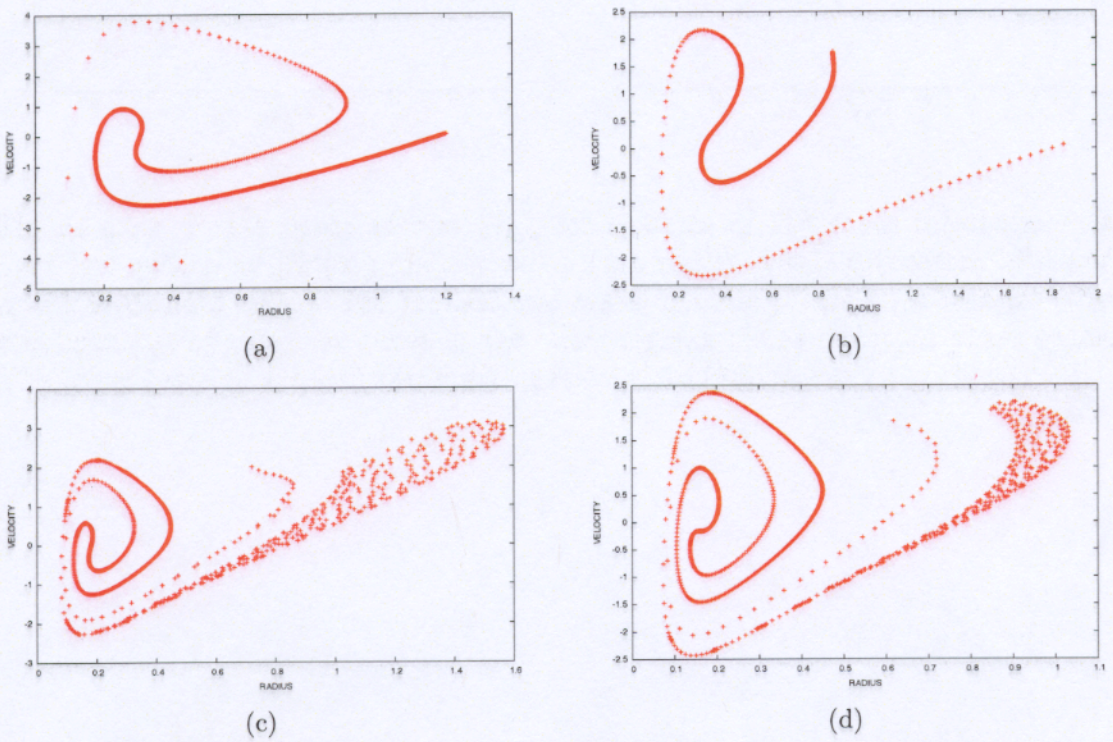

Figure 4.10: Phase space at $t = 1t_{dyn}$ for systems of 10^3 shells interacting via $1/r^{\alpha}$ law with $\alpha = 1.2$ (top left), $\alpha = 1.4$ (top right), $\alpha = 1.6$ (bottom left) and $\alpha = 1.8$ (bottom right). For the last two cases, chaotic points start to arise from two branches of a regular curve in the outer regions of the occupied phase space. The other systems are still showng a quasi-regular fashion.

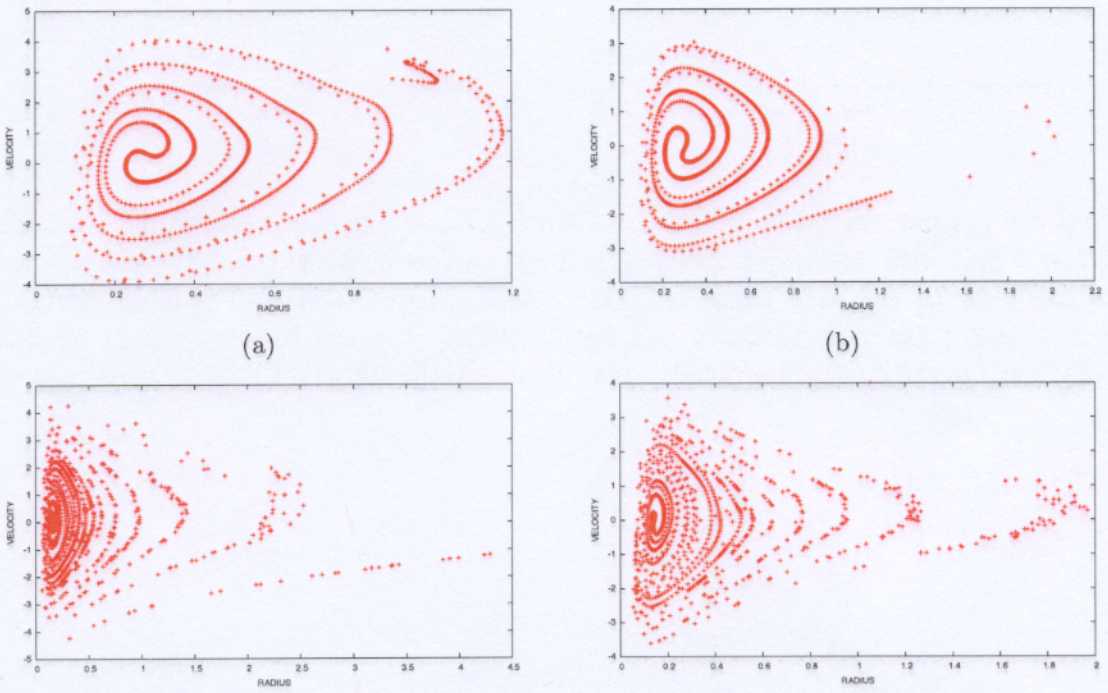

Figure 4.11: Phase space at $t = 5t_{dyn}$ for systems of 10^3 shells interacting via $1/r^{\alpha}$ law with $\alpha = 1.2$ (top left), $\alpha = 1.4$ (top right), $\alpha = 1.6$ (bottom left) and $\alpha = 1.8$ (bottom right). It is now evident at 5 dynamical times that the phase space in almost all the cases is going to be separated in a more dense inner region and a lesser dense halo. This is not already a dynamical segregation amongst the shells.

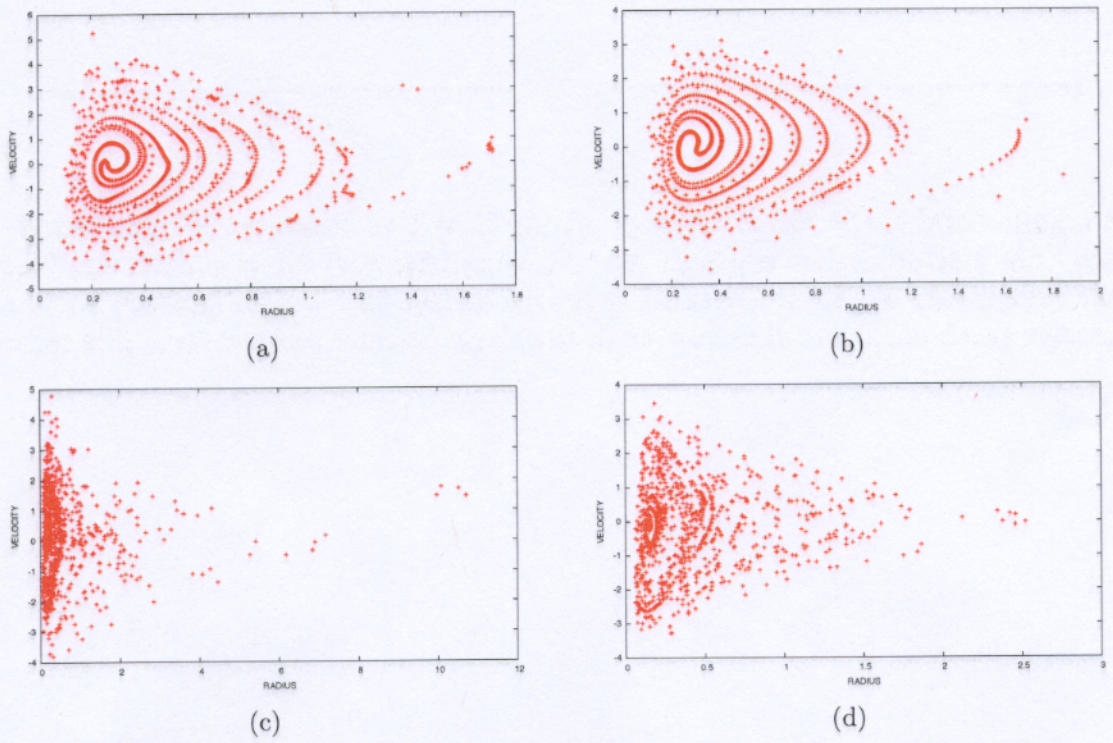

Figure 4.12: Phase space at $t = 10t_{dyn}$ for systems of 10^3 shells interacting via $1/r^{\alpha}$ law with $\alpha = 1.2$ (top left), $\alpha = 1.4$ (top right), $\alpha = 1.6$ (bottom left) and $\alpha = 1.8$ (bottom right). The system with $\alpha = 1.6$ seems to be the best mixed, the other still present some form of regularity in particular in the inner dense region.

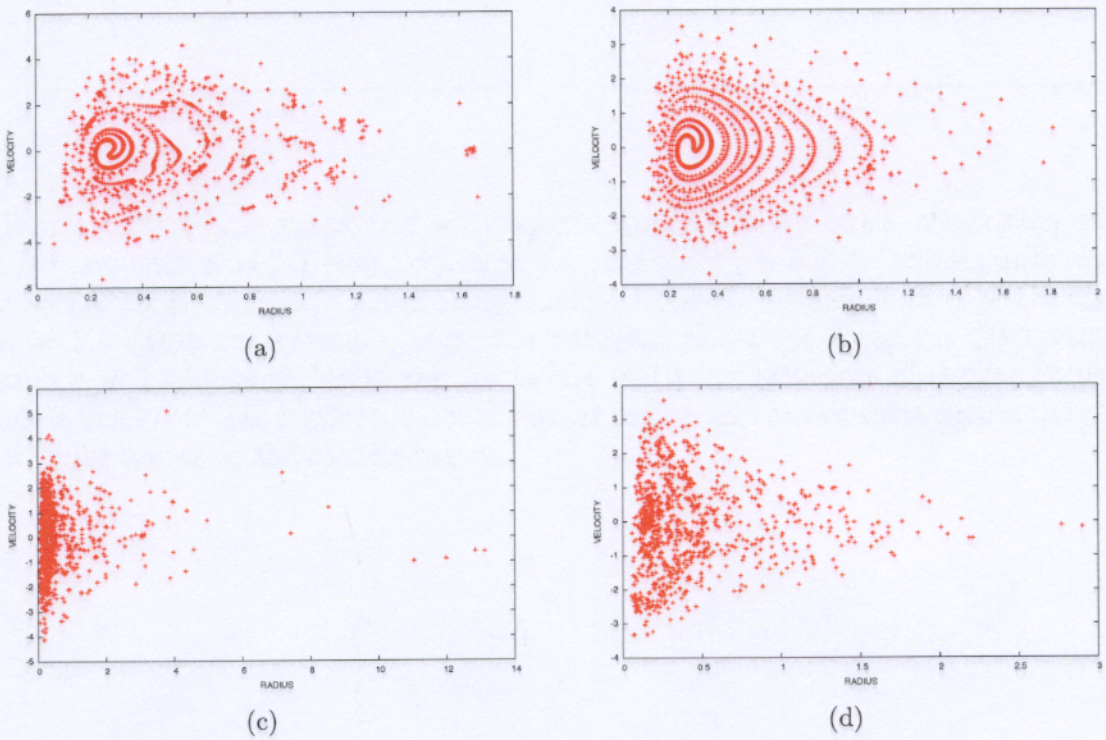

Figure 4.13: Phase space at $t = 15t_{dyn}$ for systems of 10^3 shells interacting via $1/r^{\alpha}$ law with $\alpha = 1.2$ (top left), $\alpha = 1.4$ (top right), $\alpha = 1.6$ (bottom left) and $\alpha = 1.8$ (bottom right). After 15 dynamical times in systems with $\alpha = 1.6$ and $\alpha = 1.8$ chaos has spread all over the occupied phase space region; the system with $\alpha = 1.4$ looks the most regular having still some remnants of regular curves while the $1/r^{1.2}$ has a minor internal regular region and shows some accumulation of phase points in the chaotic region.

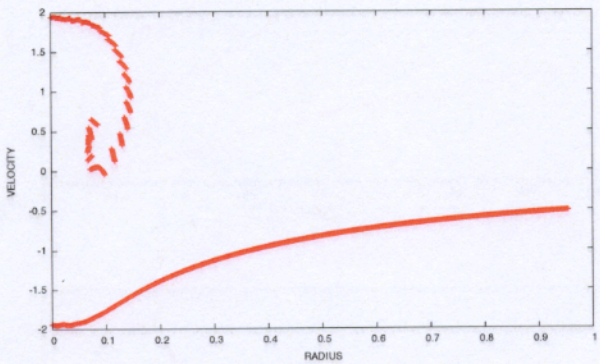

(a)

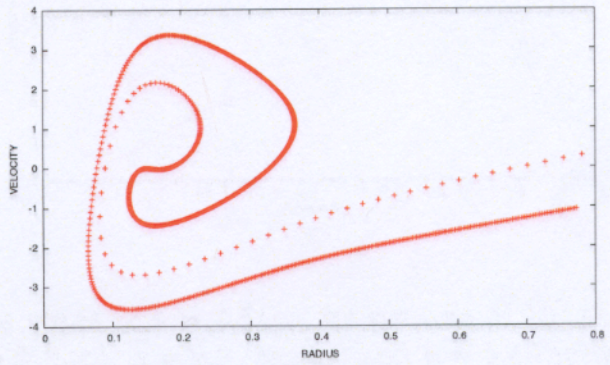

(b)

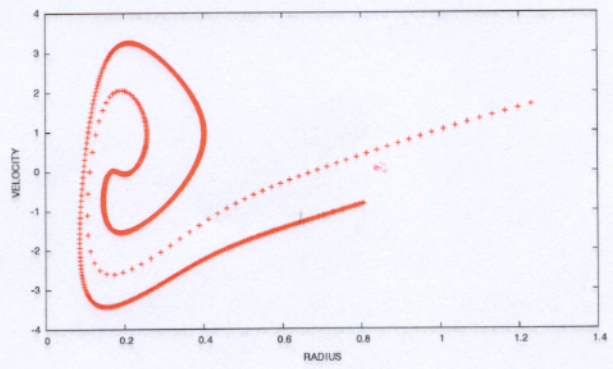

(c)

Figure 4.14: Phase space at $t = 0.5t_{dyn}$ for systems of 10^3 shells interacting via $1/r^{\alpha}$ law with $\alpha = 2$ (top), $\alpha = 2.2$ (center) and $\alpha = 2.4$ (bottom).

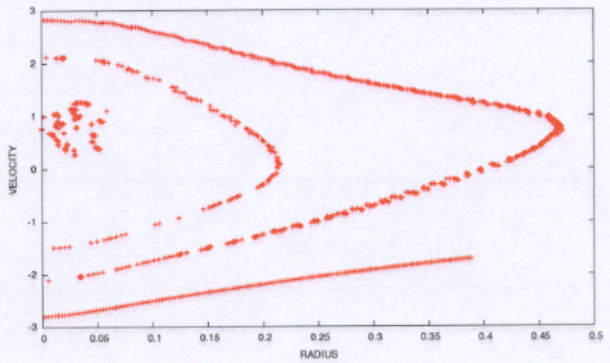

(a)

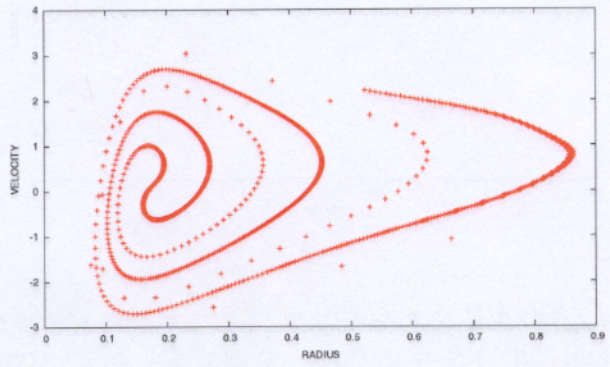

(b)

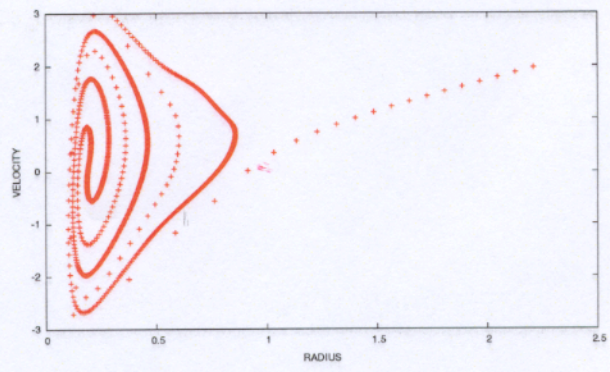

(c)

Figure 4.15: Phase space at $t = 1t_{dyn}$ for systems of 10^3 shells interacting via $1/r^{\alpha}$ law with $\alpha = 2$ (top), $\alpha = 2.2$ (center) and $\alpha = 2.4$ (bottom). The Newtonian force presents already some chaos around the smooth curves while the othe forces have still definite regions in phase space.

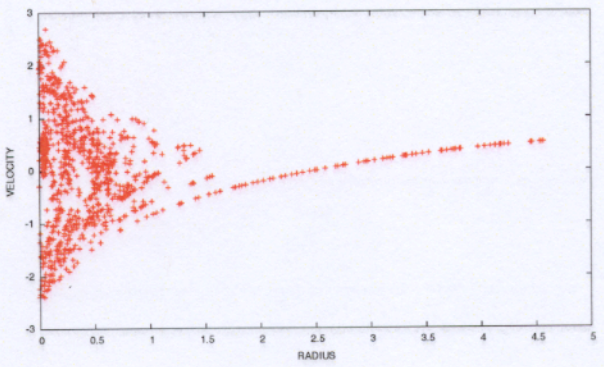

(a)

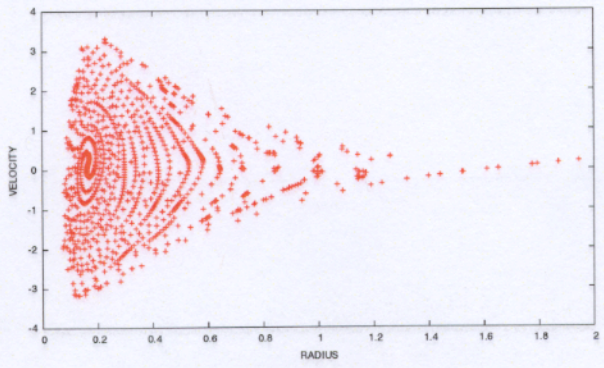

(b)

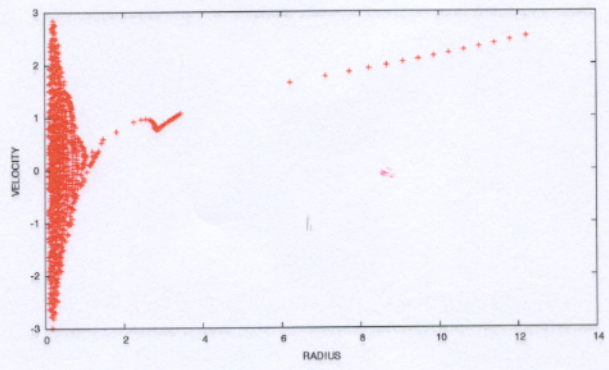

(c)

Figure 4.16: Phase space at $t = 5t_{dyn}$ for systems of 10^3 shells interacting via $1/r^{\alpha}$ law with $\alpha = 2$ (top), $\alpha = 2.2$ (center) and $\alpha = 2.4$ (bottom). At 5 dynamical times the $1/r^{2.4}$ force has the most mixed phase space, some shell seems to be candidate for evaporation.

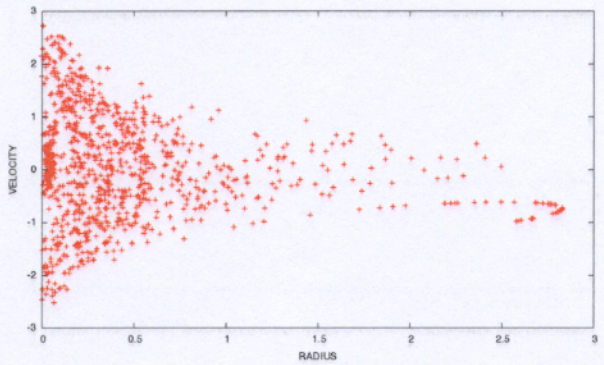

(a)

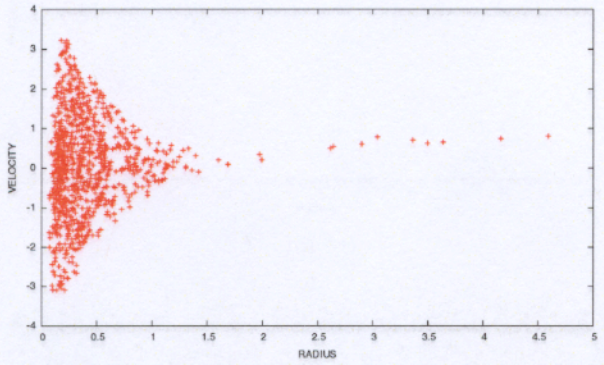

(b)

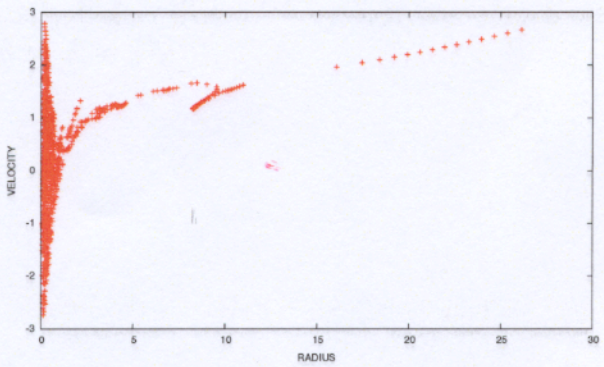

(c)

Figure 4.17: Phase space at $t = 10t_{dyn}$ for systems of 10^3 shells interacting via $1/r^\alpha$ law with $\alpha = 2$ (top), $\alpha = 2.2$ (center) and $\alpha = 2.4$ (bottom). All the systems have reached a configuration where the phase plane is divided in an inner high density core and a low density halo. The $1/r^\alpha$ system has also a well defined excapers region from $R = 16$ to $R = 27$.

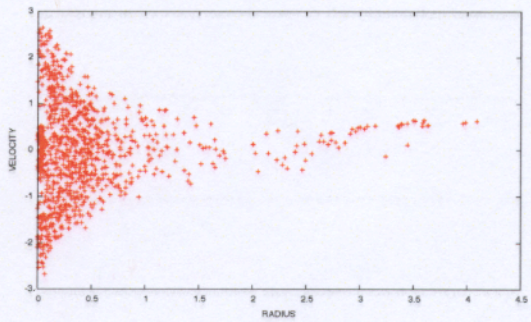

(a)

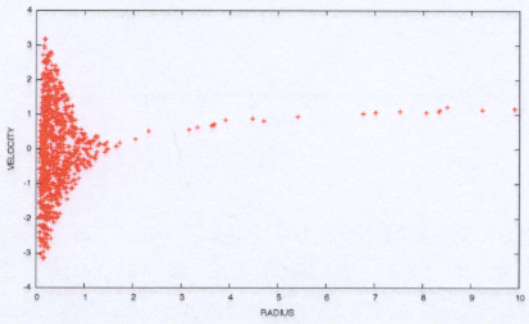

(b)

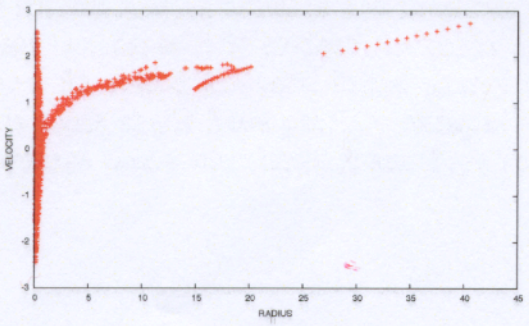

(c)

Figure 4.18: Phase space at $t = 15t_{dyn}$ for systems of 10^3 shells interacting via $1/r^{\alpha}$ law with $\alpha = 2$ (top), $\alpha = 2.2$ (center) and $\alpha = 2.4$ (bottom). At 15 dynamical times all the system continue to show a clear phase space segregation and probable excapers; it must be pointed out that contrary to $1/r^{\alpha}$ interactions with $\alpha < 2$ where the system always remains bounded due to the longer range of the interaction; in these last cases it is evident tha some internal mechanisms of evaporation may occour. So even if the total initial energy was set to be negative for all the experiments some shells have partialy excaped the system creating a separate region of the phase plane with large R and high (positive) velocity.

4.3.2 The virial ratio evolution

As we have said in the preliminaires, if a system oscillates around the relaxed state the quantity expressed in equation 2.37 oscillates around 1. We have tested it for all our experiments with different $1/r^{\alpha}$ laws finding a good agreement with the hypotesis. Picture 4.19 in the next page shows the results for four relevant cases. One will notice immediately that in all the cases the evolution of the virial ratio shows the initial violent jump from the cold initial state ($K = 0$) and then experiences the oscillating phase. For the lower αs the curve of the virial ratio looks smoother while for $\alpha \geq 2$ it shows a major presence of noise. This comes from the fact that when the range of the interaction increases (in our weak long range cases, the exponent α decreases), the mean field effect grows and erases or smothes the short range noisy effects. For example this is what happens in Plasma Physics when at sclaes larger than the Debye lenght, that discriminates the ranges where the collisional or the mean field effects are important, the collective effects dominate over the direct particle-particle effects in the dynamical evolution of the system.

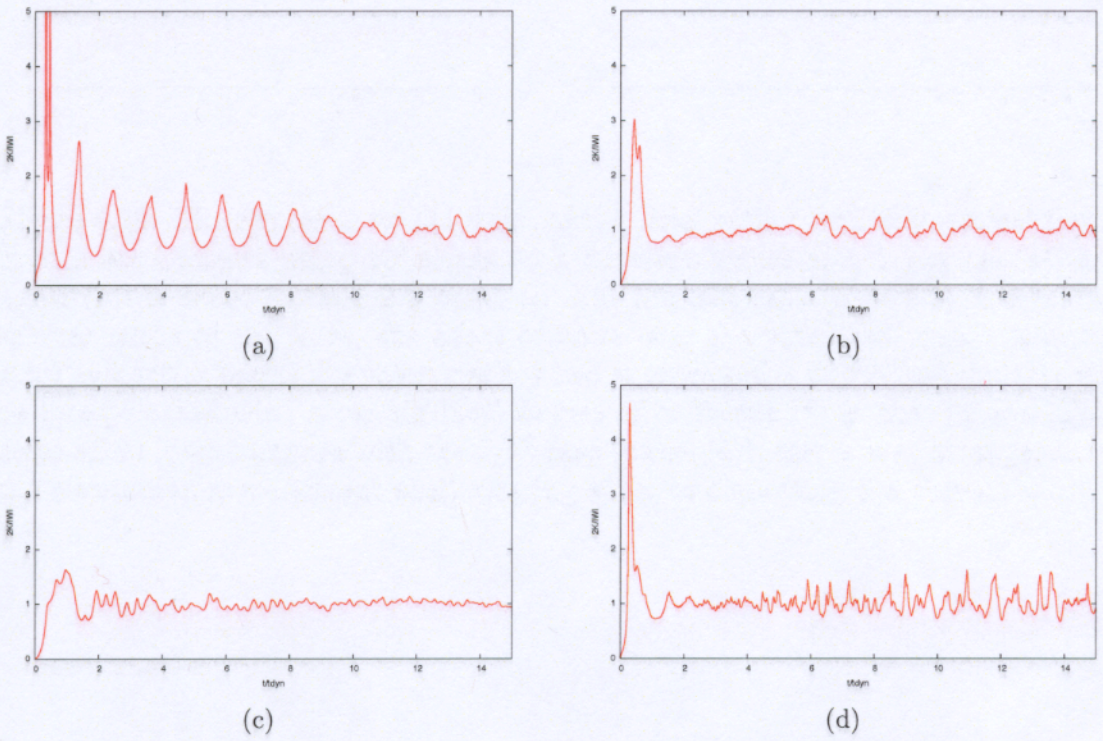

Figure 4.19: The figures show the trend of the virial ratio over 15 dynamical times in four experiments using 10^3 shells with different values of α 1.2 panel (a), 1.6 panel (b), 2 panel (c) and 2.2 panel (d). in the last case ($\alpha = 2.2$) due to the shorter range of the force, the effect of noise over the virial oscillations is much more evident, it seems like the curve has two or more scales of oscillations; this can be interpretated with a certain local degree of collisionality in the system. This noise effect if we compare with the $1/r^2$ case (panel (c)), seems even stronger than the Newtonian more efficent shell crossing effect in disturbing the curve.

4.3.3 Final velocity and energy distributions

We now show and analyze the results for the energy distribution $n(E)$, (equation 2.22) and the velocity distribution $n(V)$, defined in an analogus way from the number of particles (in our case shells) $n(v)dv$ having velocity between v and $v+dv$. The first quantity, as it is predicted by Statistical Mechanics assuming the Most Probable Distribution Principle, should have a Maxwellian form (say exponential trend), while the second, coherently with thermal phenomena in chaotic dynamics is most probably well described by a Gaussian distribution

$$n(v) = n_0 \exp\left[-\frac{(v - v_0)^2}{2\sigma^2}\right] \tag{4.10}$$

where v_0 is the value of v corresponding the peak n_0 and σ is the mean square velocity that in the curve parametrizes the width. For the gravitational case, the Maxwellian energy distribution was proved to be valid for a spherical self consistent star system by Antonov ([2] 1963), who generealized the procedure taken from the kinetic theory of the gases of maximizing the functional

$$S_L = -\int\int f \ln f d\,\vec{r}\; d\,\vec{v} \tag{4.11}$$

and then extrecting the correspondent $n(E)$. Doing the same analyticaly for a generalized $1/r^\alpha$ interaction is impossible due the fact that we do not have in this case the analogus of the Poisson equation, so we can not built self consistent density potential pairs. Apart from this problem, by integrating numericaly different shell models with various values of the parameter α and computing the energy distributions $n(E)$ in the final quasi-relaxed state we have found that effectively some esponential trend is present unless the curves (fig. 4.20) are looking very noisy, most probably due to the grid scale used to compute the distribution (100 nodes for 1000 particles). In picture 4.21 we show the linear fit for the number distribution $n(E)$ in logarithmic scale, the values of the parameter are in table 4.1. In the end in picture 4.23 there are the velocity distributions. All those last diagram show a gaussian form exept for 4.23(f) that looks like two distributions were superimposed, this fact arises from the presence of a large population of excapers in systems with greater α systems, so the second peak is due to the shells containig unbounded particles.

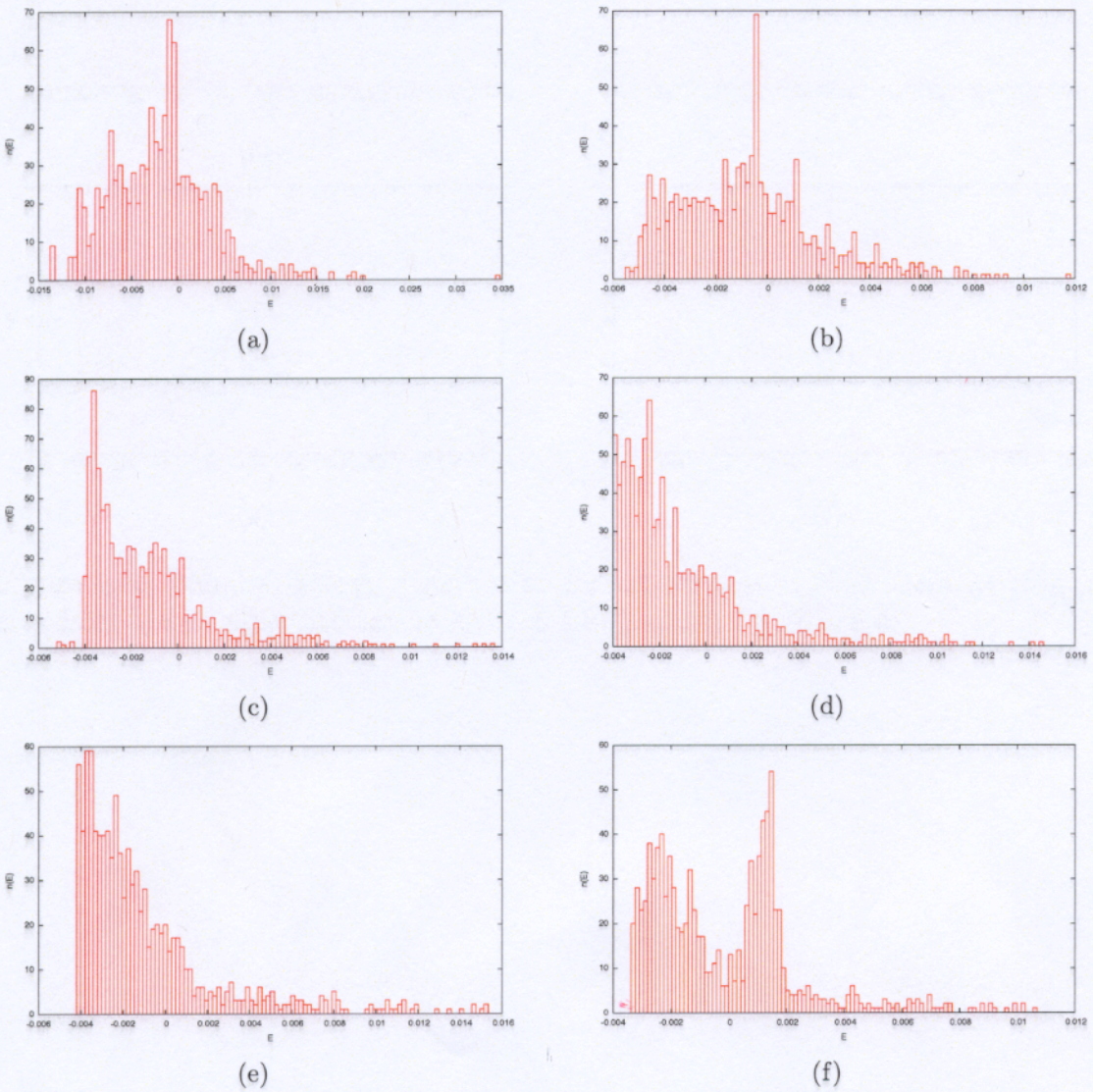

Figure 4.20: Number energy distribution for six systems of 1000 shells at $15t_{dyn}$. α is from left to right and top to bottom 1.2, 1.4, 1.6, 1.8, 2.2, 2.4.

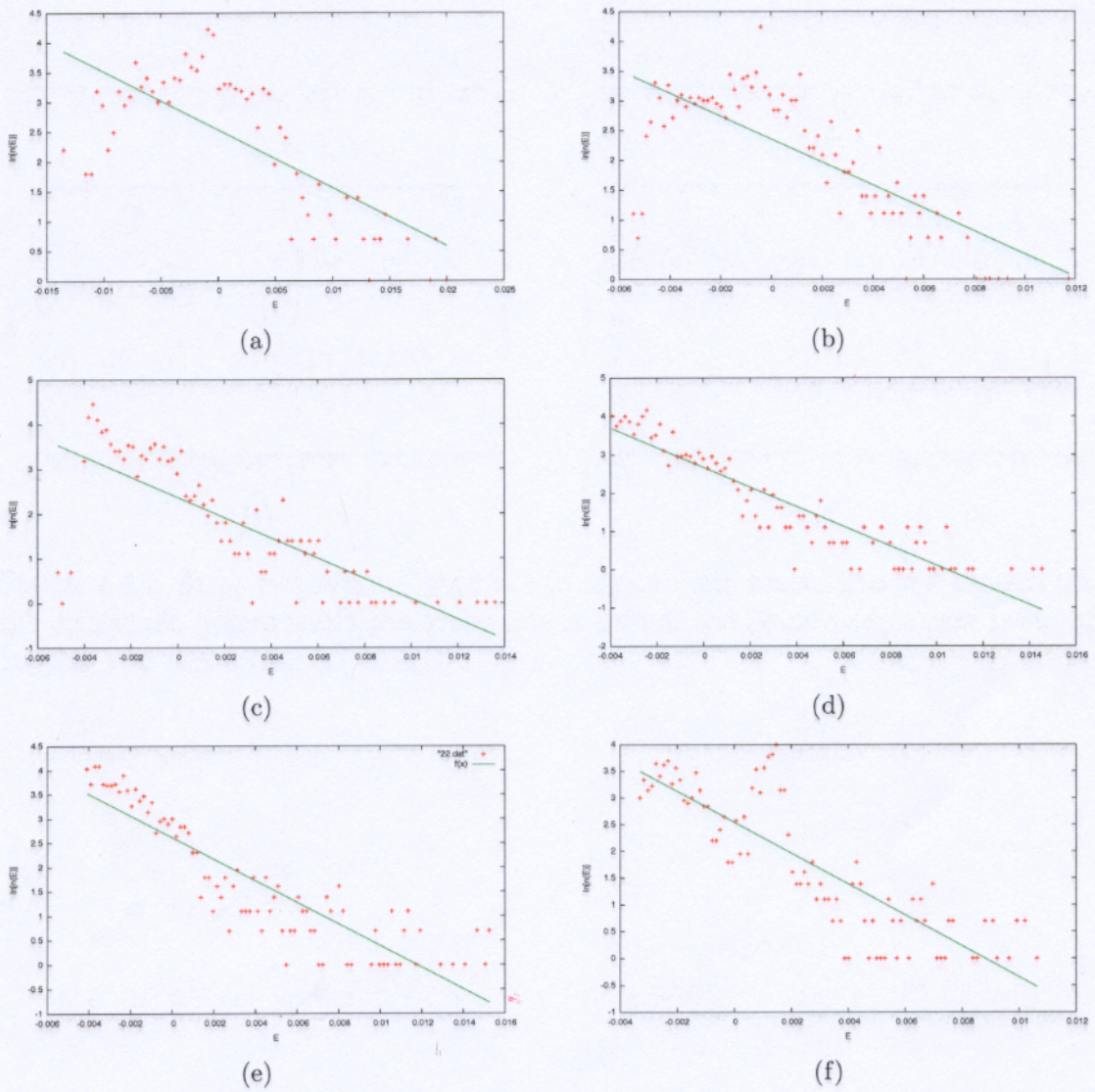

(a) (b) (c) (d) (e) (f)

Figure 4.21: Same of previous page but in logarithmic scale. The red crosses are the computed points while the green line is a fit of the (supposed) linear trend of $\ln(n(E))$ in this scale.

α	A	B
1.2	-97.500 ± 12.41	2.533 ± 0.122
1.4	-192.973 ± 12.82	2.351 ± 0.087
1.6	-227.650 ± 21.21	2.364 ± 0.115
1.8	-255.978 ± 12.33	2.660 ± 0.074
2.2	-222.154 ± 12.57	2.614 ± 0.085
2.4	-289.029 ± 19.64	2.540 ± 0.097

Table 4.1: Interpolated values for the inclination A and the intersection B for the computed logarithmic distributions with different $1/r^{\alpha}$ laws.

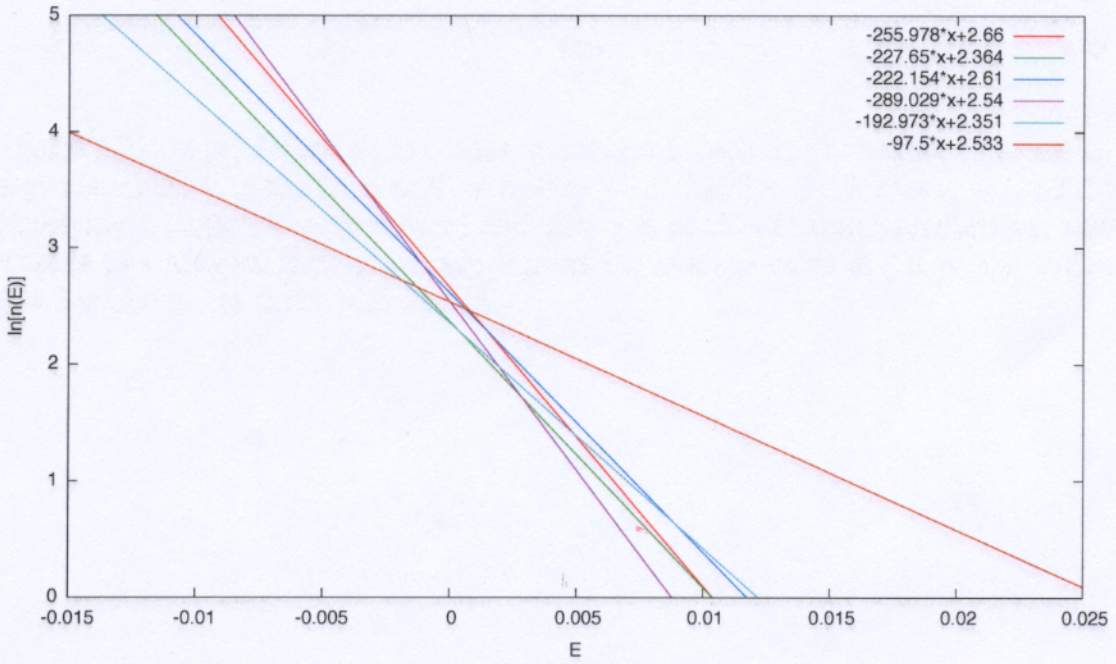

Figure 4.22: $\ln[n(E)]$ for all the cases in Table 4.1 Each line corresponds to an energy distribution in the form $n(E) = n_0 \cdot \exp[(-E/k_B T) + \xi]$. Where $A = (k_B T)^{-1}$ (implying a negative temperature) and $B = \xi$ is coefficent that parametrizes how close is to a Maxwellian. In our experimens the average value of ξ is ~ 2.4. When $\xi = 0$ we have the exact Maxwellian

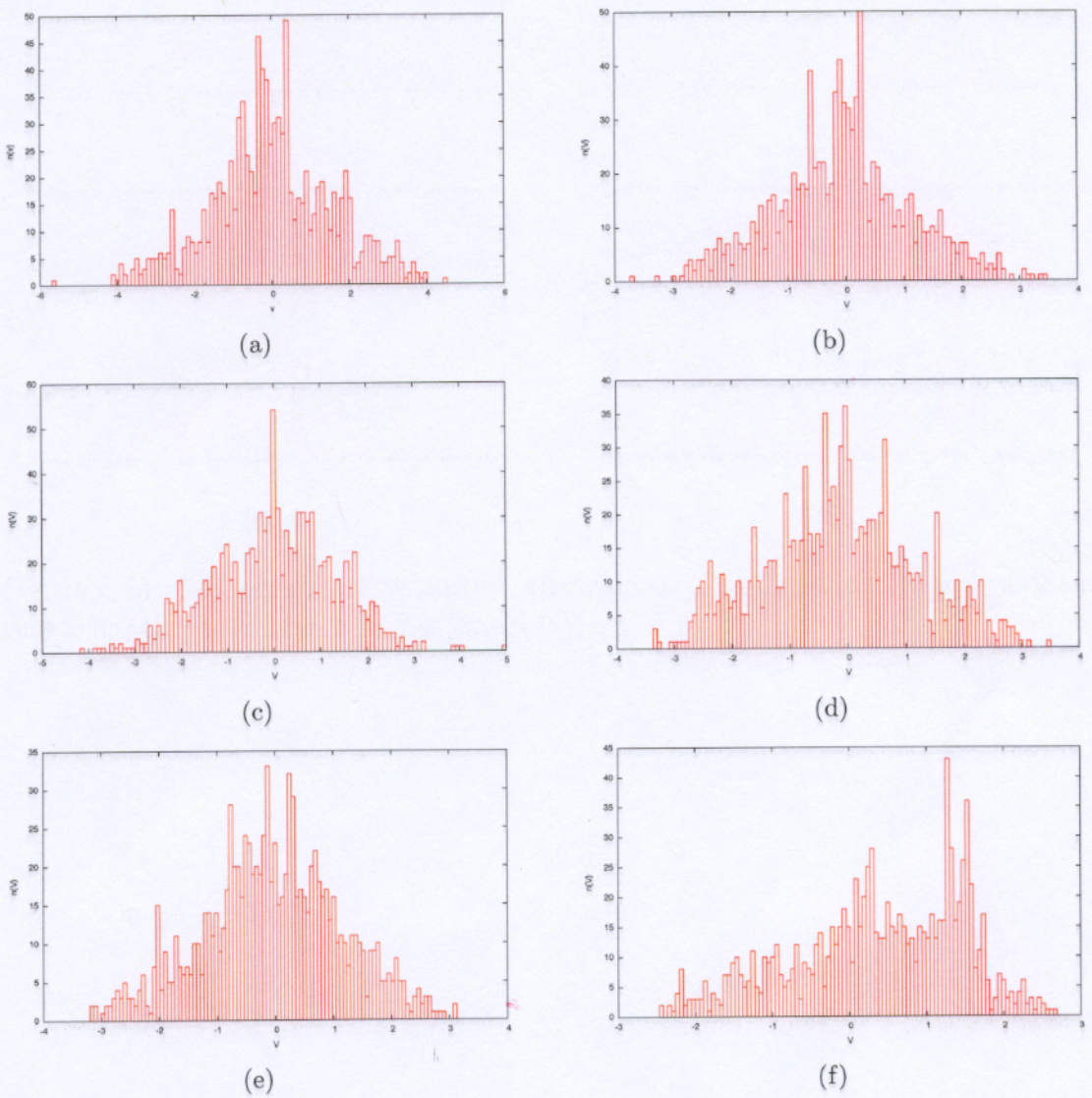

Figure 4.23: Correspondent velocity distributions. The Gaussian trend is evident except for the case with $\alpha = 2.4$ (panel (f)).

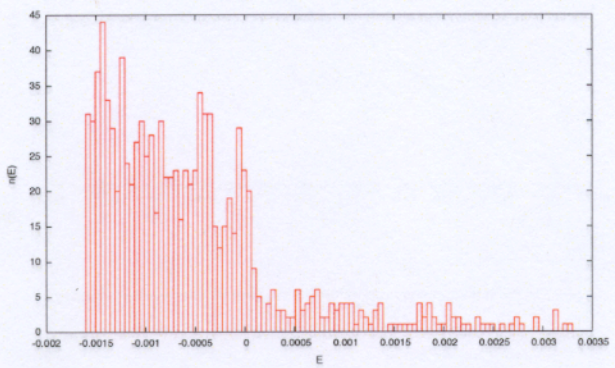

(a)

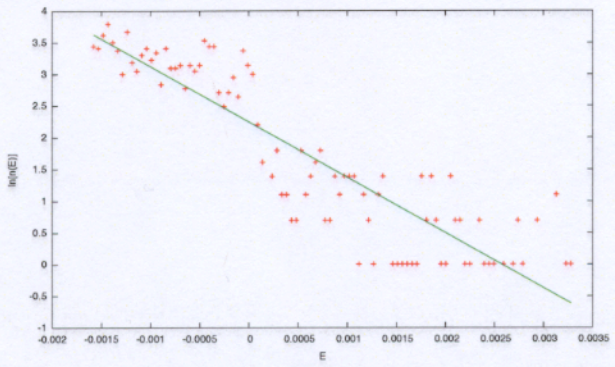

(b)

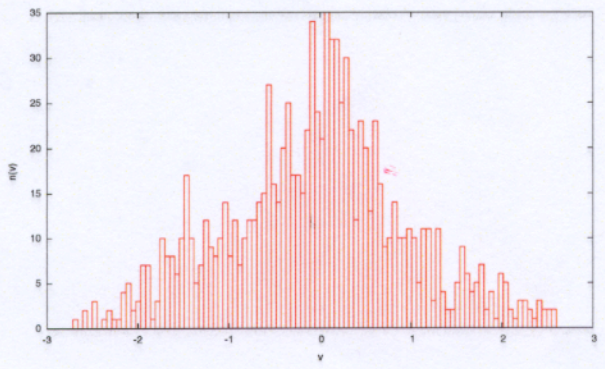

(c)

Figure 4.24: Final energy distribution $n(E)$, its logarithm and velocity distribution $n(v)$ for a Newtonian systems of 10^3 shells evolved from an initial state with uniform density and zero kinetic energy. The extrapolated inclination A of the in panel (b) is -873.07 ± 46.02 while the intersection is at $B = 2.24$ that is lower than every other in table 4.1

4.3.4 Density profiles and global radial oscillations

One last thing that has been extracted from the experiments is the final density profile for each model. As it can bee seen in picture 4.25 where we have the plots for three significant cases the profiles show a central density cusp and an exponential tail tha rapidely vanishes. Notice that in the Newtonian case the central cusp is higher, that is in agreement with the fact that in other force laws each shell has also the contribution of the external mass that opposes to the collapse, resulting in a depression of the mass profile $M(r)$ at the center that gives a lower density profile at the core and a fatter tail. The resultin density profile for the Newtonian experiment is in agreement with what we currently know on density profiles resulting from radial dissipationless collapses from other simulations: the density distribution does not fit with a γ-model having a central cusp and an exponential decrease at large radius.
The system's radius R_{max} in our experiments (picture 4.26) has different trends for the different cases, After the initial contraction that is common to all the force laws, the systems with α equal to 1.2 and 1.4 have increasing oscillations and finaly a quasi-regular oscillating phase around a particular radius $\widetilde{R}$ that is ~ 18 for both cases, Forces with $\alpha = 1.6$ and 1.8 have an increasing phase that in the second case is more complex but does not seems to relaxe over a particular value of r. Almost the same thing occurs in the Newtonian phase while for $\alpha = 2.2$ the radius of the systems increases indefinitely with a quasi-linear trend for the considered time; this is linked tho the fact that with lower range forces the possibility of evaporation increases ans so this trend is probably due to a singe shell that contains the particles that are leaving the system. In fact, as it can be seen from picture 4.18(a) the phase space of this systems is splitted in a dense region from $r \sim 0$ to $r \sim 1.6$ and a faint tail of particles at higher radius with positive velocity, (halo or excapers). The same thing happens also for a system interacting via $1/r^{2.4}$ force; (radius evolution not shown here).

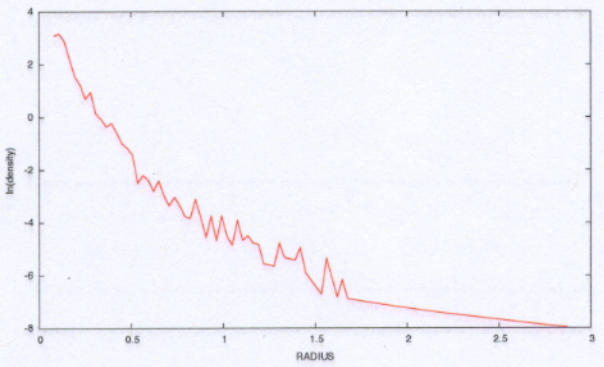

(a)

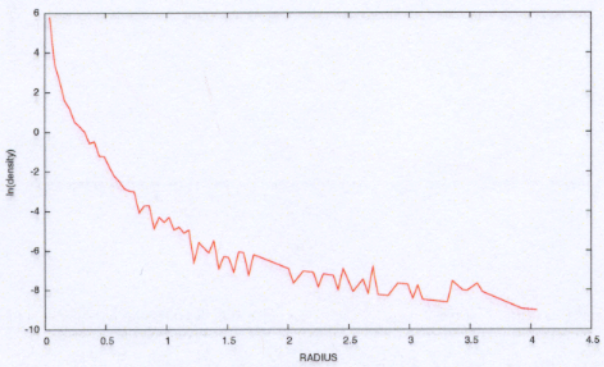

(b)

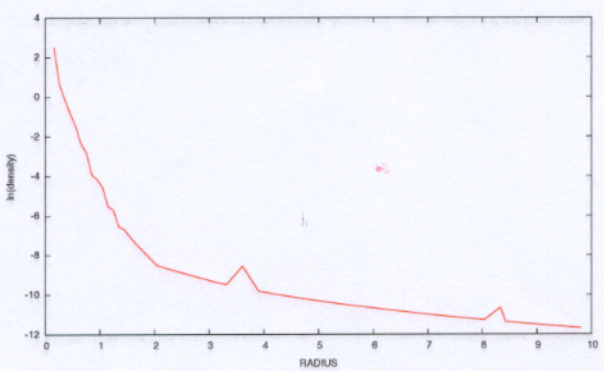

(c)

Figure 4.25: Logarithmic density profiles at $t = 15t_{dyn}$ for three particular exponents, from top to bottom α =1.8, 2, 2.2. Notice that in all cases we have a cusp in the center. The disturbance in the central part of the curve arise simply from the discreteness of the mass profile in the shell model and from the choice of the grid step in its computation.

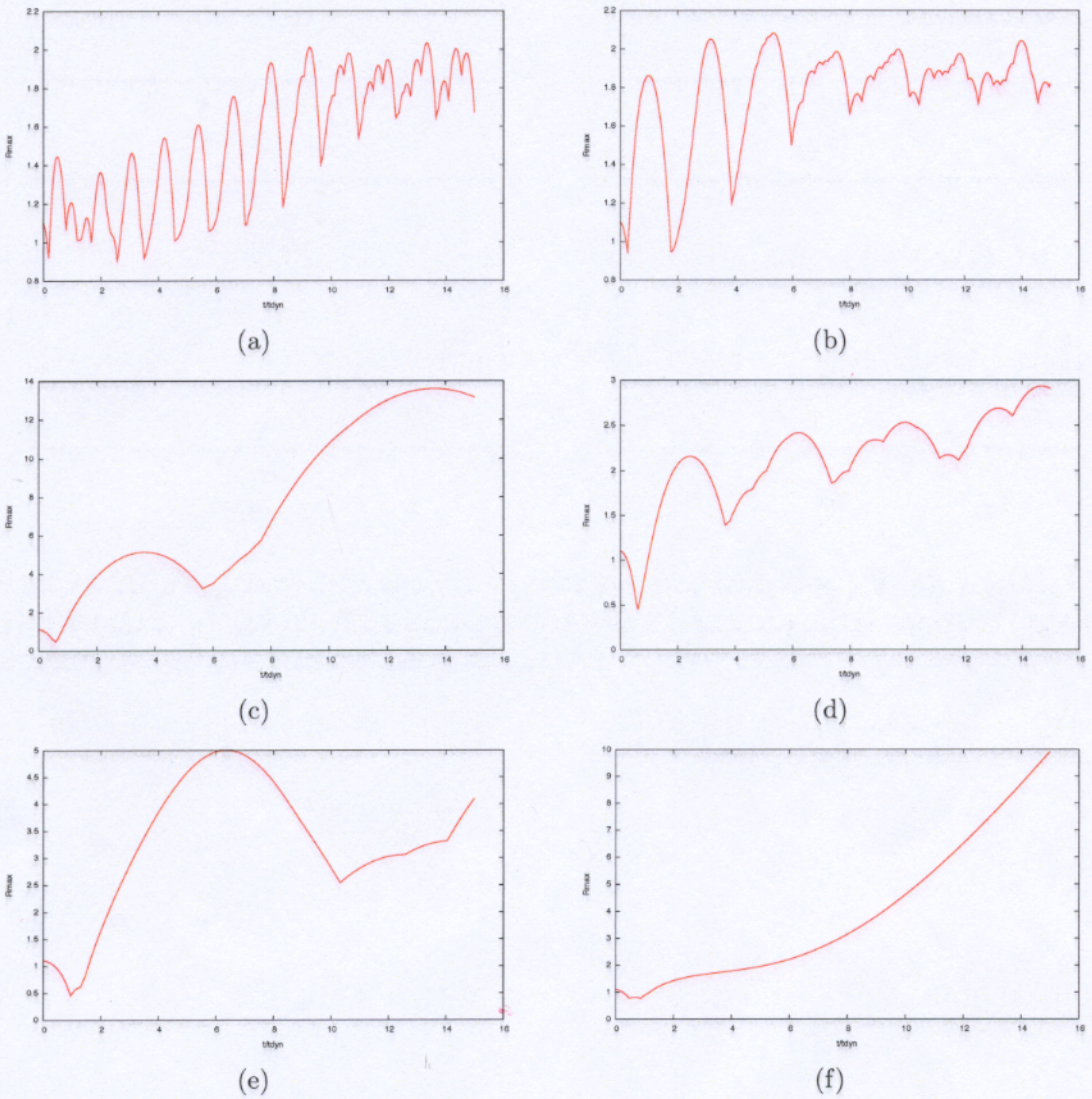

Figure 4.26: R_{max} evolution over 15 t_{dyn} for systems with $\alpha = 1.2$ (a), 1.4 (b), 1.6 (c), 1.8 (d), 2 (e), 2.2 (f). The initial radius was 1.1 and the inital constant density profile was $\rho_{in}(r) = 0.18$ for every simulation.

4.4 Flow diagrams

In this final part of the chapter we show the flow charts illustrating the functioning of the code. Again, referr to appentix C for the complete listing. Picture 4.27 shows the general structure of the code, picture 4.28 illustrates the initial segment where the initial conditions and the parameters of the model are set and finaly picture 4.29 shows how does the integration routine works.

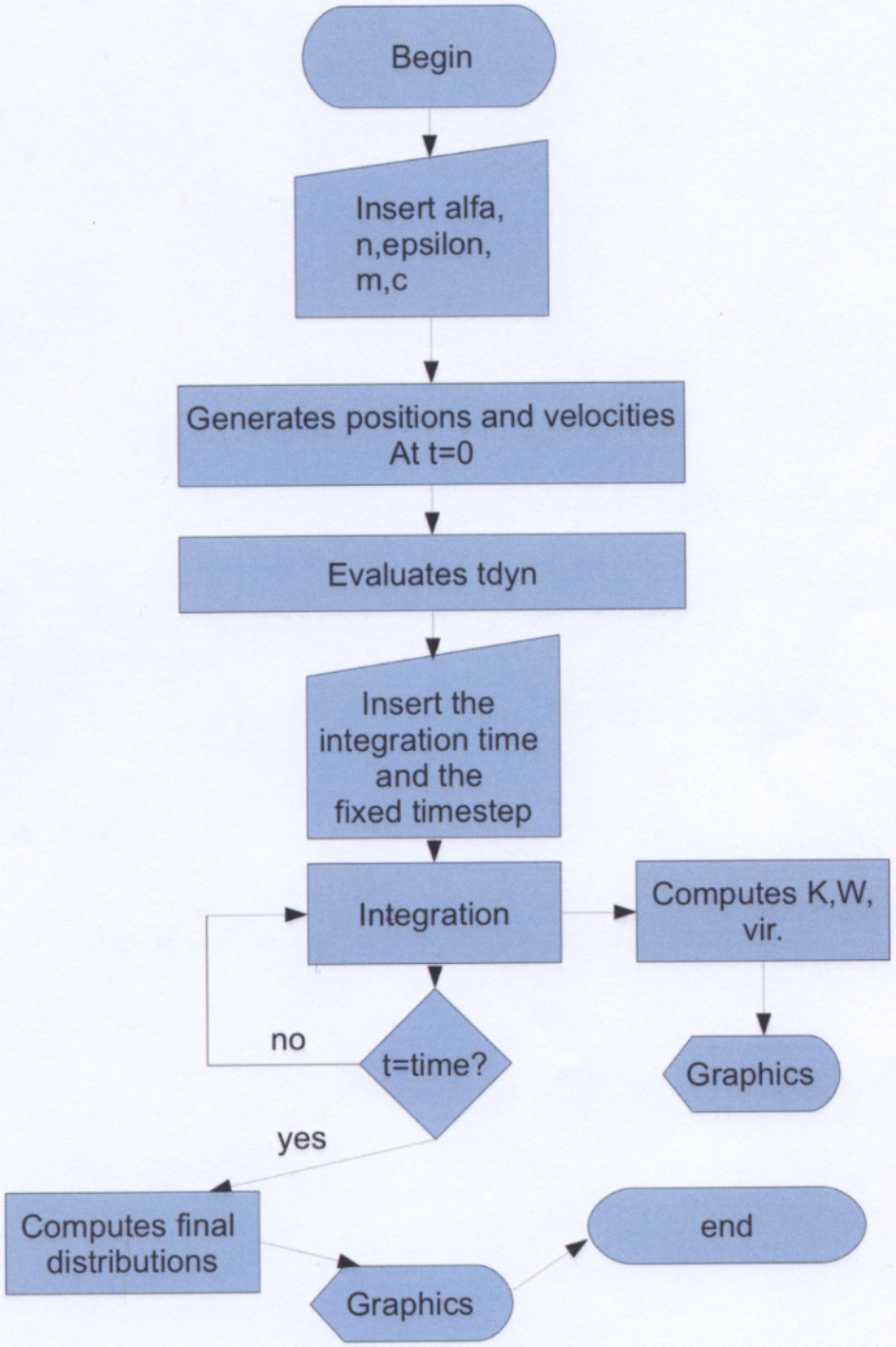

Figure 4.27: A basic sketch of the code's functioning

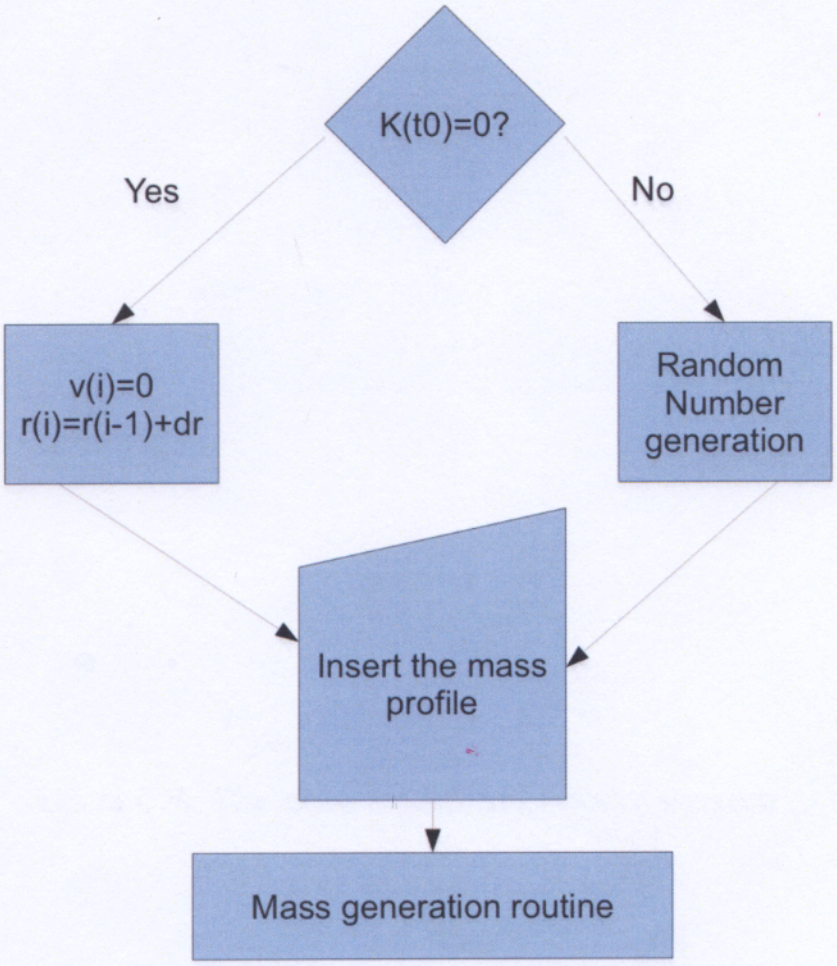

Figure 4.28: The initial conditions generator segment.

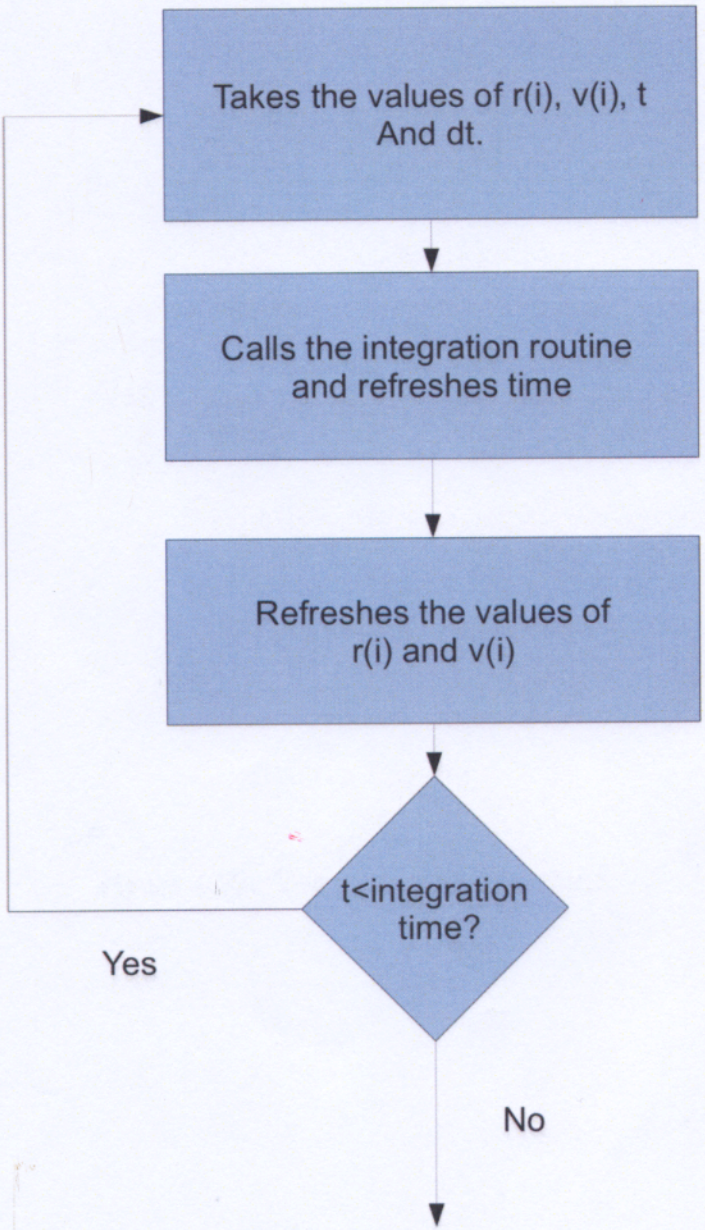

Figure 4.29: The integration segment.

Chapter 5

Discussion and conclusions

Herein we summarize the main conclusions arising from the result of the experiments presented in the previous chapter. In the end there is a final general discussion where we illustrate the possible future developments of these studies.

5.1 General Results

In this work we have studied different aspects of relaxation in dynamicla systems with long-range interactions, with numerical techniques already consolidated for Gravity in the astrophysical context.
We have found out that some features are essentially the same for all the experimented $1/r^{\alpha}$ forces while others are peculiar of some specific exponent α.
The first point that has to be mentioned is that the evolution of the virial ratio has the same trend in all the cases. Starting from the same $K = 0$ and uniform density profile configuration, the explored systems increase their virial ratios from the inital 0 value with a violent jump that in some cases takes two orders of magnitude. This always happens between 0.8 and 1 t_{dyn}. After that, the viral ratio violently decreases and then starts to oscillate around 1 with a noisy beheaviour. The only significant exception happens for $\alpha = 1.2$, fig. 4.19(a): In this case between the first peak and the oscillating phase there is a phase that looks like a logarithmically dumped decrease. This may happen because 1.2 is closer to 1 (logarithmic potential). In this last case, partially explored in Appendix B a similar trend for $2K/|W|$ is evident in fig. B.4(c).
Confronting for each exponent the phase space at 0.5 dynamical times with the phase space at 5 dynamical times we note that between those two times we have the major changes in the phase space asset.
It is between these two times that the jump occurs in all cases, this most probably can be interpreted as a clue that some sort of Violent Relaxation mechanism happens for all the explored long range forces and perhaps for all the forces of the same kind. Reproducing the exposed experiments with different non equilibrium initial conditions lead essentialy to the same trends in all cases, so we conclude that this feature is not strictly correlated with the chosen initial conditions but is intrinsic to the dynamics of that kind of forces.
Another important point is that the energy distribution appears almost in all the cases particulary similar to a Maxwell distribution while the velocity distribution $n(v)$ is nicely Gaussian. This fact is very important because it demonstrates that the assumptions of Statistical Mechanics are still valid for all those fictious long-range interaction systems.
On the other hand some interesting differences that create a rough subclassification among $1/r^{\alpha}$ interactions have been noticed. When the parameter α is between 1 and ~ 2 the systems have a well defined long range behaviour, that is to say global effects dominate over the small scale effects, relaxation times are smaller and chaos originates from a definite region of phase space and then spreads around. By contrast when α is greater than 2 (shorter range) the system shows hybrid features. The long range nature is still evident but in particular the evolution in phase space is different as chaotic point start to be evident in different zones while the collec-

tive structure is still poorly mixed (fig. 4.16(a)). This is typical of short-range interactions systems where the information takes longer times to spread from a point of space to another while, in long-range systems also two points that are far are connected.
In systems with $\alpha > 2$ we have also found out that the probability of having dynamical evaporation is higher. This is intuitive because in longer range systems the turning point of velocity happens at an inferior radius due to the longer range of the potential itself. Apart from this classification it has been seen that the $1/r^2$ force is the one that in spherical dissipationless collapses mixes better the phase space. This arises from the fact that in spherical symmetry the effect of the second Newton's theorem boosts locally the effect of energy exchange between two crossing dust shells.
One last fact that has to be mentioned is the non-linear, non-metric case of MOND that is explored in Appendix B. Essentially the present work has confirmed with 1-d simulations the results obtained in [14] and [38] for 3-dimensionl systems using this time a direct summation algorithm instead of a particle-mesh code.
We have shown that even in the case of unidimensionl pointlike gravitating masses the MOND has a longer timescales for the phase mixing and the virial ratio oscillations are higher than those of the Newtonian gravity.
One more thing concerning modified gravity that has been shown here is that, even if in the deep regime MOND has a $1/r$ asymptotic trend the structure of phase space and the evolution of quantities like total kinetic energy or the virial ratio are completely different from the pure $1/r$ with logarithmic potential case.
To summarize all, we can say that with this Thesis we have first found out, that a violent relaxation process happens for all long range inverse power law interactions, so this is not specific of Newton law or $1/r^\alpha$ law, (Levin et al. have already shown (2008) [31] that Lynden-Bell's theory of Violent Relaxation applies also for plasmas); second that there are some kind of $1/r^\alpha$ forces that have a pure long range beheaviour while other have a mixed nature and show some short range forces features such as evaporation, and third that the results about phase mixing in MOND by Nipoti et al. are solid because essentially a different code simulating a different system with a force in the same regime gives the same final conclusions.

5.2 Open problems

There is still a large amount of open problems concerning relaxation with long-range interactions, in particular when the interaction is gravity. We have mentioned some of them in the outline and in section 2.4 and here we are simply reminding some of the most important. At the state of the art the main problem concerning relaxation in astrophyical and cosmological context is related to the

time that it needs for these processes to take place. From a more general point of view it has to be mentioned that a complete theory that contains collisional and collisionless mechanisms is still missing.
The description of galaxy formation and evolution lacks of a complete treatment of how the non collisonal effects of resonances are important. Another important point is how structures other than spherical or spheroidal, such as disks or tori, relax to their seeming stable configuration and how effectively the Dark Matter halo works in these processes. Further on, at the present time we still lack of a cosmologically consistent structure formation theory in modified dynamics, this last point is particularly hard because it would imply some major changes in the current Cosmology's Standard Model. From the studies of Pogorelov and Kandrup (2003, [40]) that generalized to long range interactions the numerical experiments of thermalization in linear lattices originally done by Fermi, Ulam and Pasta [20], it is known that for long range interactions the energy trapping in certain oscillatory modes is even stronger than the short range case. It would be interesting in an astrophysical context to comprehend how this phenomena works in gravity and in particular if it has direct implication in Galactic Dynamics.

5.3 Possible future studies

We now give a list of some possible future aims for the studies around the topic of this Thesis. The first intersting point is to perform other numerical experiments considering the angular momentum, in order to experience how does the radial orbital instability works in the different $1/r^{\alpha}$ force systems. We have to remark that our experiments were all in spherical symmetry and so it would be also interesting to study systems with different symmetries and in the case of ellipsoidal shape to find exactly how the collisional and collisionless relaxation are correlated with the ellipticity. Adding other spatial degrees of freedom introduces other non trivial effects that need still to be studied. To do so performing direct $N-$body simulations will be necessary. Since the energy distribution in a MONDian system has never been treated nor derived from a Statistical Mechanics point of view, it is certainly a nice challenge for the future to try to derive it for a symple spherical system in the wisdom of Antonov's work [2] for Newtonian gravity. Some hints coming from numerical simulations [38] are in the direction that such distribution differs from the usual Maxwellian that in the present work was found to be nicely valid for almost all the tested linear long range interactions.
One last thing that has to be explored in the future is the correlation or not of the final relaxed state with the initial conditions. Our experiments were simply a toy model to emphasize the fundamental properties of long range systems, making finer and more accurate experiments will certainly show some features that we

have not seen in the present work.

Appendix A

Two body relaxation time with $1/r^{\alpha}$ force

We now give a rough extimate of the t_{2b} for a $1/r^{\alpha}$ gravity-like force. See [8] and [44] for the explicit calculations in the gravitational case. Let us consider a test particle of mass m_1 and velocity $\vec{v}$ moving towards a spherical distribution of N particles of the same kind of masses $m_1 = M_{tot}/N$ interacting via a force Cm_1/r^{α}, we now focus on a single weak scattering with a field particle. Defining the impact parameter b as

$$b = \frac{L}{\mu V(+\infty)} \tag{A.1}$$

where μ is the reduced mass and L and $V(+\infty)$ are the moduli of the total angular momentum in the baricentric frame and asymptotic relative velocity, we can say roughly speaking that the acceleration Cm_1/b^{α} due to m_1 on m_2 acts for an effective time $2b/v$ and produces a component Δv barely perpendicular to the unperturbed direction of $\vec{v}$

$$\Delta v = \frac{2Cm_1}{b^{\alpha-1}}. \tag{A.2}$$

At this point if $\Delta v \ll v$ we can say that the deflection angle Ψ can be expressed at the first order as

$$\Psi \simeq \frac{\Delta v}{v} + \mathcal{O}(\Delta v^2), \tag{A.3}$$

if we choose for typical b the mean particle separation $\sqrt{M_{tot}/\rho}$ and for typical square v the total potential by unity of mass that we neglect but approximate as

$CM_{tot}/(\alpha-1)R^{\alpha-1}$ where R is the radius of the system, we have that the average scattering angle is

$$\tilde{\Psi} \approx \frac{\Delta v}{v} \approx \frac{2(\alpha-1)}{(\frac{4\pi}{3})^{\frac{\alpha-1}{3}}} N^{-\frac{4-\alpha}{3}}. \tag{A.4}$$

We now want an approximate expression for the mean square velocity change that is function of the contribution of all the scattering events. We now take $m_2 = m_1 = m$, and consider the average number of scattering events occouring to a particle with velocity between v and $v + dv$ and having impact parameter between b and $b + db$, such number is

$$dn = 2\pi f(v,t) v dt db dv \tag{A.5}$$

where $f(v,t)$ is now the velocity distribution. We now make the strong assumptions that $f(v,t)$ in the neighborhood of every particle is isotropic and does not changes in time, this is formaly true only in the steady state, so we can neglect the dependance on time and simply write $f(v)$. Multiplying both sides of the last equation by the square of the velocity change we have to integrate

$$\int_0^{+\infty} \int_0^{t_*} \int_{b_{min}}^{b_{max}} \frac{8\pi f(v) C^2 m^2}{v b^{2\alpha-3}} dv dt dv = (\Delta v)^2 \int_1^N dn. \tag{A.6}$$

With the previous assumptions the integration in dv of $f(v)/v$ leads to the average inverse velocity $n\langle v^{-1}\rangle$, the integraton over b is simply:

$$\int_{b_{min}}^{bmax} \frac{db}{b^{2\alpha-3}} = \frac{b_{max}^{4-2\alpha} - b_{min}^{4-2\alpha}}{4-2\alpha}, \tag{A.7}$$

then if we identify $\langle v^{-1}\rangle$ with the inverse of the velocity dispersion σ and we divide both sides by the square of such quantity, integrating over t the l.h.s. of equation A.6 we obtain the total mean square perturbation

$$\left(\frac{\Delta v}{\sigma}\right)^2 \approx \frac{8\pi C^2 m^2 N}{\sigma^3} \left(\frac{b_{max}^{4-2\alpha} - b_{min}^{4-2\alpha}}{4-2\alpha}\right) t_*. \tag{A.8}$$

In order to define the two body relaxation time for collisional relaxation t_{2b}, as it is usually done for gravity we set $\Delta v/\sigma = 1$ and then taking $Nm = M_{tot}$ we evaluate t_* obtaining

$$t_{2b} = \frac{\sigma^3}{8\pi C^2 m M_{tot}} \left(\frac{b_{max}^{4-2\alpha} - b_{min}^{4-2\alpha}}{4-2\alpha}\right)^{-1}. \tag{A.9}$$

Notice that if $\alpha = 2$ like in the gravitational case the last expression is indetermined, this is due to the fact that the integration in db gives in this special case a logarithmic term $\ln(b_{max}/b_{min})$ that for an oculated choice of b_{min} and b_{max} can be substituted with $\ln(N)$, the so called Coulomb logarithm. in our (more general) power law force we can simply put $b_{min} = 0$ because here we have no ultraviolet divergence and $b_{max} = \tilde{R}$ where $\tilde{R}$ is the radius where the average kinetic energy of the particles is around one half of their potential energy in the system

$$\tilde{R} \approx \left(\frac{CmN}{\langle v \rangle^2} \right)^{\frac{1}{\alpha - 1}}, \tag{A.10}$$

so plugging these last constraints into equation A.9 we finally obtain that for a general $1/r^\alpha$ interaction the two body scales as

$$t_{2b} \approx N^{\frac{2\alpha - 4}{\alpha - 1} - 1} \tag{A.11}$$

with the number of particles in the system. In order to estimate numericaly the trend with α of dynamical friction's efficiency we have preformed a set of direct integrations of the trajectorys of particles suffering from long range scatters in background of fixed targets for different values of the parameter. We have taken as our index of energy's redistribution the quantity $\tilde{k}$ that we have called decorrelation parameter, defined as

$$\tilde{k} = \sqrt{\frac{1}{N_c} \sum_{i=1}^{N_c} \left(k_i \frac{1}{N_c} \sum_{i=1}^{N_c} \int_0^{t_*} \frac{\partial k_i}{\partial t} dt \right)^2} \tag{A.12}$$

where N_c is the number of sampled orbits, k_i one paricle's kinetic energy and $\partial k_i / \partial t$ is its variation during time over its orbit. The strategy and the code used are very simple, for first the code generates with a Box-Muller algorithm a random distribution for 10^4 particles with positions projecitons x_i, y_i, z_i and initial velocities with components vx_i, vy_i, vz_i, the velocity distribution is then normalized to one while the positions were set inside a sphere of radius 4 in scaled unities. After choosing a number N_c of test particles (say for example 100) it performs N_c times a one body problem inside a frozen distribution of scatterators. During the orbit integrations the code computes test particle's kinetic energy variations and evaluates its time integral from $t = 0$ to $t = t_*$, the simulation's time. In the end, after doing this for all the sampled particles $\tilde{k}$ is calculated. We repeated the experiment for different α, the results are in table A.1.

α	$\widetilde{k}$	$\langle k \rangle$
1	6.04×10^{-5}	2.92×10^{-5}
1.2	5.86×10^{-5}	2.53×10^{-5}
1.4	5.77×10^{-5}	2.34×10^{-5}
1.6	5.98×10^{-5}	2.62×10^{-5}
1.8	7.19×10^{-5}	2.95×10^{-5}
2	2.54×10^{-4}	7.80×10^{-5}
2.2	3.74×10^{-3}	6.55×10^{-4}
2.4	0.19	2.17×10^{-2}
2.6	6.54	0.92

Table A.1: Trend of the decorrelation parameter $\widetilde{k}$ and the mean integral kinetic energy exchange $\langle k \rangle$ with α from simulations with 10^2 on 10^4 sampled particles. In all the experimens the integration is carried on for 10 dynamical times and the softening lenght is fixed to $8 \cdot 10^{-3}$ that is an average value tha keeps the error on the force under the 20%. For the studied interactions the trend of the energy exchange has first a decrease between $\alpha = 1$ and $\alpha = 1.4$ and then increases.

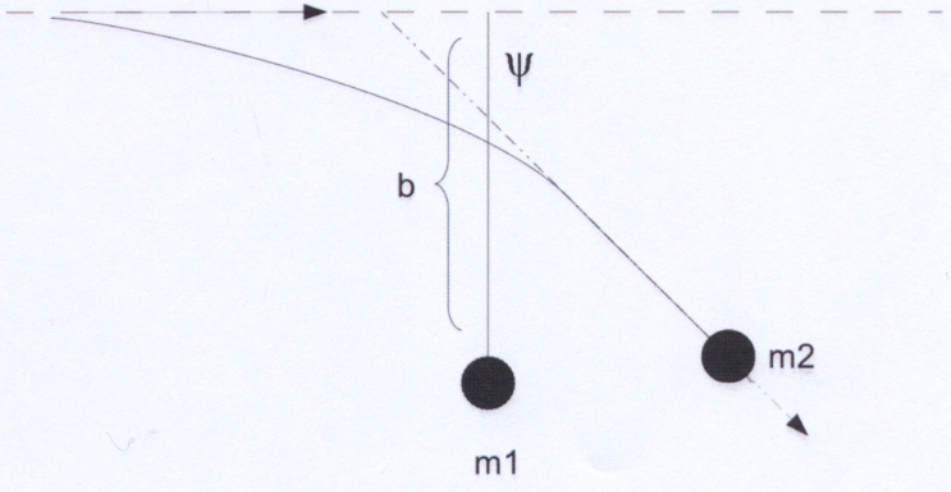

Figure A.1: Orbit of a deflected particle.

Appendix B

The MOND case

In this appendix we will make some considerations about MOND, although this theory is more complex, having non linear field equation it is intresting because of its $1/r$ asymptotic trend which makes of MOND a more-than-gravity long range interaction. Here after a brief introductory review we give only a bunch of very simple arguments and we hope that these will set the basis for further studies in that direction. Modified dynamics was first introduced by Milgrom in 1983 ([34]) to solve the problems of the missing mass and the rotation curves of disk galaxies in an alternative way. He proposed along with Bekenstein in an action derived theory ([5]) a replacement of the Poisson field equation for the gravitational potential with

$$\nabla \cdot \left[\mu \left(\frac{\| \nabla \phi \|}{a_0} \right) \nabla \phi \right] = 4\pi G \rho \tag{B.1}$$

where $a_0 \simeq 1.2 \cdot 10^{-10} m s^{-2}$ is a scale acceleration and μ is a constraint funcion such that $\mu(y) \sim y$ when $y \ll 1$ (deep MOND regime) and $\mu(y) \sim 1$ when $y \gg 1$ (Weak MOND regime, say Newtonian regime[1]). It is immediately evident the higly non linear nature of this theory i.e. the potential intensity itself is related to the ratio of the field and a newly introduced nature's constant a_0; this implies that the motion of a particle inside a MONDian field is more strictely influenced by the local changing of the field rather than its position inside the distribution of matter. It is interesting to express equation B.1 in terms of the related Newtonian field $\vec{g_N} = -\nabla \phi_N$ associated to the same distribution of mass ρ. If we eliminate the last using the two field equations we obtain

$$\nabla \cdot \left[\mu \left(\frac{\| \nabla \phi \|}{a_0} \right) \nabla \phi - \nabla \phi_N \right] = 0; \tag{B.2}$$

[1] In fact when $\mu(\| \nabla \phi \| / a_0)$ is exactely 1 one obtains the classical Poisson equation $\Delta \phi = 4\pi G \rho$

by the means of a vectorial identity we can write the last equation as

$$\mu\left(\frac{g}{a_0}\right)\vec{g}=\vec{g_N}+\nabla\times\vec{h} \tag{B.3}$$

where $\vec{g}$ is the MONDian field and $\vec{h}$ is a certain vectorial field. When such field can be neglected one obtains that the the force $\vec{F}$ acting on a particle of mass m is related to the the acceleration $\vec{a}$ by

$$\vec{F}=m\mu\left(\frac{a}{a_0}\right)\vec{a} \tag{B.4}$$

so that the modified field and the Newtonian field are related by

$$\mu\left(\frac{g}{a_0}\right)\vec{g}=\vec{g_N}\,. \tag{B.5}$$

It has been demonstrated in [5] that for particular symmetries of the mass distribution (spherical, cylindrical or planar) and in the limit of great distance, the curl term in B.3 vanishes; in this case the relation B.3 reduces

$$g^2 = a_0 g_N. \tag{B.6}$$

As one can see the MOND as an inertia modifing theory [35] it must be noticed also that the dynamics of a particle is influenced also by its mass and velocity. The most important fact is that in this wisdom the superposition principle is not valid anymore, so basicaly MOND would be outside of our models. We decided to include it in our discussion because of its asymptotic long-range beheaviour, and in particular for its strangeness in relaxation. We now present a discussion on dynamical friction in MOND, basically following [13] and [37]. Consider two barely equal masses m_1 and m_2, it has been shown that in the deep regime the force exchanged between the two is

$$F \simeq \frac{m_1 m_2}{\sqrt{m_1+m_2}}\frac{\sqrt{Ga_0}}{r}=\frac{Gm_1m_2}{rr_0}, \tag{B.7}$$

where r is their spatial separation and

$$r_0 \equiv \sqrt{\frac{G(m_1+m_2)}{a_0}} \tag{B.8}$$

is a MOND scale radius that for stars of $\sim 1M_{sun}$ is of the order of 10^{17}cm that is smaller than the average star distance in normal systems. This leads to nearly

all the encounters being in the deep regime. Taking m_1 and m_2 to be equal to m and using as we have done in appendix A the impulsive approximation, the perpendicular variation Δv of the asymptotic velocity $\vec{V}$ is

$$\Delta v \simeq \frac{2b}{V}\frac{F(b)}{m} = \frac{2Gm}{r_0 V}. \tag{B.9}$$

Notice that the impact parameter b vanishes from this last formula and so in the deep MOND regime the deflection is independent from the impact parameter. In a system of N stars with scale radius R (for example the half-mass radius) and total mass $M = Nm$ the number of encounters with impact parameter between b and $b + db$ is

$$dn = \frac{N}{2\pi R^2} 2\pi b db = \frac{Nb}{R^2} db, \tag{B.10}$$

again as we have done for the general $1/r$ force we write in integral form the quadratic cumulative velocity change

$$\Delta v^2 = \frac{N}{R^2}\left(\frac{2Gm}{r_0 V}\right)^2 \int_0^R b db = 2N\left(\frac{2Gm}{r_0 V}\right)^2. \tag{B.11}$$

Now if we define the crossing time for MOND as

$$t_{cross} = \frac{R}{v_{typ}} \tag{B.12}$$

where v_{typ} is the typical velocity in a MONDian system defined as $v_{typ} = (GMa_0)^{1/4}$, we write the two body relaxation time t_{2b} in function of t_{cross} as

$$t_{2b} \simeq \frac{v_{typ}^4 r_0^2 N}{2G^2 M^2} t_{cross}. \tag{B.13}$$

At this point by substituting the expressions for r_0 and v_{typ} into the last relation one can notice immediately that in deep MOND regime systems, the collisional relaxation scale t_{2b} is almost equal to the crossing time; this arises from the important fact expressed by equation B.9 that distant encounters produce larger velocity changes compared to the Newtonian case making larger contributions to the collisional relaxation's efficency. Referring to [13] comparing the t_{2b}^M in a MOND system and the t_{2b}^N in a Newtonian system with the same number of stars but embedded in a proper Dark Halo it has been shown that

$$\frac{t_{2b}^M}{t_{2b}^N} = \frac{\sqrt{2} g_0^2}{a_0^2} \tag{B.14}$$

where g_0 is a uniform gravitational field around which whe have to expand equation B.1. Writing the last in the deep MOND regime and eliminating a_0 we obtain

$$\frac{t_{2b}^M}{t_{2b}^N} = \frac{\sqrt{2}g_N^2}{g_0^2} = \frac{\sqrt{2}}{(1+\mathcal{R})^2} \tag{B.15}$$

where $\mathcal{R}$ is the ratio of the Dark Matter mass costituting the halo in the Newtonian system to the stellar mass (equal in both models). We have to point out that this treatment of dynamical friction in modified dynamics is little naive, in fact due to the non linearity of the field equation and our basic ignorance on the real form of μ the degree of approximation is higher compared to the treatmant of calssical gravity, moreover there is another questionable point, in MOND every orbit is bounded, i.e. we do not have for example hyperbolic orbits, so impulsive approximation itself theoreticaly crumbles because of the arbitrariety of the so called close interaction time. We now review what we currently know from numerical simulations about the Phase Mixing in modified dynamics, these results can be found in [14] and [38]. At the state of the art the knowledge of this aspect of dynamical evolution in modified dynamics systems is quite poor; due to the non linearity of the field equation an analytic treatment is particulry threacherous and also pure MOND numerical simulations present a lot of important difficulties. Currently the only complete MOND 3-dimensional N-body experiments are those made in 1999 by Brada and Milgrom [9] to study the stability of disk galaxies and those by Tiret and Combes in 2007 to study the bar formation and the external field effect. Other efforts have been meade during the previous years setting arbitrarely to 0 the curl term contribute. The simulations of MONDian dissipationless collapse made by Nipoti, Londrillo and Ciotti ([14] and[38]) with a modified gravity particle-mesh N-body code showed essentialy that the Phase-Mixing is less efficent than in Newtonian theory plus Dark Halo's contribution; contemporarely it was also found that the projection of final relaxed stellar distributions well fit the Sersic law (equation 2.38) with m between 2 (deep MOND) and 4. In those experiments the systems have spherical symmetry in order to formaly reduce $\nabla \times \vec{h} = 0$. As one can see from the graphs in the next page coming from a radial collapse experiment with frozen angular component, for the deep MOND systems the virial ratio shows long last oscillations while in the Newtonian case it relaxes to one with less scatter.

All these results are a clear prove that stellar systems in MOND have a relaxation process that is completely different from the Newtonian description. In classical gravity's scenario galaxies and clusters move towards the equilibrium configuration through a Violent Relaxation phase and dynamical mixing process, collisional systems as the globular clusters relax via dynamical friction and eventualy environement driven pulsations, by contrast in MOND it seems that the dynamical friction is more efficent also for galaxies, while the Phase Mixing has longer time

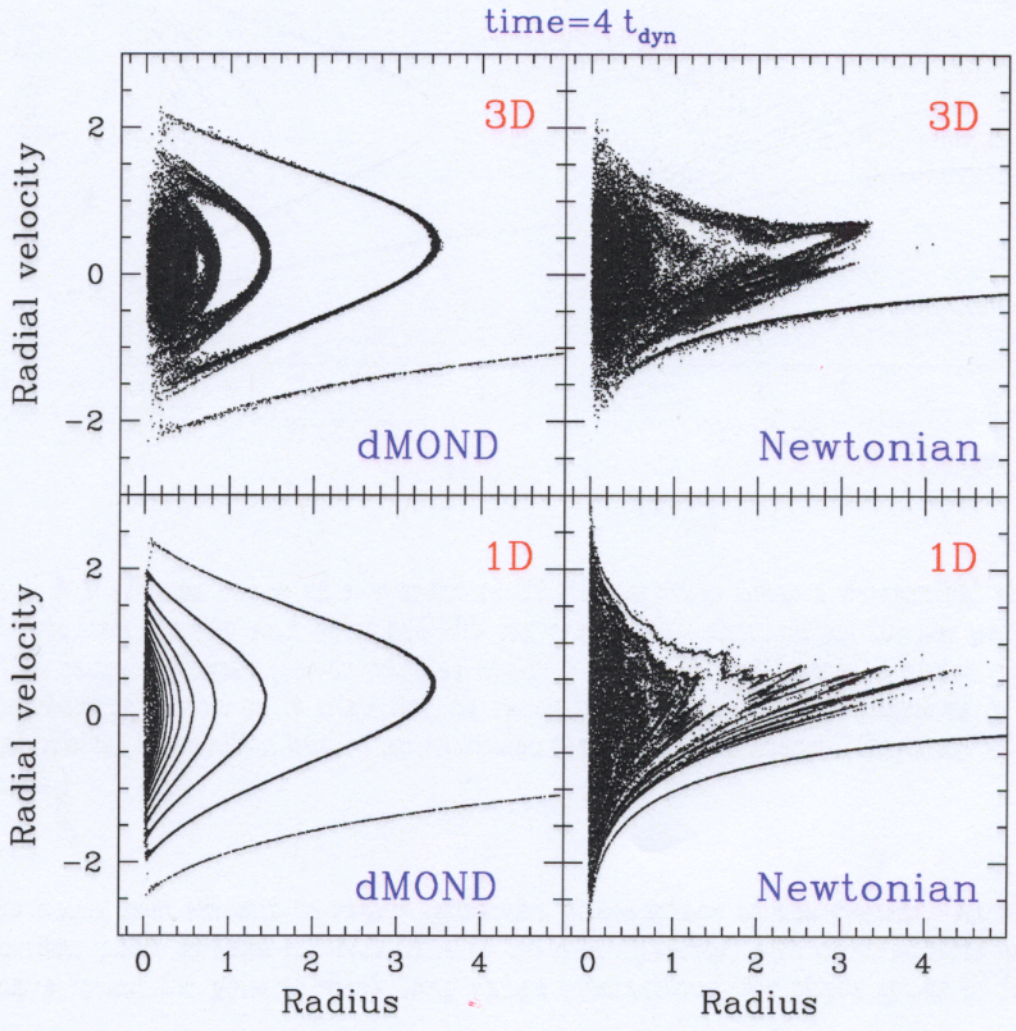

Figure B.1: Phase space of a system of 32000 particles after 4 dynamical times in Newtonian gravity and deep MOND regime. In 3D simulations (upper panels) and 1D radial collapse (lower panels) MOND shows in both cases a minor phase space reorganization so it may not be recondicted to a different efficence of the radial orbital instability but to an intrinsec feature of the theory.(Courtesy of the authors.)

scales being less efficent in rearranging the phase space of the system. Another important point is that MOND (due to its non linearity) also contraddicts what we have found for generic weak long range interactions, for those types of force

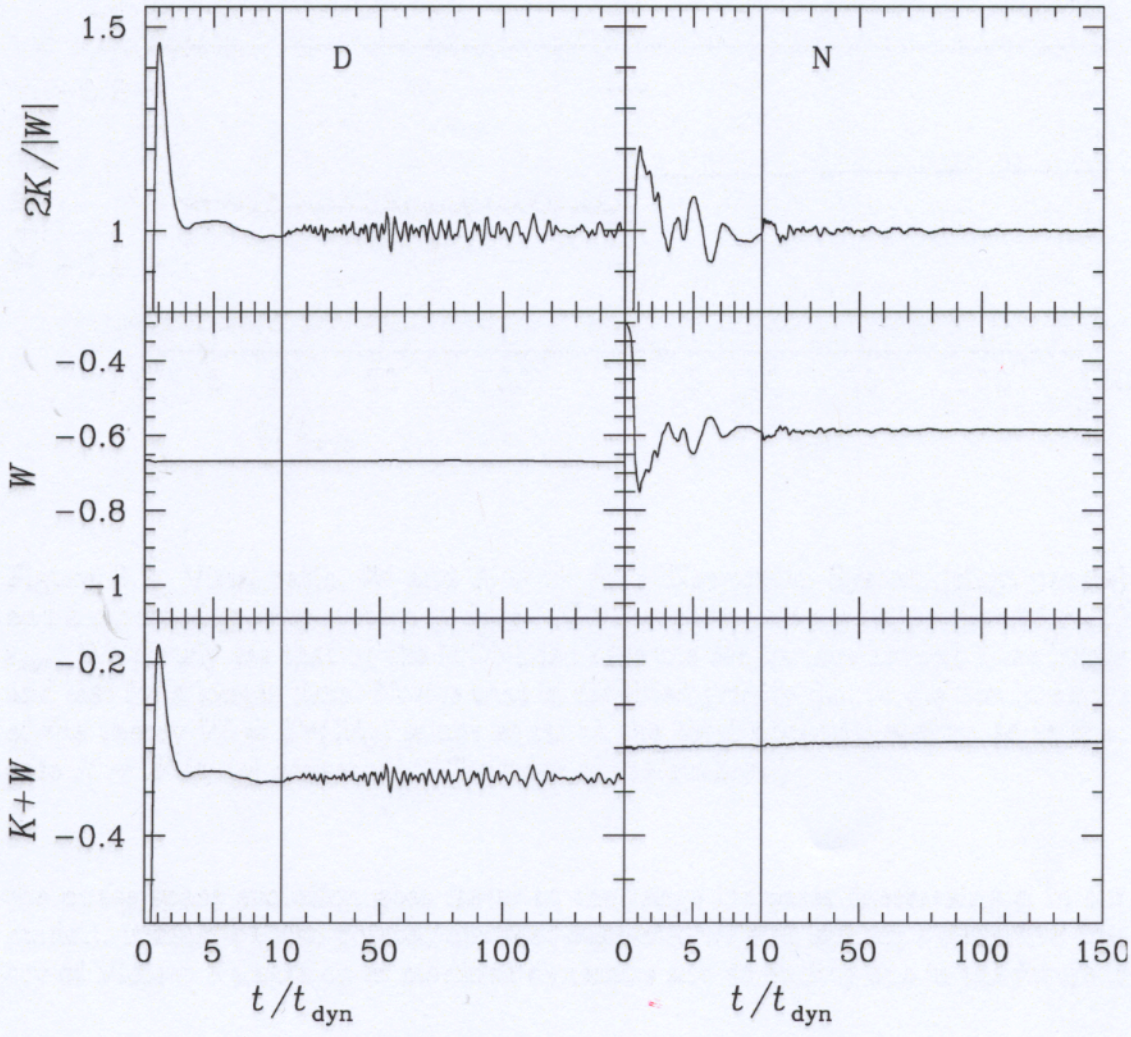

Figure B.2: Virial ratio, W and $K + W$ for a Newtonian System (right panels) and a modified gravity system in deep MOND regime (left panels), evolved for 150 t_{dyn}. We clearly see that in the MONDian case the oscillations around 1 are larger and last for a longer time. Notice that in modified gravity due to the non linearity of the theory $W = Tr(W_{ij})$ is not equal to the total potential energy, so in that case $K + W$ is not conserved. (Courtesy of the authors.)

the phase space evolution goes faster as the range increases (decreasing α in our model). it must be also pointed out that currently we still lack for a definitive theory of Violent Relaxation in modified dynamics and so finding one in the future it

would be a very interesting challenge for further studies. In the present work we have also used our code to perform simulations of 1-d systems with equal masses interacting via $1/r^2$ Newtonian gravity, deep MOND regime and $1/r$ force. In the experiments this time we do not consider shells but instead point masses arranged on a row[2], as was experimented with Newtonian gravity by Gabrielli et al. [21] in a cosmological context. We have considered ghost particles (in the sense that during a collision they cross each other) and so the situation is pretty unphysical, indeed this is not a problem because we are only intersted in phase space rearranging and virial ratio evolution. At $t = 0$ the particles have been set immoble and equispaced so that initially the total kinetic energy and the virial ratio are both zero, we defined the dynamical times for Newton gravity, deep MOND and $1/r$ force as

$$t_{dyn}^{N} = 2r_e^{3/2}(GM)^{-1/2}, \tag{B.16}$$

$$t_{dyn}^{dM} = 2r_e(GMa_0)^{-1/4} \tag{B.17}$$

and

$$t_{dyn}^{1/r} = 2r_e(|CM\ln(r_e/2)|)^{-1/2} \tag{B.18}$$

where r_e is taken as the scale radius of the system and M is the total mass. We have chosen for the stellar cases a normalization where $M = G = 1$ so that $a_0 \sim 0.18$ and in the $1/r$ fictious interaction we arbitrarely set the coupling constant C also equal to 1. the systems then have been evolved in each case for $30t_{dyn}$; during the integration the code took snapshots of the phase space at certain fixed times and computed the virial ratio $2K/|W|$ and the Jacobi identity $\ddot{I} = 2K + W$. The experiments showed that also in one dimensional systems MOND has a significantly longer mixing time as its phase space structure is still poorly mixed after the same number of dynamical times compared to the gravitational case. This is another clear proof that the lower phase mixing efficency is an intrinsec property of dMOND regime and it is not imputable to a different beheaviour of the radial orbital instability. It must be pointed out that the $1/r$ force is the least efficent in mixing; the phase space looks incredibely regular unless the convergence to 1 of the virial ratio seems the most rapid of the three(figure B.3 (c)).

[2]Such arrangement can be reconduced to a particular case of cylindrical symmetry, so for modified gravity the assumption of the curl term being zero can be taken as valid also in our experiments.

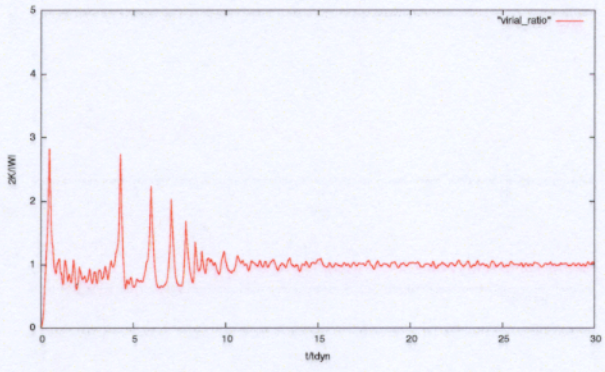

(a)

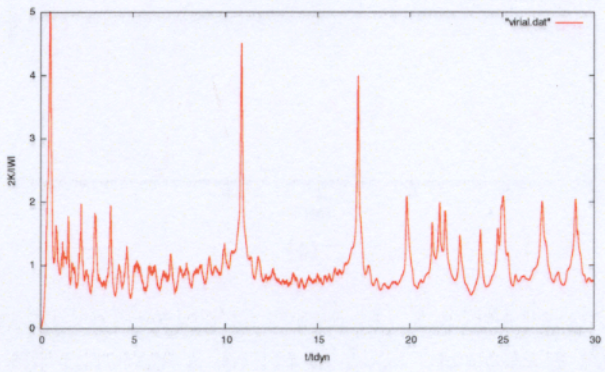

(b)

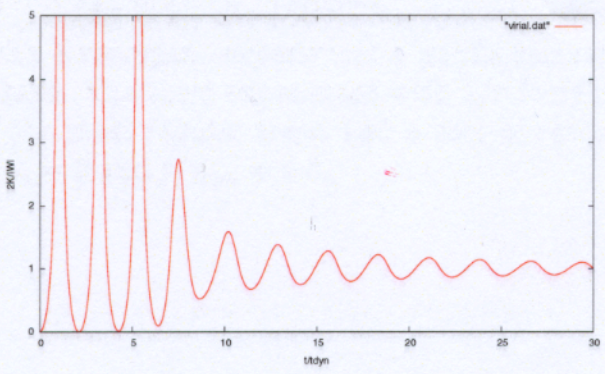

(c)

Figure B.3: Virial ratio for Newtonian sytem (a), modified gravity (b) and $1/r$ force system (c). In our experiments a lattice of 5000 particles is evolved for 30 t_{dyn} in all three cases from an initial cold state (K=0). The simulations are consistent with the results of [14] (fig B.2), the MONDian system shows long lasting noisy oscillations while the Newtonian, experiences a gentle relaxation around 1 after an initial violent phase. The third experiment with $1/r$ force is different from the others as it shows the most regular trend and a sort of recurrence of the initial frozen state at $t/t_{dyn} = 2$ and $t/t_{dyn} = 4.5$.

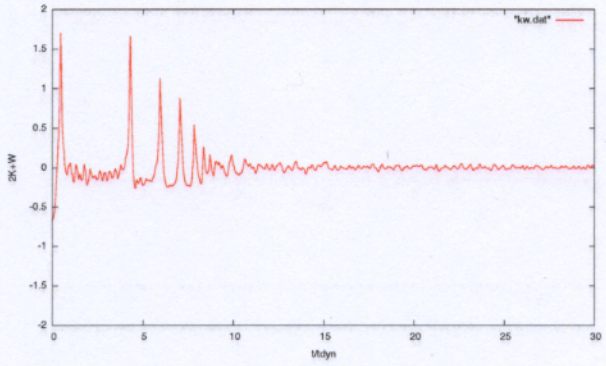

(a)

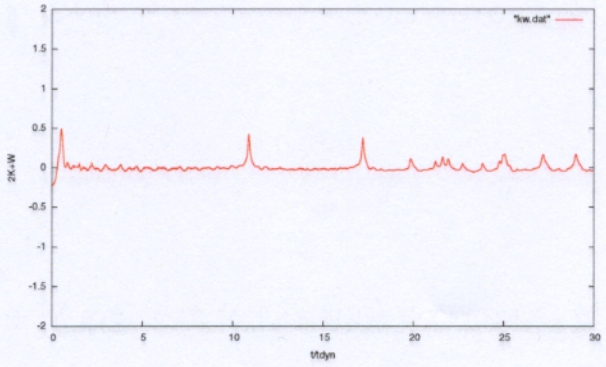

(b)

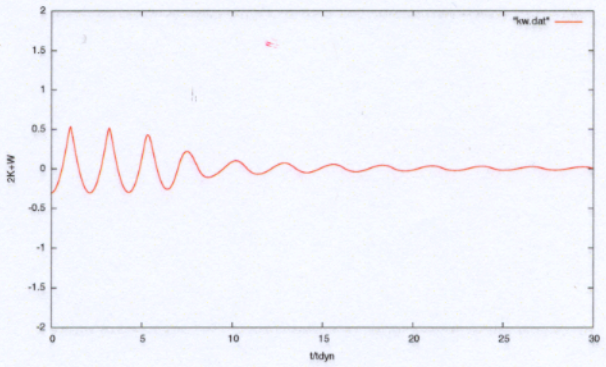

(c)

Figure B.4: $2K + W$ evolution for the same experiments of previous panels.

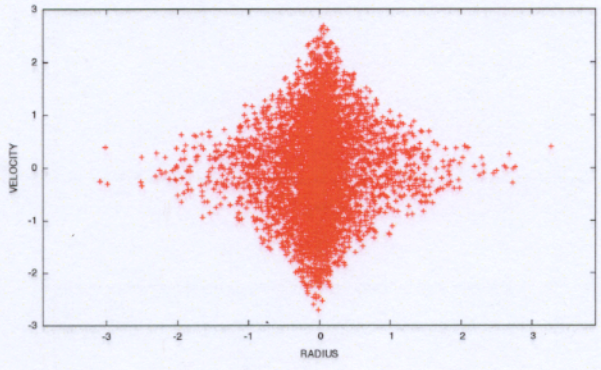

(a)

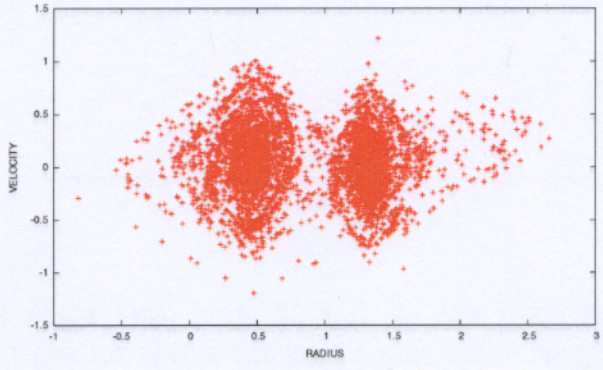

(b)

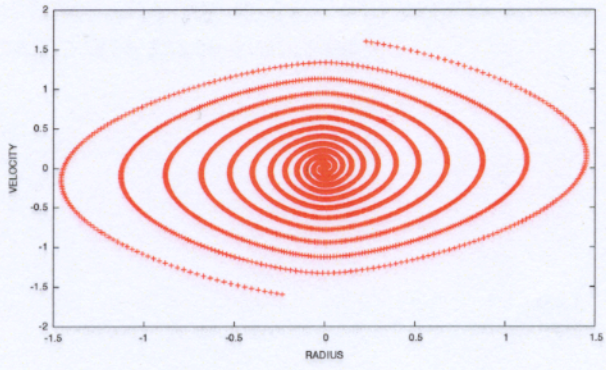

(c)

Figure B.5: Phase space asset after 30 t_{dyn} for the three experiments. Notice that the Newtonian system shows the best phase space rearrangement, dMOND is divided in two subsystems and is still manifesting some sort of regularity while $1/r^{\alpha}$ looks still unmixed. Gravity in dMOND regime and $1/r^{\alpha}$ law do not show any similarity in their phase space evolution.

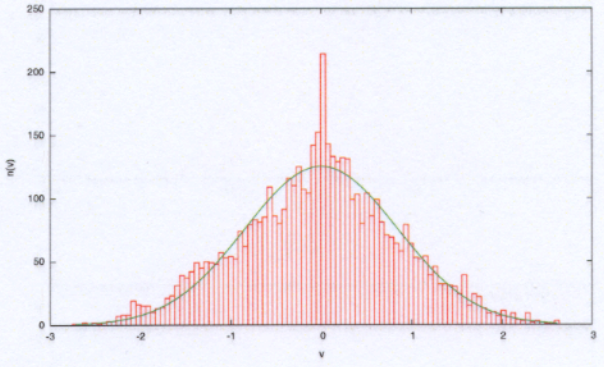

(a)

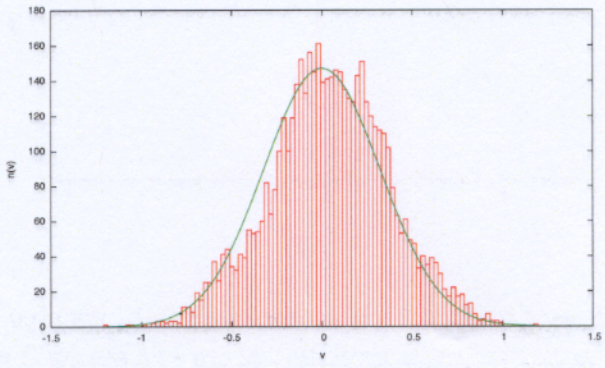

(b)

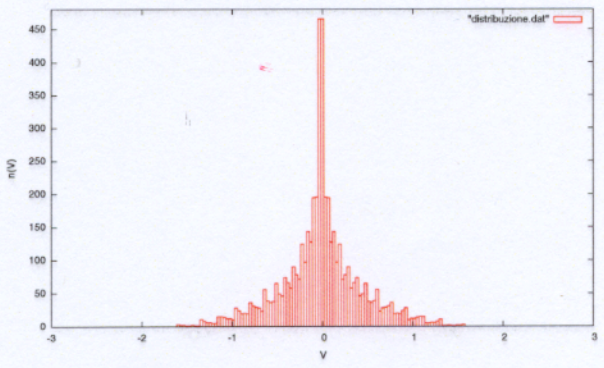

(c)

Figure B.6: Final velocity distributions $n(V)$ for the three models. The initial distributions at $t = 0$ where the same (uniform distribution $v_i = 0$).

Appendix C

The code's listing

Here we add the FORTRAN 90 listing of the code that we have wrote and used in almost all the numerical experimens of this thesis. After the CONTAINS statement at the end of the main one can find the subroutines that execute the different procedures. They can be changed at need or put in separated files to be included in the main.

```
PROGRAM powerlawforceshells

implicit none

!data declaration and parameter settings

real*8 :: finaltime,timestep,time,constant,alpha,kinetic,potential,step,&
energy,energy0,potential0,kinetic0
real*8 :: tdyn,rmax,rmin,vir,radius,w,i2dot,mtot,plw
real*8,allocatable,dimension(:) :: positions0,velocity0,positions,&
velocity,tot,pe,self0,field0,velocity1,potential00&
,griglia,mass,densy,gr,distro
integer :: nshell,i,ci,cj,mp,vp,tempi,tss,t05,t1,t5,t10,t20,t50,t100

write(*,*)"insert the number of shells used in the simulation,&
 (the total mass will be always 1)"
read(*,*) nshell

write(*,*) "insert the exponent of the 1/r^a law"
read(*,*) alpha

write(*,*)"chose the coupling constant G"
```

```
read(*,*) constant

write(*,*) "press 1 to consider the self-force,2 to neglect it"
read(*,*) ci

write(*,*)"press 1 to use an uniform value of the masses,&
2 for a normal profile,3 for a power-law,4 for two mass families"
read(*,*) mp

write(*,*)"insert the softening lenght"
read(*,*) rmin

!vector allocation

allocate(positions0(1:nshell))
allocate(velocity0(1:nshell))
allocate(velocity1(1:nshell))
allocate(tot(1:nshell))
allocate(pe(1:nshell))
allocate(self0(1:nshell))
allocate(field0(1:nshell))
allocate(distro(1:100))
allocate(griglia(1:100))
allocate(mass(1:nshell))
allocate(densy(1:100))
allocate(gr(1:100))

!setting the mass profile for the shells

if (mp==1) then
do i=1,nshell
mass(i)=1./nshell
end do

else if (mp==2) then
do i=1,nshell
call boxmuller(mass(i))
end do
do i=1,nshell
mass(i)=abs(mass(i))
end do
```

```
else if(mp==4) then
do i=1,nshell
call boxmuller(mass(i))
end do
do i=1,nshell
if (mass(i)<=0.0) then
mass(i)=0.5
else if (mass(i)>0.0) then
mass(i)=0.0005
end if
end do

else if (mp==3) then
write(*,*)"insert the exponent of the mass power-law"
read(*,*) plw
call rejection(mass,nshell,plw)
end if

!normalizing to 1 the total mass of the system

mtot=0.0
do i=1,nshell
mtot=mtot+mass(i)
end do

do i=1,nshell
mass(i)=mass(i)/mtot
end do

mtot=1.0

write(*,*)"insert 1 to start the shells from an initial cold state&
 (K=0),2 to generate random radii and velocities"
read(*,*) vp

if (vp==1) then

step=1./nshell
positions0(1)=0.1
do i=2,nshell
```

```
positions0(i)=positions0(i-1)+step
end do

do i=1,nshell
velocity0(i)=0.0
end do

else if (vp==2) then
do i=1,nshell
call boxmuller(positions0(i))
end do

do i=1,nshell
positions0(i)=abs(positions0(i))
end do

do i=1,nshell
call boxmuller(velocity0(i))
end do

end if

!estimates the dynamical time and asks the&
 parameters for the integration

radius=maxval(positions0)

tdyn=radius/sqrt(constant*mtot/radius**(alpha-1.))

write(*,*) "the estimated dynamical time for the system is:"
write(*,*) tdyn

write(*,*)"for how many dynamical times do&
 you want to integrate? (it must be an integer value)"
read(*,*) tempi

finaltime=tempi*tdyn

write(*,*)"chose the fixed timestep dt"
read(*,*) timestep
```

```
!writes a file with the initial conditions

open(10,file="initial.dat")
do i=1,nshell
write(10,*) positions0(i),velocity0(i)
end do
close(10)

!computes and outputs the initial W, K K+W and 2K+W

kinetic0=0.0

do i=1,nshell
kinetic0=kinetic0+0.5*mass(i)*velocity0(i)**2
end do

call force(nshell,ci,constant,mass,rmin&
,positions0,field0,alpha)

w=0.0

do i=1,nshell
w=w+positions0(i)*mass(i)*field0(i)
end do

vir=2.*kinetic0/abs(w)


write(*,*) "the initial value of K is"
write(*,*) kinetic0

write(*,*) "the initial value of W is"
write(*,*) w

write(*,*) "the initial value of 2K/|W| is"
write(*,*) vir

write(*,*) "the initial value of 2K+W is"
write(*,*) 2.0*kinetic0+w

write(*,*) "the initial value of K+W is"
```

```
write(*,*) kinetic0+w


!advances the velocities of half dt&
! (when the integrator is leapfrog)

do i=1,nshell
velocity0(i)=velocity0(i)+field0(i)*0.5*timestep
end do

!allocates the vectors
!for the new velocities and positions

allocate(positions(1:nshell))
allocate(velocity(1:nshell))

t05=0.5*tdyn/timestep
t1=tdyn/timestep
t5=5*tdyn/timestep
t10=10*tdyn/timestep
t20=20*tdyn/timestep
t50=50*tdyn/timestep
t100=100*tdyn/timestep

time=0.0
tss=0

!integration begins, the code
!opens the files to store K, W 2K/|W| etc.


open(14,file="K.dat")
open(15,file="W.dat")
open(16,file="KplusW.dat")
open(23,file="virial.dat")
open(77,file="2KplusW.dat")
open(333,file="radius.dat")

do while(time<=finaltime)

call integration (positions0,velocity0,positions,velocity&
```

```
,nshell,timestep,mass,constant,rmin,pe,time,ci,velocity1,alpha)

!time is advenced

time=time+timestep

tss=tss+1

!here the code opens the files to store
!the phase space at certains given values of time

if(tss==t05)then
open(50,file="0.5tdyn")
do i=1,nshell
write(50,*) positions(i),velocity1(i)
end do
close(50)
end if


if(tss==t1)then
open(60,file="1tdyn")
do i=1,nshell
write(60,*) positions(i),velocity1(i)
end do
close(60)
end if

if(tss==t5)then
open(65,file="5tdyn")
do i=1,nshell
write(65,*) positions(i),velocity1(i)
end do
close(65)
end if

if(tss==t10)then
open(70,file="10tdyn")
do i=1,nshell
write(70,*) positions(i),velocity1(i)
end do
```

```
close(70)
end if


if(tss==t20)then
open(80,file="20tdyn")
do i=1,nshell
write(80,*) positions(i),velocity1(i)
end do
close(80)
end if


if(tss==t50)then
open(90,file="50tdyn")
do i=1,nshell
write(90,*) positions(i),velocity1(i)
end do
close(90)
end if

if(tss==t100)then
open(100,file="100tdyn")
do i=1,nshell
write(100,*) positions(i),velocity1(i)
end do
close(100)
end if

!computes again the field acting on each shell

call force(nshell,ci,constant,mass,rmin,positions,field0,alpha)

!computes K, W, 2K+W, 2K/|W|

radius=maxval(positions)

write(333,*) time/tdyn,radius


kinetic=0.0
```

```
do i=1,nshell
kinetic=kinetic+0.5*mass(i)*velocity1(i)**2
end do

w=0.0
do i=1,nshell
w=w+mass(i)*positions(i)*field0(i)
end do

vir=2.*kinetic/abs(w)


i2dot=2.*kinetic+w

write(14,*) time/tdyn,kinetic
write(15,*) time/tdyn,w
write(16,*) time/tdyn,kinetic+w
write(23,*) time/tdyn,vir
write(77,*) time/tdyn,i2dot


!the conditions are refreshed

do i=1,nshell
positions0(i)=positions(i)
end do

do i=1,nshell
velocity0(i)=velocity(i)
end do

!the integration is finished

end do


close(14)
close(15)
close(16)
close(23)
close(77)
```

```
close(333)

!computes the fina velocity and energy distributions

write(*,*)"the integration is finished, i compute the distributions"

call distribution(pe,nshell,distro,griglia)

open(44,file="logdistribuzione.dat")
do i=1,100
write(44,*) log(griglia(i)),log(distro(i))
end do
close(44)


open(455,file="distribuzione.dat")
do i=1,100
write(455,*) griglia(i),distro(i)
end do
close(455)



open(11,file="final.dat")
do i=1,nshell
write(11,*) positions(i),velocity1(i),mass(i)
end do
close(11)

call massdist(mass,nshell,densy,gr,positions)

open(199,file="den.dat")
do i=1,100
write(199,*) gr(i),densy(i)
end do
close(199)



open(299,file="logden.dat")
do i=1,100
```

```
write(299,*) log(gr(i)),log(densy(i))
end do
close(299)

call distribution(velocity1,nshell,distro,griglia)
open(45,file="vdistr.dat")
do i=1,100
write(45,*) griglia(i),distro(i)
end do
close(45)

write(*,*)"you can find the plotable files .dat in the current directory"

CONTAINS

subroutine integration (p0,v0,p,v,n,t,m,k,mini,part,tempo,c1,v1,alp)

!this subroutine integrates the system with leapfrog algorithm

integer :: j,l
integer,intent(in) :: n,c1
real*8,intent(in) :: k,mini,tempo,alp
real*8,intent(in) :: p0(1:n),v0(1:n),m(1:n)
real*8,intent(in) :: t
real*8,intent(out) :: p(1:n),v(1:n),part(1:n),v1(1:n)
real*8,allocatable,dimension(1:n) :: total(:),epote(:)

allocate(total(1:n))
allocate(epote(1:n))


call force (n,c1,k,m,mini,p0,total,alp)

do j=1,n
v(j)=total(j)*t+v0(j)
end do

do j=1,n
p(j)=v(j)*t+p0(j)+0.5*total(j)*t**2
end do
```

```
!regolarize the scattering in the origin

do j=1,n
do l=1,n
if (p(l)<=0.0) then
v(l)=-(v0(l))
p(l)=p0(l)
else if (p(l)>0.0) then
p(l)=p(l)
v(l)=v(l)
end if
end do
end do

!interpolates the velocity at t+dt/2

do j=1,n
v1(j)=0.5*(v(j)+v0(j))
end do

do j=1,n
do l=1,n
if (v1(l)==0.0) then
v1(l)=v(l)
end if
end do
end do

!recomputes the field and the particles individual energies

call force (n,c1,k,m,mini,p,total,alp)


!call poten (epote,p,n,m,k,total,mini,alp)

do j=1,n
part(j)=0.5*m(j)*v1(j)**2+total(j)*p(j)*m(j)
end do

end subroutine
```

```
subroutine force(nm,k1,cost,mu,mi,rh,g,aleph)

! This subroutine computes the field acting on each shell

integer,intent(in) :: nm,k1
real*8,intent(out) :: g(1:nm)
real*8,intent(in) :: rh(1:nm),mu(1:nm)
integer :: l,o
real*8,intent(in) :: cost,mi,aleph

do l=1,nm
g(l)=0.0
end do

do l=1,nm
do o=1,nm
if (o/=l) then
g(l)=g(l)+(0.5*cost*mu(o)/(1.-aleph))*(((rh(l)+rh(o))&
*((abs(mi+rh(l)**2+rh(o)**2-2.*rh(l)*rh(o)))**(0.5-0.5*aleph)&
+(abs(mi+rh(l)**2+rh(o)**2+2.*rh(l)*rh(o)))&
**(0.5-0.5*aleph)))/(rh(l)*rh(o))-((abs(mi+rh(l)**2+&
rh(o)**2-2.*rh(l)*rh(o)))**(1.5-0.5*aleph)+(abs(mi+rh(l)**2+rh(o)**2&
+2.*rh(l)*rh(o)))**(1.5-0.5*aleph))/(rh(o)*(3.-aleph)*rh(l)**2))
end if
end do
end do

if(k1==1) then
do l=1,nm
g(l)=g(l)-0.5*(4.*cost*mu(l))/((3.-aleph)*(abs(2.*(rh(l)+mi)))**aleph)
end do
else if(k1==2)then
do l=1,nm
g(l)=g(l)
end do
end if

end subroutine

subroutine boxmuller(x)
```

```
!generates random numbers with uniform distribution

implicit none
real*8,intent(out) :: x
real*8 :: uu,vv
do
call random_number (uu)
call random_number (vv)
uu=2.*uu-1.
vv=2.*vv-1.
if ((uu**2+vv**2)<1.) then
x=uu*sqrt((-2.*log(uu**2+vv**2))/(uu**2+vv**2))
exit
endif
end do
end subroutine

subroutine poten(ep,rr,nn,ms,cstn,f0,rmm,al)

!calcola l'energia potenziale

real*8,intent(out)::ep(1:nn)
integer,intent(in)::nn
real*8,intent(in)::rr(1:nn),f0(1:nn),ms(1:nn)
real*8,intent(in)::cstn,rmm,al
real*8,allocatable,dimension(1:nn) :: den(:)
integer::j,l
allocate(den(1:nn))

ep=0.0

do j=1,nn
den(j)=0.0
end do

do j=1,nn
do l=1,nn
if(rr(l)<rr(j))then
den(j)=den(j)+ms(j)
end if
```

```
end do
end do

do l=1,nn
ep(l)=-ms(l)*den(l)*cstn/sqrt((rr(l)**2+rmm**2))&
+(-cstn*ms(l)**2/sqrt((rr(l)**2+rmm**2)))
end do

end subroutine

subroutine distribution(particlee,nb,dist,grid)
integer,intent(in)::nb
real*8,intent(in)::particlee(1:nb)
real*8,intent(out)::grid(1:100),dist(1:100)
real*8::emin,emax,gridstep
integer::j,l

emin=minval(particlee)
emax=maxval(particlee)
gridstep=abs(emax-emin)/100
grid(1)=emin
do j=2,100
grid(j)=grid(j-1)+gridstep
end do

do j=1,100
dist(j)=0
end do

do l=1,nb
do j=1,99
if(grid(j)<=particlee(l).and.particlee(l)<grid(j+1)) then
dist(j)=dist(j)+1
end if
end do
end do

do l=1,nb
if(particlee(l)>=grid(100)) then
dist(100)=dist(100)+1
end if
```

```
end do
end subroutine

subroutine massdist(masss,nb,distr,gri,raggi)
integer,intent(in)::nb
real*8,intent(in)::masss(1:nb),raggi(1:nb)
real*8,intent(out)::gri(1:100)
real*8::rgmin,rgmax,gristep
integer::j,l
real*8,intent(out)::distr(1:100)
rgmin=minval(raggi)
rgmax=maxval(raggi)
gristep=abs(rgmax-rgmin)/100
gri(1)=rgmin
do j=2,100
gri(j)=gri(j-1)+gristep
end do

do j=1,100
distr(j)=0
end do

do l=1,nb
do j=1,99
if(gri(j)<=raggi(l).and.raggi(l)<gri(j+1)) then
distr(j)=distr(j)+masss(l)
end if
end do
end do

do l=1,nb
if(raggi(l)>=gri(100)) then
distr(100)=distr(100)+masss(l)
end if
end do
end subroutine

SUBROUTINE rejection (mm,sh,wlp)
!generates the masses with a rejection method
implicit none
```

```
real :: e,u
integer :: i
integer,intent(in) :: sh
real*8,intent(out) :: mm(sh)
real*8,intent(in) :: wlp

do i=1,sh

do
call random_number (mm(i))
mm(i)=2.*mm(i)-1.
if (mm(i)<1.) then



mm(i)=sqrt(2.*mm(i))


e=mm(i)

call random_number (u)
if (u<e**(wlp)/1.0) then
exit
endif
endif
end do
end do
END SUBROUTINE



END PROGRAM powerlawforceshells
```

Bibliography

[1] Aarseth, S.J., 2003, *Gravitational N-body simulations*, Cambridge monographs on Mathematical Physics, Cambridge University press, Cambridge UK.

[2] Antonov, V.A., 1984, *Most probable phase distribution in spherical star systems and conditions for its existence*, Dynamics of Star Clusters, IAU symposiums proceedings, Goodman and Hut (eds) vol. 113, pp 525-540. Original version to be found in: Vest Leningrad University 7, 135; 1962 (In Russian).

[3] Athanassoula, E., Bosma, A., Lambert, J.C., Makino, J., 1998 *Performance and accuracy of a GRAPE-3 system for collisionless N-body simulations*, MNRAS, N.293, pp 369-380.

[4] Arfken, G.B. & Weber, H.J., 1995, *Mathematical methods for physicists*, fourth ediction, Academic Press eds. A Division of Harctourt Brace & co. San Diego, USA.

[5] Bekenstein, J. & Milgrom, M., 1984, *Does the missing mass problem signal the Newtonian gravity breakdown?*, ApJ N. 286, pp 7-14.

[6] Benedetti, C., Rambaldi, S., Turchetti, G., 2005, *Relaxation to Boltzmann equilibrium of 2D Coulomb oscillators*, Physica A, vol. 364, pp 197-212.

[7] Binney, J., 1982, *The phase space structure of $r^{1/4}$ galaxies: Are these galaxies isothermal after all?*, MNRAS, N.200, vol.1, pp 951-964.

[8] Binney, J. & Tremaine, S., 1987, *Galactic Dynamics*, Princeton University Press, Princeton, USA.

[9] Brada, R, & Milgrom, M., 1999, *Stability of Disk Galaxies in the Modified Dynamics*, ApJ, N. 519, pp 590-598.

[10] Chandrasekhar, S., 1943, *Principles of Stellar Dynamics*, University of Chicago Press. Chicago, USA.

[11] Chavanis, P.H. 2008, *Dynamics and thermodynamics of systems with long-range interactions: interpretation of the different functionals*, Dynamic and Thermodynamics of systems with long-range interactions: Theory and Experiments. AIP Conference Proceedings, Volume 970, pp. 39-90.

[12] Ciotti, L., 1991, *Stellar systems following the $R^{1/m}$ luminosity law*, A& A N. 249, pp 99-106.

[13] Ciotti, L. & Binney, J. 2004, *Dynamical friction in modified newtonian dynamics*, MNRAS, N. 351, pp 285-29.

[14] Ciotti, L., Nipoti, C., Londrillo, P., 2007, *Phase Mixing in MOND*, arXiv:astro-ph/0701826, To appear in the Proceedings of the International Workshop "Collective Phenomena in Macroscopic Systems", G. Bertin, R. Pozzoli, M. Rome, and K.R. Sreenivasan, eds., World Scientific, Singapore.

[15] Dehnen, W., 2001, *Towards optimal softening in three-dimensional N-body codes - I, minimizing the force error*, MNRAS, N. 324, pp 273-291.

[16] de Vaucouleurs, G., 1948, *Recherches sur les nebuleuses extragalactiques*, Annales d'Astrophysique, Annèe 11, pp 247-287 (In French).

[17] Durand, E., 1953, *Electrostatique et Magnétostatique*, Masson eds, Paris, France, (In French).

[18] Dwight, H.B., 1961, *Tables of Integrals and other Mathematical Data*, ed. Macmillan, Toronto Canada.

[19] Efthymiopoulos, N., Voglis, N., Kalapotharakos, C., 2006, *Special features of Galactic Dynamics*, unpublished lecture notes.

[20] Fermi E., Pasta J., Ulam S., 1955, *Studies of nonlinear problems. I. Los Alamos report LA-1940*, published later in Collected Papers of Enrico Fermi, E. Segré (Ed.), University of Chicago Press (1965).

[21] Gabrielli, A., Joyce, M., Sicard, F., 2009 *One-dimensional gravity in infinite point distributions*, PhysRev. E, vol. 80, Issue 4, id. 041108.

[22] Heggie, P. & Hut, P., 2003, *The Gravitational Million-body Problem: A multidisciplinary approach to Star Cluster Dynamics*, Cambridge University press, Cambridge, UK.

[23] Hénon, M. *Sur l'Evolution Dynamique des Amas Globulaires*, 1961, Annales d'Astrophysique, Annèe 24, vol.5, pp 369-419 (In French).

[24] Hénon, M., *Evolution Initiale d'un Amas spherique*, 1964, Annales d'Astrophysique, Annèe 27, vol.2, pp. 83-91(In French).

[25] Ipser, J.R. & Kandrup, H.E., 1980, *Stability theory of the orbit-averaged Boltzmann equation*, ApJ N. 241, pp 1141-1147.

[26] Jackson, J.D., 1998, *Classical Electrodynamics*, Third ediction, J. Wiley & Sons Inc. eds, Hoboken, USA.

[27] Kandrup, H.E., 1998, *Violent Relaxation, Phase Mixing, and Gravitational Landau Damping*, ApJ N. 500, pp 120-128.

[28] Kandrup, H.E., 1999, *Collisionless Relaxation of Stellar Systems*, Galaxy Dynamics, APS Conference Series Vol. 182, pp 197-208, Merritt, Sellwood and Valluri eds.

[29] Kandrup, H.E., 2001, *Energy relaxation induced by an external environment and/or incoherent internal Pulsations*, MNRAS, N. 323, pp 681-687.

[30] Kellogg, O.D., 1954, *Foundations of Potential Theory*, ed. Courier Dover Publications. J. Braine & E. Brinks.

[31] Levin, Y., Pakter, R., Teles, T.N. 2008, *Collisionless relaxation in non-neutral plasmas*, Ph.Rev. letters, Vol. 100 issue 4, pp 604-607.

[32] Lynden-Bell, D., 1967, *Statistical mechanics of Violent Relaxation in stellar systems*, MNRAS, N.136, pp 101-121.

[33] Merritt, D., 1996, *Optimal smoothing for N-body codes*, AJ, N.111 vol.6, pp. 2462-2464.

[34] Milgrom, M. 1993, *A modification of the Newtonian dynamics as a possible alternative to the hidden mass hypothesis*, ApJ N. 270, pp 365-370.

[35] Milgrom, M. 2006, *MOND as modified inertia*, EAS Publications Series, Volume 20, pp 217-224.

[36] Mukamel, D., 2009, *Statistical Mechanics of Systems with Long-Range Interactions*, Lectures notes for the XII International Summer School in Fundamental Problems of Statistical Physics, Leuven (B), Unpublished.

[37] Nipoti, C., Ciotti, L., Binney, J., Londrillo, P., 2008, *Dynamical friction in modified Newtonian dynamics*, MNRAS, N. 386, pp 2194-2198.

[38] Nipoti, C., Londrillo, P., Ciotti, L., 2007, *Dissipationless collapse in modified Newtonian dynamics*, ApJ, N. 660, pp 256-266.

[39] Pitaevskji, L.P., Lifshitz, E.M., Landau, L.D., 1970, *Physical Kinetics*, course of Theoretical Physics vol. 10, Butterworth-Heinemann press, London UK.

[40] Pogorelov, I.V. & Kandrup, H.E., 2005, *Energy trapping in loaded string models with long- and short-range couplings*, Annals of the New York Accademy of Sciences vol. 1045: Non linear dynamics in Physics and Astronomy, in memory of Henry Kandrup. ed Wiley InterSciences.

[41] Press, W.H., Teukolsky, S.A., Vetterling, W.T., Flannery, B.P., 2007, *Numerical Recipes, the Art of Scientific Computing*, third ed., Cambridge University press, Cambridge, UK.

[42] Rambaldi, S., Salustri, G., Benedetti, C, 2006, *Hard sphere gas state equation*, Physica A, vol. 361, pp 180-194.

[43] Rodionov, S.A. & Sotnikova, N.Ya., 2005, *Optimal choice of the Softening Lenght and Time-step in N-body simulations*, Astr.Rep. , year 49, vol.6 pp.470-476.

[44] Saslaw, W.C. 1985, *Gravitational Physics of stellar and galactic systems*, Cambridge monographs on Mathematical Physics, Cambridge University press, Cambridge UK.

[45] Sersic, J.L., 1963, *Photometry of Southern Galaxies. IX: NGC1313*, Boletin de la Asociacion Argentina de Astronomia, Vol. 6, p.99.

[46] Spitzer, L., 1987, *Dynamical evolution of globular clusters*, Princeton University Press, Princeton, USA.

Acknowledgements

After these two years of Master Program and at the end of my Thesis work there is a large number of of people that I want to thank for their support during this period. I apologize immediately to those of you that I have forgot to mention! Firts my gratitude goes to my Advisor, Professor Luca Ciotti who always inspired me during my my second thesis work with him and helped me in always applying seriously to this research, hoping that such nice collaboration will go on in the future. I would like to thank dr. Carlo Nipoti (Dipartimento di Astronomia) and dr. Pasquale Londrillo (INAF-OAB) for their precious help in developing my numerical codes. I would also say a big thank you to all the nice people that I have met during my stay in Utrecht University last summer, in particular to Michela Tomasi (University of Trento) and Matin Hallaij (University of Teheran). Amongst my friends and colleagues at the departement of Astronomy in Bologna I would like to thank Francesco D'Eugenio (now at Oxford University) and Gabriele Pezzulli for the useful and precious discussions, Federico Lelli, Roberto Iaconi and Antonino Marasco for the time that we have spent together in the laboratory, Marco Sirotti for its patience and Alessandro "Spugna" Ballone for its friendship. I am grateful to my family (Mum and Dad) for the support that they give me during those years and for always believing me. I thank all the people that I have met in the last year for what they have done and in particular my flat mates Damiano, Michele, Stefano, Loris and Fabio for the last months together. Finally I would like to thank Monica, for being the nicest person I ever knew.